

## Chapter I. OBJECTIVES

**I.1 Objective 1--Use the transcriptional profiling procedure, Fluorescent Differential Display (FDD), to identify genes that are altered in their ability to show differential expression during alkaloid biosynthesis, by comparing a wild type to a low alkaloid (LA21) regulatory mutant.**

To identify novel genes related to nicotine synthesis, mRNA from Burley 21 (*AABB*) and LA21 mutant (*aabb*) tobacco root cultures that have been treated to induce alkaloid biosynthesis will be screened for differential expression using FDD. Gene fragments isolated by FDD will be cloned and sequenced.

**I.2 Objective 2--Confirm differential expression of known alkaloid biosynthetic genes and new genes identified as FDD clones in Burley 21 and LA21 cultivars using Quantitative Real Time Polymerase Chain Reaction (QRT PCR) and Northern blot analysis.**

Differential expression of genes represented by newly isolated FDD clones will be confirmed by comparing Northern blots of transcripts of these genes to known alkaloid biosynthetic genes: arginine decarboxylase (*ADC*), ornithine decarboxylase (*ODC*), putrescine N-methyltransferase (*PMT*) and quinolinate phosphoribosyltransferase (*QPRT*). The role of *A* and *B* loci in differential expression of genes represented by FDD clones and known biosynthetic genes will be examined using QRT PCR to measure transcript levels of these genes in tobacco genotypes differing in alkaloid content: *AABB*, *AAbb*, *aaBB*, and *aabb*.

### **I.3 Justification**

Goals of this research are both basic and applied. Alkaloids contribute a significant portion of plant-derived pharmaceuticals and provide chemical defense to plants against animal herbivory. A thorough understanding of alkaloid biosynthesis and the role of secondary metabolism in plant defense will promote both pharmaceutical and crop development.

## Chapter II. BACKGROUND AND LITERATURE REVIEW

### II.1 Secondary metabolism: function and significance

Many of the organic compounds synthesized by plants are not required for the primary physiological functions supporting life: respiration, photosynthesis, growth, and reproduction. These non-essential plant compounds are frequently referred to as secondary metabolites, and are associated with the plant's adaptation to its environment. Although not directly involved in the essential functions of primary metabolism, secondary metabolites that benefit the plant (such as chemicals toxic to predators or attractive to pollinators) may ultimately determine the viability and fitness of the plant.

Primary metabolites (e.g. amino acids, sugars and fatty acids) are precursors for various secondary metabolites, thus linking primary and secondary metabolism. Unlike the primary metabolic pathways that characterize essentially all living organisms, secondary metabolic pathways may not occur universally among species. Plant secondary metabolites, such as terpenoids, phenylpropanoids or alkaloids, are classified according to the type of molecule from which the compounds are derived (Croteau et al. 2000). The diversity of secondary metabolites results in part from molecular modifications, such as oxidation, acylation, glucosylation, or methylation of chemical functional groups of precursors, either primary metabolites or intermediate secondary compounds (De Luca and St. Pierre 2000). Although products of secondary metabolism are often unique to individual plant species, secondary metabolic pathways may have co-evolved in other species; orthologs of enzymes associated with secondary metabolism in plants, such as methyltransferases, are found in animals and bacteria (Kutchan 2001). There is also evidence in plants for evolution of enzymes associated with a specific secondary metabolic pathway from enzymes associated with a different secondary metabolic pathway. For example, acridone synthase (ACS) and chalcone synthase (CHS), which are plant polyketide synthases of alkaloid and phenylpropanoid biosynthesis, respectively, share significant primary amino acid sequence homology. Lukacin et al. (2001) studied ACS and CHS in *Ruta graveolens*, and found that replacing just three amino acids of ACS with the corresponding amino acids in CHS transforms ACS to a functional CHS with marginal ACS activity. Consistent with the derivation of secondary metabolites from less complex primary

metabolites, some secondary metabolic enzymes may have originated from homologous enzymes involved in primary metabolism (De Luca and St. Pierre 2000). Putrescine methyltransferase (PMT), an enzyme specifically associated with nicotine and tropane alkaloid synthesis, is speculated to have evolved from the primary metabolic enzyme spermidine synthetase (SPDS), involved in polyamine synthesis, as these enzymes share significant sequence homology (Hibi et al. 1994).

## II.2 Regulation of secondary metabolism

Plant secondary metabolism that occurs in response to stress, wounding, or pathogens is initiated by stress signals or elicitor molecules. Elicitors are defined as non-race-specific compounds that induce a plant defense reaction (Darvill and Albersheim 1984). Chemical stress signals, including oligosaccharides (Bishop et al. 1981) and reactive oxygen species (Bradley et al. 1992), and physical stress signals, such as hydraulic change (Boari and Malone 1993) and electric currents (Wildon et al. 1992), have been identified. Plant stress or elicitor signal transduction may be mediated by phytohormones, including auxin (Yasumatsu 1967, Bush and Saunders 1977, Shinshi et al. 1987, Baldwin 1989, Hibi et al. 1994), cytokinins (Shinshi et al. 1987), ethylene (Ecker and Davis 1987), and methyl jasmonate (MeJA) (Gundlach et al. 1992). MeJA has been the most thoroughly characterized phytohormone associated with regulation of plant defense responses. MeJA synthesis and accumulation during plant wounding or elicitor treatment leads to induction of plant defense genes, such as proteinase inhibitors (Doares et al. 1995, Peña-Cortés et al. 1995), and up-regulates secondary metabolic pathways, leading to increased terpenoid synthesis (Choi et al. 1994, Mirjalili and Linden 1996), phenylpropanoid synthesis (Gundlach et al. 1992, Mizukami et al. 1993), and alkaloid synthesis (Baldwin et al. 1994). Although it is not well understood how MeJA regulates stress response in the plant, a model describing the role of MeJA in regulating terpenoid indole alkaloid (TIA) biosynthetic gene expression has been developed (Memelink et al. 2001). The first enzyme in the TIA biosynthetic pathway, strictosidine synthase (STR), catalyzes a condensation reaction leading to strictosidine, which is a precursor for a range of TIAs in several plant species. *Str* and other TIA biosynthetic genes are inducible by MeJA (Geerlings et al. 2000, van der Fits et al. 2000). The promoter of the strictosidine synthase gene (*Str*) has been found to contain two jasmonate and elicitor responsive sequences: the BA region and the jasmonate- and elicitor-responsive element

(JERE) (Menke et al. 1999; van der Fits et al. 2000). Two AP2/ERF-type transcription factors, which are characterized by the AP2/ERF DNA-binding domain (Riechmann and Meyerowitz 1998), were found to bind to the JERE promoter element, and were identified as octadecanoid-responsive *Catharanthus* AP2-domain proteins (ORCAs) (Menke et al. 1999; van der Fits and Memelink 2000). The model proposed by Memelink et al. (2001) for MeJA induction of TIA synthesis involves elicitor perception, kinase activation, and subsequent  $\text{Ca}^{2+}$  influx into the cytosol, leading to increased MeJA synthesis. MeJA accumulation then leads to activation and/or induction of ORCA proteins (van der Fits and Memelink 2001), which in turn bind to the *Str* cis-elements, increasing *Str* expression.

Secondary metabolism is dependent on the availability of primary metabolites, thus supporting the concept of coordinate regulation of primary and secondary metabolic pathways. For example, tryptophan is a primary metabolite precursor in TIA secondary metabolite synthesis. Coordinate regulation by the transcription factor ORCA3 activates genes leading to both tryptophan and TIA synthesis, in a stress response mediated by methyl jasmonate (van der Fits and Memelink 2000).

Plant secondary metabolites benefit plants by increasing plant fitness and are useful to humans as pharmaceuticals; however, genetic engineering of secondary metabolic pathways in plants to enhance or reduce metabolite production is limited by the current understanding of these pathways and their regulation in response to environmental conditions. In order to characterize a biosynthetic pathway of secondary metabolism with respect to its regulation as a defense response, many studies have focused on one class of secondary metabolites, the alkaloids.

### II.3 Plant alkaloids

Plant alkaloids, low-molecular-weight nitrogenous bases derived from an amino acid, are secondary metabolites that may be synthesized in an inducible defense response to animal or insect herbivory (Baldwin 1999). Approximately 20% of flowering plant species contain a unique combination of alkaloids, of which over 16,000 different structures have been identified (Memelink et al. 2001). Alkaloid synthesis may be tissue-specific or accompany certain stages of development, such as senescence (Burton et al. 1988, Anderson et al. 1989). Increased alkaloid synthesis can also occur in response to environmental stimuli such as wounding (Baldwin, 1989)

and water stress (Atkinson et al. 1969), conditions associated with damage to the plant by animal or insect herbivores (Baldwin and Prestin 1999, Baldwin 1989).

Toxicity and unpalatability to animals and insects accounts for the role of alkaloids in plant defense. Caffeine, for instance, is an alkaloid toxic to the tobacco hornworm at levels well below that actually found in the coffee bean or leaves (Croteau et al. 2000). Nicotine, isolated from various tobacco species, has been used commercially as an insecticide (Bauer and Zenk 1991). The biological activity of alkaloids has prompted the fortuitous identification of many alkaloids as effective pharmaceutical agents. Pharmacologically active and medically significant plant alkaloids include the antimalarial quinine, anticancer agents vinblastine, vincristine and camptothecin, antibacterial berberine, analgesic codeine, and the anesthetic (and narcotic) agents cocaine and morphine (Memelink et al. 2001). Understanding alkaloid biosynthesis and the role of secondary metabolism in plant defense is therefore relevant to both agricultural crop development and pharmaceutical discovery.

#### II.4 *Nicotiana tabacum* as a model plant for alkaloid biosynthesis research

The study of alkaloid biosynthesis is fostered by using a model plant system that is tractable to experimentation and characterization. *Nicotiana tabacum* (domestic tobacco) is particularly well suited for this purpose. Most agriculturally important plants that contain alkaloids (such as other Solanaceous species, including tomato, potato and pepper) have been bred to reduce their alkaloid content, because these alkaloids are frequently toxic and/or impart an unpleasant flavor. In contrast, nicotine has historically been a desirable component of commercially grown tobacco, and *N. tabacum* has therefore been cultivated specifically to optimize its nicotine content. Thus, years of tobacco breeding has resulted in well-characterized tobacco accessions with differing levels or composition of alkaloids, including the development of near-isogenic tobacco cultivars that differ only in alkaloid content. In the tobacco plant, nicotine is synthesized in root tissue (Dawson 1941), in an inducible, hormone-mediated response to apical stem or leaf wounding (Baldwin et al. 1994), then transported to the shoots and leaves and stored in the vacuoles (Dawson 1941, 1942). Since tobacco roots (the site of nicotine synthesis) can be grown alone in culture, induction and measurement of nicotine biosynthesis can be performed specifically and reproducibly. Finally, the availability of *N. tabacum* genomic and cDNA libraries and the

relative ease with which *N. tabacum* plant cells are transformed (Cramer et al. 1996) allow the use of molecular techniques to isolate and express complete alkaloid biosynthetic genes. For example, Hibi et al. (1994) used a subtractive hybridization technique to isolate a cDNA from *N. tabacum* cv Burley 21 coding for putrescine N-methyltransferase. Shoji et al (2000) performed *Agrobacterium rhizogenes* and *A. tumefaciens* transformations of *N. sylvestris* with promoter::GUS fusions of *NsPMT1*, *NsPMT2* and *NsPMT3* genes previously isolated by Hashimoto et al. (1998) and demonstrated that a 250 bp portion of the conserved 5' gene flanking region mediated root tissue-specific and jasmonate-inducible *PMT* gene expression.

## II.5 Cultural practices

The experimental conditions used in the present study simulate cultural practices that have been shown to affect nicotine synthesis in tobacco. Although Tso (1990) writes that “every step in tobacco production that affects plant metabolism will influence the level of alkaloid content to a certain degree,” cultural practices that induce alkaloid biosynthesis by their effect on plant maturity, root development, leaf integrity, or apical dominance are most relevant to this study.

Nicotine is found in mature seed of *N. tabacum* (Weeks and Bush 1974), and nicotine synthesis and accumulation begins as early as 48 to 96 hours after seed germination, increasing as the plants mature. Senescence of mature plant tissue, accompanied by a further increase in nicotine content, occurs after the apical meristem is “topped”, or decapitated (a standard cultural practice intended to improve tobacco quality) (Atkinson and Sims 1973). Agricultural practices that lead to increased adventitious root growth (such as decreased plant density) also increase nicotine production (Wolf and Bates 1964). However, subsoiling, or deep tillage to reduce soil compaction, was found to increase root development without significantly affecting nicotine synthesis (Vepraskas and Miner 1987).

Damage to the leaves or apical meristem (associated with mechanical wounding, insect or animal herbivory) of tobacco plants leads to increased nicotine levels in xylem and undamaged leaves, which suggests that a signaling process is involved in the detection of leaf wounding and subsequent induction of alkaloid synthesis in roots (Baldwin 1989). Wounding-associated alkaloid synthesis is mediated by the phytohormone jasmonic acid (JA) or its methyl ester

(MeJA) (Creelman et al. 1992, Doares et al. 1995, Sembdner and Parthier 1993). Endogenous jasmonate levels increase within two hours of tobacco plant wounding (Baldwin et al. 1997), and MeJA applied to the tobacco leaf or root promotes nicotine synthesis (Baldwin et al. 1994, Ohnmeiss et al. 1997). MeJA treatment of cultured tobacco cells induces nicotine biosynthetic gene mRNA synthesis and causes accumulation of nicotine precursors and nicotine (Imanishi et al. 1998a).

The phytohormone auxin stimulates leaf and root growth but negatively affects nicotine synthesis (Yasumatsu 1967). Auxin is synthesized in the apical meristem and moved downward (via polar transport) to sites of activity in other plant tissues (Philips 1975). Removal of the apical meristem results in decreased auxin levels in the root, which may de-repress or induce expression of genes related to nicotine biosynthesis. Mechanical “topping”, or decapitation of the tobacco plant, is a cultural practice that stimulates nicotine production by removing the apical meristem and source of auxin synthesis. Increased nicotine production associated with herbivory may also result from apical meristem damage and decreased levels of auxin.

## II.6 Genetic regulation of alkaloid biosynthesis in tobacco

The use of tobacco cultivars that differ phenotypically in alkaloid content facilitates the characterization of biosynthetic enzyme inducibility. The majority of nicotine accumulation in tobacco is controlled by two non-linked loci, designated *A* and *B* (Legg et al. 1969). Because transcript levels and/or enzyme activities of multiple nicotine biosynthetic genes are reduced by mutations at either loci (Saunders and Bush 1979, Hibi et al. 1994), the *A* and *B* loci are thought to encode regulatory proteins which coordinate alkaloid biosynthetic enzyme expression (Hibi et al. 1994). A low alkaloid tobacco cultivar LA Burley 21 was developed as a genetically stable (for alkaloid content) breeding line, by introgressing mutant alleles *a* and *b* from low alkaloid tobacco varieties (Valleau 1949) into the *N. tabacum* Burley 21 background (Legg et al. 1969). Although the phenotype of LA21 does not differ from the parental Burley 21 with respect to days to flowering, plant height, and leaf size and number, the reduced nicotine content of LA21 makes it more susceptible to insect damage (Legg et al. 1970). Legg and Collins (1971) also derived single mutant genotypes HI21 (*AAbb*) and LI21 (*aaBB*) in Burley 21. The Burley 21 genotype (*AABB*) and the homozygous recessive LA21 genotype (*aabb*) produce high and low alkaloid

levels, respectively, and the single mutant genotypes HI21 (*AAbb*) and LI21 (*aaBB*) produce intermediate alkaloid levels. Legg and Collins (1971) measured the percentage of total alkaloid levels in dry leaves of Burley 21, HI21, LI21 and LA21, and showed that alkaloid content was correlated with genotype in the order: Burley 21 (*AABB*) > HI21 (*AAbb*) > LI21 (*aaBB*) > LA21 (*aabb*). The *a* and *b* mutant alleles have an additive (semi-dominant) effect on alkaloid levels and the mutant *a* allele was found to be 2.4 times as effective as the *b* allele in the reduction of alkaloid content (Legg and Collins 1971). The characterization of *A* and *B* as unique genes has not been confirmed because a genetic complementation study is complicated by the tetraploid tobacco genome and the semidominant action of the *a* and *b* alleles.

## II.7 Nicotine

Nicotine constitutes between 0.6 and 9% of the dry weight of leaves, depending on the tobacco cultivar as well as growing conditions (Dewick 1997). Although nicotine has been postulated to function in the plant as a nitrogen reserve, a growth factor, a waste product, and a detoxification product, as well as a chemical defense agent against predators, only the defense role is well supported experimentally. Baldwin et al. (1998), showed that nicotine production in *N. attenuata* increased to represent 6% of the plant's nitrogen content following herbivory, with increased nicotine content correlated to increased insect resistance. Nicotine toxicity is due to its structural similarity to acetylcholine, whereby nicotine can bind to acetylcholine receptors, affecting nervous system function (Wink 1998).

## II.8 Nicotine biosynthetic pathway

Nicotine, with a chemical structure consisting of one pyridine and one pyrrolidine ring, is classified as a pyridine alkaloid. The pyridine ring, derived from quinolinic acid condenses with the N-methylated pyrrolinium ring, derived from putrescine, and naturally produced nicotine consists entirely of the (-)-2'S-nicotine isomer (Leete 1967). The nicotine biosynthesis pathway is conducive to research because it consists of relatively few biosynthetic steps. Portions of a hypothetical biosynthetic pathway have been proposed based on radiolabeled precursor studies and biochemical enzyme analysis (reviewed in Leete 1983), but other steps in the pathway are speculative and the genetic regulation of nicotine biosynthesis has not been determined. Figure 2.1 shows a currently accepted pathway for the synthesis of nicotine from pyridine and

pyrrolidine ring precursor molecules. The steps in red have not been confirmed experimentally and have been proposed based on principles of organic chemistry.

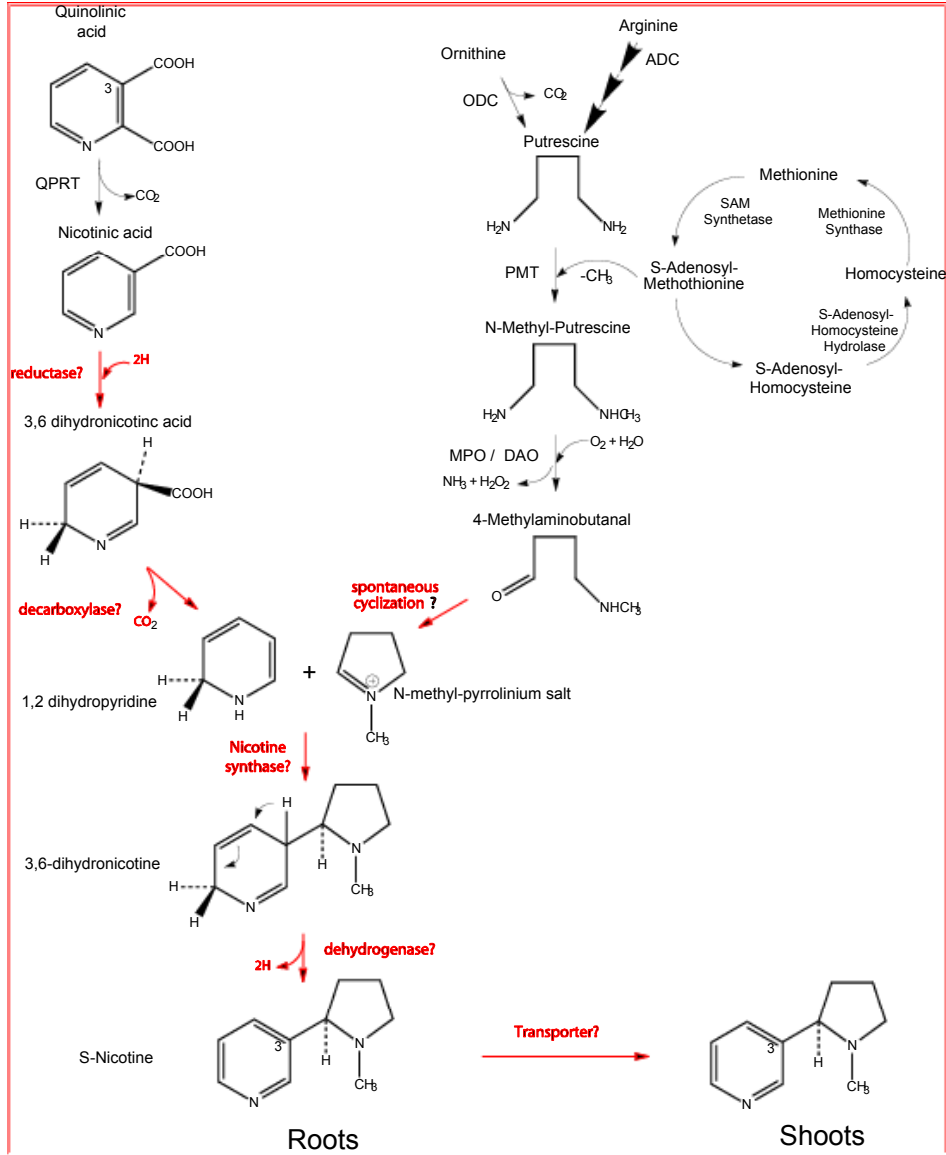


**Figure 2.1. Nicotine biosynthetic pathway. Arginine decarboxylase (ADC); diamine oxidase (DOA); methyl putrescine oxidase (MPO); ornithine decarboxylase (ODC); putrescine methyltransferase (PMT); quinolinate phosphoribosyltransferase (QPRT).**

### II.8.1 Formation of the pyrrolinium ring

Putrescine originates from the decarboxylation of either ornithine (directly) or arginine (indirectly) by ornithine and arginine decarboxylase, respectively (Leete 1980, Tiburcio and Galston 1986, Misuzaki et al. 1973, reviewed by Smith, 1985). Putrescine is utilized as an intermediate in other metabolic pathways, including synthesis of the polyamines spermine and spermidine, primary metabolites involved in stress response, senescence and morphogenesis (Galston 1989). Putrescine targeted for nicotine synthesis is methylated by putrescine methyltransferase (PMT) to produce N-methyl putrescine (Misuzaki et al. 1971). Methylation of putrescine by PMT is the first committed step in the nicotine pathway and the supply of putrescine available for methylation may limit nicotine synthesis (Misuzaki et al. 1973, Bush et al. 1993 p.13). The source of the methyl moiety transferred by PMT is S-adenosyl methionine (SAM) (Misuzaki et al. 1971). The N-methyl putrescine is oxidatively deaminated by a diamine oxidase or putative methyl putrescine oxidase (MPO) to form the aldehyde, 4-methyl aminobutanal (Leete 1967, Misuzaki et al. 1972), and this aldehyde is believed to spontaneously cyclize *in vivo* to yield an imine, the N-methyl pyrrolinium ion (Leete 1967, Misuzaki et al. 1968).

### II.8.2 Formation of the pyridine ring

Quinolinic acid is derived from glyceraldehyde 3-phosphate and L-aspartic acid (Dewick 1997 p.292). The decarboxylation of quinolinic acid via quinolinic acid phosphoribosyltransferase (QPRT) produces nicotinic acid. It is speculated that for nicotine synthesis, nicotinic acid is reduced and decarboxylated to form 1,2-dihydropyridine (Dawson and Osdene 1972, Leete 1977, Leete 1980), which combines with the N-methyl pyrrolinium ion to form nicotine. Friesen and Leete (1990) isolated a cell-free enzyme extract from *N. glutinosa* and *N. tabacum* roots that catalyzed the synthesis of nicotine from 1-methyl- $\Delta^1$ -pyrrolinium chloride and [2-<sup>3</sup>H]-labeled nicotinic acid, and concluded that the enzyme extract contained an enzyme or enzyme complex that was termed “nicotine synthase”; however, this nicotine synthase enzyme or complex has not been further characterized. Newly synthesized nicotine may be actively transported from its source in root cells to the xylem, where it is carried to the shoots and leaves. A transporter protein may facilitate the transfer of nicotine across the root cell wall.

## II.9 Biochemistry/inducibility of known biosynthetic enzyme activities

Genetic regulation of nicotine biosynthesis is supported by measurement of enzyme levels and steady-state mRNA levels in mutant genotypes of tobacco varying in alkaloid content (Saunders and Bush 1979, Wagner et al. 1986, Hibi et al. 1994, Sinclair et al. 2000) and/or in response to alkaloid-inducing conditions (Saunders and Bush 1979, Wagner et al. 1986, Hibi et al. 1994, Imanishi et al. 1998a, Sinclair et al. 2000, Wang et al. 2000). Enzymes involved in nicotine biosynthesis that have been partially purified by traditional biochemical isolation methods include putrescine methyltransferase (PMT) (Misuzaki et al. 1971) and N-methylputrescine oxidase (MPO) (Misuzaki et al. 1972). The biosynthetic activity of PMT, MPO, ornithine decarboxylase (ODC) and quinolinate phosphoribosyltransferase (QPRT) has been characterized with respect to tissue localization and alkaloid content in *N. tabacum* cultivars Bursa (high alkaloid), Samsun (intermediate alkaloid) and Bursanica (low-alkaloid) tobacco cultivars (Wagner et al. 1986). Similarly, PMT, MPO and QPRT activity have been measured in the Burley 21, HI21, LI21, and LA21 tobacco genotypes following induction of alkaloid synthesis by topping (Saunders and Bush 1979). Induction of the following nicotine synthetic genes in tobacco has also been studied: *PMT*, induced by leaf wounding (Sinclair et al. 2000), topping (Hibi et al. 1994, Reichers and Timko 1999), and auxin removal (Hibi et al. 1994); *QPRT*, induced by leaf wounding (Sinclair et al. 2000) and MeJA treatment (Imanishi et al. 1998); *ODC*, induced by topping (Wang et al. 2000) and MeJA treatment (Imanishi et al. 1998); and arginine decarboxylase (*ADC*), induced by induced by topping (Wang et al. 2000). The characterization of known nicotine biosynthetic enzymes ODC, ADC, PMT, QPRT, and PMT with respect to enzyme activity levels and steady-state mRNA levels, in genotypes of tobacco that vary in alkaloid content and in response to alkaloid-inducing conditions, is described below.

### II.9.1 ODC

Ornithine decarboxylase (ODC) generates putrescine, which is a precursor for both nicotine and general polyamine synthesis in tobacco. Putrescine synthesis in plants differs from other eukaryotes, but is similar to bacteria, in that putrescine can be derived from either ornithine or arginine, via arginine decarboxylase (ADC) (Smith 1985). Since ornithine and arginine are readily inter-converted, the exact amino acid origin of putrescine is not certain (Smith 1985). Originally, ornithine was considered the primary source of putrescine for nicotine synthesis,

based on evidence showing ODC activity to be concentrated in roots (the site of nicotine synthesis) (Misuzaki 1973, Wagner et al. 1986), correlated to nicotine content in tobacco roots following topping (Misuzaki 1973), and correlated to nicotine content in roots of high-nicotine versus low-nicotine tobacco cultivars (Wagner et al. 1986). However, Tiburcio et al. (1985) examined the levels of both ADC and ODC activity in relation to changes in tobacco alkaloid content of tobacco callus and found that ADC activity, but not ODC activity, corresponded to alkaloid content. Tiburcio and Galston (1986) measured the effects of an ADC inhibitor, DL- $\alpha$ -difluoromethylarginine (DFMA) and an ODC inhibitor, DL- $\alpha$ -difluoromethylornithine (DFMO) on nicotine synthesis in tobacco calli and found that while the ADC inhibitor reduced nicotine levels by as much as 60%, the ODC inhibitor did not significantly affect nicotine synthesis. The authors also showed that labeled arginine was incorporated into nicotine more than three times as efficiently as labeled ornithine in tobacco calli. Tiburcio and Galston (1986) therefore concluded that ADC is the primary route in generating putrescine for nicotine synthesis, while ODC functions primarily in polyamine synthesis and cell growth. Hiatt et al. (1986) found that inhibition of ODC was lethal to tobacco cell suspension cultures, while ADC inhibition was only lethal during growth initiation, which corroborates the role of ODC in cell growth, as suggested by Tiburcio and Galston (1986). However, experimental support for the role of ODC in nicotine synthesis is found in a study by Imanishi et al. (1998a) demonstrating that mRNA levels of ODC in tobacco cell suspension cultures are increased by MeJA, while mRNA levels of ADC are unaffected. Induction of ODC mRNA by MeJA was reduced by addition of auxin to the culture media, suggesting that genetic regulation of ODC is sensitive to both MeJA and auxin (Imanishi et al. 1998a). Hamill et al (1990) transformed *N. rustica* plants with yeast ODC, resulting in increased levels of N-methyl putrescine and marginally increased nicotine content. Conversely, overexpression of oat ADC activity in transgenic *N. tabacum* cv. Xanthi tobacco did not change nicotine levels (Burtin and Michael 1997). Further support for a role of both ODC and ADC in nicotine synthesis is contributed by Wang et al (2000), who found full-length and partial *ODC* cDNAs and a full length *ADC* cDNA in a subtractive hybridization screen of topped Burley 21 tobacco plants and showed that mRNA levels of both ODC and ADC increased in tobacco roots following topping (Wang et al. 2000). Wang et al. (2000) also found that *N. tabacum* ODC is represented by a gene family consisting of five to seven members.

### II.9.2 ADC

In plants, arginine decarboxylase (ADC) catalyzes the decarboxylation of arginine to agmatine, which is converted to putrescine via an N-carbamoylputrescine intermediate (Smith and Garraway 1964); this reaction may provide the primary source of putrescine for nicotine synthesis in tobacco (Tiburcio and Galston 1986). Wang et al (2000) found ADC mRNA to be inducible by topping and localized to root and floral tissue. Although tobacco ADC mRNA levels are not affected by MeJA, unlike ODC (Imanishi et al. 1998a), both ADC and ODC mRNA are induced by topping (Wang et al. 2000), which may indicate that genetic regulation of *ADC* and *ODC* is coordinated to a limited extent. Additional regulation of ADC activity in tobacco may occur post-translationally, since the *ADC* cDNA isolated by Wang et al. (2000) in a subtractive hybridization screen encoded a 720 a.a. protein similar in size to the oat ADC, which encodes a 66 kDa proenzyme that is post-translationally processed to yield two polypeptides (Malmberg et al. 1992). Wang et al (2000) determined that *N. tabacum* ADC is encoded by a small gene family consisting of at least two members.

### II.9.3 PMT

Mizusaki et al (Misuzaki et al. 1971) partially purified an enzyme from tobacco roots that catalyzed the transfer of the methyl moiety from SAM to putrescine to form N-methyl putrescine, the first committed step of pyrrolidine ring synthesis. This enzyme was termed putrescine methyltransferase (PMT). Evidence for PMT activity and its involvement in nicotine synthesis was observed by Misuzaki et al. (1971), who reported that labeled N-methyl putrescine is incorporated into the pyrrolidine ring of nicotine. The formation of 4-methylaminobutanal from N-methyl putrescine was proposed by Leete (1967), and Mizusaki et al. (1968) determined that 4-methylaminobutanal derived from ornithine is a precursor for nicotine synthesis. PMT activity was detected exclusively in root tissue and was increased 12 fold following plant topping, indicating that PMT activity is inducible under conditions that promote nicotine synthesis (Misuzaki et al. 1971). Saunders and Bush (1979) examined PMT levels following topping in roots of near-isogenic genotypes of *Nicotiana tabacum* cv Burley 21 that differed in alkaloid content and found that PMT activity corresponded to nicotine levels in each genotype: Burley 21 (*AABB*) > HI21 (*aaBB*) > LI21 (*AAbb*) < LA21 (*aabb*). This result was later confirmed by Hibi et al (1994), who also performed a subtractive hybridization screen of Burley 21 versus

low alkaloid LA21 *N. tabacum* root cDNA libraries, to detect and isolate differentially expressed genes related to nicotine biosynthesis. One cDNA clone isolated by this method had high sequence homology to the spermidine synthase (*SPDS*) gene, which encodes a primary metabolic enzyme catalyzing spermidine (polyamine) formation from decarboxylated SAM and putrescine (Smith 1981). However, expression of the cDNA clone produced an enzyme lacking SPDS activity but showing PMT activity, and the authors deduced that the isolated gene was *PMT*. Hibi et al. (1994) also found that the *PMT* clone transcript levels were inducible with plant topping and with removal of auxin from root culture growth media. Northern blot analysis of the *PMT* clone transcript levels showed a transient peak one hour after topping or removal of auxin from root culture media, although Reichers and Timko (1999) examined *PMT* transcript levels by semi-quantitative RT-PCR and found that *PMT* gene expression steadily increased up to 24 hours after topping, which corroborated earlier results by Mizusaki et al (1973) and Saunders and Bush (1979) showing that *PMT* enzyme activity peaked 24 hours after topping. MeJA treatment of cultured tobacco BY-2 cells also increased *PMT* mRNA levels, which peaked between one and six hours after induction (Imanishi et al. 1998a). Reichers and Timko (1999) and Hibi et al (1994) concluded from quantitative RT-PCR and Northern blot analysis, respectively, that *PMT* was inducible by topping in *N. tabacum* Burley 21, but not inducible in the low alkaloid mutant (LA21) cultivar. Consistent with these results, Northern blot analysis by Sinclair et al. (2000) showed that *PMT* was inducible by leaf wounding in the wild-type *N. tabacum* NC95 cultivar, but not in the corresponding low-alkaloid mutant *N. tabacum* LAF53 cultivar. Hibi et al. (1994) probed genomic DNA from *N. tabacum* with the *PMT* clone, which showed *PMT* to be comprised of a multigene family with two to five members. Hashimoto et al. (1998) and Reichers and Timko (1999) separately confirmed that the *PMT* gene family in *N. tabacum* consists of 5 genes, referred to as *PMT 1*, *2*, *3*, *4* and *5*.

#### II.9.4 QPRT

Quinolinic acid phosphoribosyltransferase (QPRT) decarboxylates quinolinic acid to produce nicotinic acid supplying the pyridine ring of nicotine. QPRT activity is induced following topping (Saunders and Bush 1979), and QPRT activity levels are correlated with nicotine content in near-isogenic genotypes of tobacco differing in alkaloid content (Burley 21, HI21, LI21, and LA21) (Saunders and Bush 1979). *QPRT* mRNA levels correspond to QPRT activity levels and

are concentrated in root tissue of *N. tabacum*. Sinclair et al. (2000) performed Northern blot analysis demonstrating that *QPRT* is inducible by leaf wounding in a wild-type *N. tabacum* NC95 cultivar, but not in the corresponding low-alkaloid mutant *N. tabacum* LAFC53 cultivar. Imanishi et al. (1998) found a MeJA-inducible *QPRT* cDNA in *N. tabacum* BY-2 cell culture. Since nicotinic acid is also a primary metabolite and precursor for NAD<sup>+</sup>/NADP<sup>+</sup> coenzyme synthesis, *QPRT* is linked to primary metabolism, and *QPRT* activity is therefore subject to regulation of both a primary and secondary metabolic pathway. Sinclair et al. (2000) found that *QPRT* is represented by a small gene family consisting of at least two members, which may encode separately regulated enzymes to accommodate both primary and secondary metabolic pathways.

#### II.9.5 MPO

Misuzaki et al. (1972) partially purified a cell-free extract of *N. tabacum* roots with enzyme activity that catalyzed the oxidative deamination of N-methylputrescine-<sup>14</sup>CH<sub>3</sub> to produce radiolabeled N-methylpyrrolinium chloride (the pyrrolidine ring precursor of nicotine). The enzyme was termed methyl putrescine oxidase (MPO) and classified as a diamine oxidase. Misuzaki et al. (1972) found that MPO activity was localized to root tissue, and was inducible by topping. Saunders and Bush (1979) confirmed the inducibility of MPO activity by topping. Saunders and Bush (1979) found MPO activity correlated with alkaloid content in *N. tabacum* Burley 21 and LA21. MPO activity levels in the high intermediate alkaloid genotype (HI21) was not significantly different from the low intermediate alkaloid (LI21), although the MPO activity levels of both intermediate genotypes was between LA21 and Burley 21. A tobacco *MPO* gene has not been cloned.

#### II.10 Alkaloid gene discovery by differential gene expression

To date, none of the nicotine biosynthetic enzymes have been isolated to homogeneity, thus blocking a reverse genetic approach to gene characterization. Recent efforts, using molecular approaches that circumvent the problems associated with biochemical techniques, are focused on cloning nicotine biosynthetic genes and characterizing encoded enzymes, identifying additional enzymes in the biosynthetic pathway, and elucidating the genetic regulation of nicotine biosynthesis in response to stress and plant wounding.

In response to alkaloid-inducing conditions, nicotine biosynthetic genes show differential expression (Hibi et al. 1994, Imanishi et al. 1998, Wang et al. 2000, Sinclair et al. 2000). Molecular methods for alkaloid biosynthetic gene discovery have included subtractive hybridization (Hibi et al. 1994, Wang et al. 2000) and differential polypeptide expression (Imanishi et al. 1998). While these methods have been used successfully to isolate cDNAs associated with conditions inducing alkaloid biosynthesis, the present study applies fluorescence differential display (FDD), a transcription profiling technique offering several advantages to other methods of gene discovery.

#### II.10.1 Subtractive hybridization

Subtractive hybridization of wild-type B21 cDNA and low alkaloid LA21 cDNA from roots was performed by Hibi et al. (1994). Two positive clones were sequenced and the genes expressed in *E. coli*. One clone was identified as a putrescine methyltransferase and the other was termed a reductase, although it could not conclusively be assigned a role in nicotine synthesis. Both cDNAs were coordinately induced (down-regulated by auxin) and were root-specific. Wang et al. (2000) performed another subtractive hybridization procedure using cDNA generated from B21 root tissue before and 24 hours after topping to induce nicotine synthesis. They were able to isolate and sequence 60 cDNAs associated with the topping procedure.

#### II.10.2 Differential protein expression

Imanishi et al. (1998a, 1998b) used 2-D electrophoresis to screen differentially expressed translation products in cultured *N. tabacum* cells, and found six MeJA-inducible cDNAs, including cDNAs with homology to ODC, SAMS, QPRT and one cDNA with homology to a glycosyltransferase, which is believed to be an early stress response gene.

#### II.10.3 FDD

Differential display (DD) was originally developed by Liang and Pardee (1992) and uses reverse transcriptase-polymerase chain reaction (RT-PCR) to synthesize cDNA from total RNA samples, then PCR to generate radio-labeled cDNA fragments that can be analyzed on a high-resolution gel. The RT-PCR reaction is performed with reverse transcriptase and an anchored oligo(dT) primer designed to anneal to the 3' poly-A tail of messenger RNA (mRNA). The first-strand

cDNAs generated in the RT-PCR reaction are used as template in a PCR reaction with a combination of the anchored oligo(dT) primer and an arbitrary primer. The use of a small (10-mer) arbitrary primer permits non-specific priming, thus generating a population of cDNA PCR products (biased to 3' ends of genes) that can be screened simultaneously. PCR products are labeled by incorporating <sup>35</sup>S-labeled dCTP during the PCR reaction, and are then separated on a denaturing sequencing gel to create an expression "fingerprint" of the original RNA sample. The fingerprints of two or more RNA samples are compared in adjacent lanes on the gel, and the resulting pattern of bands are screened to identify labeled PCR fragments that are differentially expressed. DD has been used successfully to isolate novel genes in secondary product pathways, including genes involved in flavonoid (Schopfer and Ebel 1998, Latunde-Dada et al. 2001) and taxol synthesis (Schoendorf et al. 2001); however, the effectiveness of the DD method as a screening tool is limited. The incorporation of radio-labeled nucleotide in the PCR reaction of DD presents several disadvantages: 1. factors other than PCR fragment abundance can affect band intensity, such as fragment length and C content; 2. radioisotope decay (with diminishing signal strength of the radio-labeled PCR product) makes it impractical to compare samples after a certain time period; and 3. gel autoradiography is time and labor intensive and involves risk of radiation exposure.

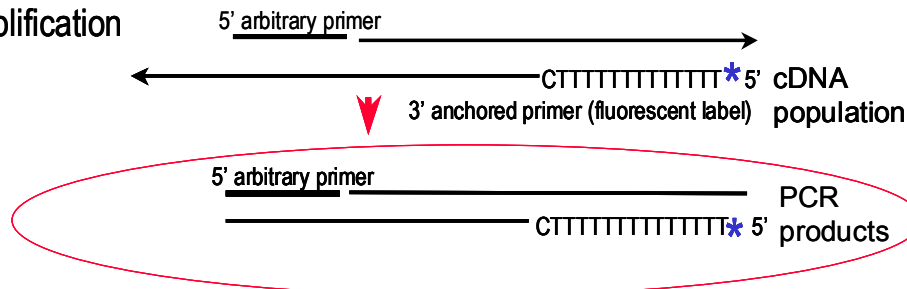
Ito et al. (1994) developed a modification of the original DD procedure that utilizes fluorescent-labeled anchored oligo(dT) primers in place of radio-labeling of PCR products, called Fluorescent Differential Display (FDD). FDD improves reproducibility, operational safety and allows high throughput screening. The FDD procedure (Figure 2.2) involves the combination of fluorescent-labeled 3' anchored oligo dT primers and arbitrary 5' primers to produce fluorescent-labeled cDNAs. Fluorescent-labeled PCR fragments from control and treated samples are separated, detected and recorded on an automated DNA sequencer, and band patterns representing the desired differential gene expression are evaluated by visual inspection. Labeled PCR product that is differentially expressed is detected as a band that is darker or lighter than the corresponding band from a control sample. Selected bands, representing potentially differentially expressed genes, are cut from the gel, and the PCR products cloned and sequenced. An FDD screen to detect novel transcriptionally regulated genes is only limited by the number of primer pair combinations used to generate cDNA populations (estimated at 100 to 150 cDNAs per

primer pair), so that the combination of three 3' anchored primers with 200 available arbitrary 5' primers theoretically permits the screening of over 100,000 gene fragments.

1. Reverse transcribe mRNA



2. PCR amplification



3. Separate PCR products on automated DNA sequencer

Figure 2.2. Fluorescent differential display (FDD) procedure. Messenger RNA (mRNA), complement DNA (cDNA), polymerase chain reaction (PCR).

FDD offers several advantages over subtractive hybridization. Multiple samples can be compared simultaneously, thus refining the search for relevant genes. FDD allows increased detection of very low-abundance genes and genes that are differentially expressed by less than two-fold (Kuno and Furuya 2000) and FDD requires only a small amount of RNA (Uchida et al. 1998). FDD is also suitable for detecting both up- and down-regulated genes in the same assay, which is not possible with subtractive hybridization. Because FDD allows the comparison of multiple mRNA populations, different sample genotypes and treatment conditions can be screened simultaneously. For example, to identify genes associated with a certain physiological response, two samples that differ only in their ability to respond to conditions inducing the response can be compared during both inducing and non-inducing conditions. Kuno et al. (2000) used an FDD screen to identify 15 genes in *Arabidopsis Landsberg erecta* regulated by phytochrome A (PhyA) in a screen of wild type and *phyA-201* single mutant seedlings exposed to PhyA-inducing light conditions.

#### II.11 Experimental approach

In this study, FDD was used to screen mRNA from root tissue of Burley 21 (*AABB*) and LA21 mutant (*aabb*) tobacco grown under both alkaloid-inducing and non-inducing conditions in order to identify differentially expressed genes regulated by the *A* and/or *B* genes. FDD gene fragments expressed at a high basal level and inducible in Burley 21, and expressed at a low basal level and not inducible or weakly inducible in LA21 may represent alkaloid biosynthetic genes that are affected by the *a* and *b* mutations. The pattern of differential expression of gene fragments identified by FDD in Burley 21 and LA21 was confirmed by Northern blot analysis. The role of *A* and *B* loci in differential expression of genes represented by FDD clones and known biosynthetic genes *ADC*, *ODC*, *PMT*, and *QPRT* was examined using Quantitative Real Time Polymerase Chain Reaction (QRT PCR) to measure mRNA accumulation levels of these genes in wild type and mutant A, B tobacco genotypes.

## II.12 Bibliography

Aerts, R.J., Gisi, D., De Carolis, E., De Luca, V., Baumann, T.W. 1994. Methyl jasmonate vapor increases the developmentally controlled synthesis of alkaloids in *Catharanthus* and *Cinchona* seedlings. *Plant J.* 5: 635-643.

Anderson, R.A., Fleming, P.D., Burton, H.R. 1989. N'-Acyl- and N'-nitroso-pyridine alkaloids in alkaloid lines of burley tobacco during growth and air-curing. *J. Agric. Food Chem.* 37: 44-50.

Atkinson, W.O., Ragland, J.L., Sims, J.L., Bloomfield, B.J. 1969. Nitrogen composition of burley tobacco. I. The influence of irrigation on the response of burley tobacco to nitrogen fertilization. *Tob. Sci.* 13: 123-126.

Atkinson, W.O., Sims, J.L. 1973. Nitrogen composition of burley tobacco. II. Influence of nitrogen fertilization, suckering practice, and harvest date on yield, value and distribution of dry matter among plant parts. *Tobacco Science* 17: 63-66.

Baldwin, I.T. 1989. Mechanism of damage-induced alkaloid production in wild tobacco. *J. Chem. Ecol.* 15(5): 1661-1680.

Baldwin, I.T., Schmelz, E.A., and Ohnmeiss, T.E. 1994. Wound-induced changes in root and shoot jasmonic acid pools correlate with induced nicotine synthesis in *Nicotiana sylvestris* Spegazzini and Comes. *J. Chem. Ecol.* 20: 2139-2157.

Baldwin, I.T., Zhang, Z.-P., Diab, N., Ohnmeiss, T.E., McCloud, E.S., Lynds, G.Y., Schmelz, E.A. 1997. Quantification, correlations and manipulations of wound-induced jasmonic acid and nicotine in *Nicotiana sylvestris*. *Planta* 201: 397-404.

Baldwin, I.T., Gorham, D., Schmelz, E.A., Lewandowski, C., Lynds, G.Y. 1998. Allocation of nitrogen to an inducible defense and seed production in *Nicotiana attenuata*. *Oecologia* 115: 541-552.

Baldwin, I.T. 1999. Inducible nicotine production in native *Nicotiana* as an example of adaptive phenotypic plasticity. *J. of Chem. Ecol.* 25: 3-30.

Baldwin, I.T., Prestin, C.A. 1999. The eco-physiological complexity of plant responses to insect herbivores. *Planta* 208: 137-145.

Bauer, W. and M.H. Zenk 1991. Two methylenedioxy bridge forming cytochrome P-450 dependent enzymes are involved in (S) stylophine biosynthesis. *Phytochemistry* 30: 2953.

Bishop, P.D., Makus, D.J., Pearce, G. and Ryan, C.A. 1981. Proteinase inhibitor-inducing factor activity in tomato leaves resides in oligosaccharides enzymically released from cell walls. *Proc. Natl. Acad. Sci. USA* 78: 3526-3540.

Boari, F. and Malone, M. 1993. Rapid and systemic hydraulic signals are induced by localized wounding in a wide range of species. *J. Exp. Bot.* 44: 741-746.

Bradley, D.J., Kjellbom, P., Lamb, C.J. 1992. Elicitor- and wound-induced oxidative cross-linking of a proline-rich plant cell structural protein: a novel, rapid plant defense response. *Cell* 70: 20-30.

Burtin, D. and Michael, A.J. 1997. Overexpression of arginine decarboxylase in transgenic plants. *Biochem. J.* 325: 331-337.

Burton, H.R., Anderson, R.A., Fleming, P.D. 1988. Changes in chemical composition of burley tobacco during senescence and curing. *J. Agric. Food Chem.* 36: 579-584.

Bush, L.P., Fannin, F.F., Chelvarajan, R.L., Burton, H.R. 1993. Biosynthesis and metabolism of nicotine and related alkaloids. In: *Nicotine and Related Alkaloids: Absorption, Distribution, Metabolism and Excretion*. Gorrod, J.W., Wahren, J., eds. Chapman & Hall. London, England. pp. 1-29.

Bush, L.P. and Saunders, J.W. 1977. Accumulation, manipulation and regulation of nicotine content in tobacco. In: *Recent Advances in the Chemical Composition of Tobacco and Tobacco Smoke*. Proc. Am. Chem. Soc. Symp. New Orleans. pp. 389-425.

Chattopadhyay, M.K. and Gosh, B. 1998. Molecular analysis of polyamine biosynthesis in higher plants. *Curr. Sci.* 74: 517-522.

Choi, D., Bostock, R.M., Avdiushko, S., and Hildebrand, D.F. 1994. Lipid-derived signals that discriminate wound- and pathogen-responsive isoprenoid pathways in plants: methyl jasmonate and the fungal elicitor arachidonic acid induce different 3-hydroxy-3-methylglutaryl-coenzyme A reductase genes and antimicrobial isoprenoids in *Solanum tuberosum* L. *Proc. Natl. Acad. Sci. USA* 91 (6): 2329-2333.

Chou, W. and Kutchan, T.M. 1998. Enzymatic oxidations in the biosynthesis of complex alkaloids. *Plant J.* 15(3): 289-300.

Cramer, C.L., Weissenborn, D.L., Oishi, K.K., Grabau, E.A., Bennett, S., Ponce, E., Grabowski, G.A., Radin, D.N. 1996. Bioproduction of human enzymes in transgenic tobacco. In: *Engineering Plants for Commercial Products and Applications*. Collins, G.B. and Shepherd, R.J., eds. Ann. N.Y. Acad. Sci. New York, pp. 62-71.

Creelman, R.A., Tierney, M.L., and Mullet, J.E. 1992. Jasmonic acid/methyl jasmonate accumulation in wounded soybean hypocotyls and modulate wound gene expression. *Proc. Natl. Acad. Sci. USA* 89: 4938-4941.

Croteau, R., Kutchan, T.M., Lewis, N.G. 2000. Natural products (secondary metabolites). In: *Biochemistry and Molecular Biology of Plants*. Buchanan, B.B., Gruissem, W., Jones, R.L., eds. American Society of Plant Physiologists. Rockville, Md., pp. 1250-1318.

- Darvill, A.G. and Albersheim, P. 1984. Phytoalexins and their elicitors- a defense against microbial infection in plants. *Annu. Rev. Plant Phys.* 35: 243.
- Dawson, R.F. 1941. The localization of the nicotine synthetic mechanism in the tobacco plant. *Science* 94: 396-397.
- Dawson, R.F. 1942. Accumulation of nicotine in reciprocal grafts of tomato and tobacco. *Am. J. Bot.* 29: 66-71.
- Dawson, R.F., Osdene, T.S. 1972. A speculative view of tobacco alkaloid biosynthesis. In: *Structural and Functional Aspects of Phytochemistry. Recent Advances in Phytochemistry, Vol. 5.* Runcles, V.C., Tso, T.C., eds. Academic Press. New York. pp. 317-338.
- De Luca, V. and St. Pierre, B. 2000. The cell and developmental biology of alkaloid biosynthesis. *Trends Plant Sci.* 5(4): 168-173.
- Dewick, P.M. 1997. Alkaloids. In: *Medicinal Natural Products.* John Wiley & Sons, Chichester, England. p. 293.
- Doares, S.H., Syrovets, T., Weiler, E.W., Ryan, C.A. 1995. Oligogalactouronides and chitosan activate plant defensive genes through the octadecanoid pathway. *Proc. Natl. Acad. Sci. USA* 92: 4095-4098.
- Ecker, J.R. and Davis, R.W. 1987. Plant defense genes are regulated by ethylene. *Proc. Natl. Acad. Sci USA.* 84(15): 5202-5206.
- Facchini, P. 1999. Plant secondary metabolism: out of the evolutionary abyss. *Trends Plant Sci.* 4: 382-384.
- Friesen, J.B. and Leete, E. 1990. Nicotine synthase- an enzyme from *Nicotiana* species which catalyzes the formation of (S)-nicotine from nicotinic acid and 1-methyl- $\Delta^2$ -pyrrolinium chloride. *Tetrahedron Lett.* 31: 6295-6298.
- Galston, A.W. 1989. Polyamines and plant response to stress. In: *The Physiology of Polyamines, Vol. 2.* Bachrach, U., Heimer, Y.M., eds. CRC Press. Boca Raton, Fla. pp. 99-106.
- Geerlings, A., Martinez-Lozano Ibanez, M., Mamelink, J., van der Heijden, R., Verpoorte, R. 2000. Molecular cloning and analysis of strictosidine  $\beta$ -D-glucosidase, an enzyme in terpenoid indole alkaloid biosynthesis in *Catharanthus roseus*. *J. Biol. Chem.* 275: 3051-3056.
- Gundlach, H., Muller, M.J., Kutchan, T.M., Zenk, M.H. 1992. Jasmonic acid is a signal transducer in elicitor-induced plant cell cultures. *Proc. Natl. Acad. Sci USA.* 89: 2389-2393.
- Hamill, J.D., Robins, R.J., Parr, A.J., Evans, P.M., Furze, J.M., Rhodes, M.J.C. 1990. Over-expressing a yeast ornithine decarboxylase gene in transgenic roots of *Nicotiana rustica* can lead to enhanced nicotine accumulation. *Plant Mol. Biol.* 15: 27-38.

Hashimoto, T., Shoji, T., Mihara, T., Oguri, H., Tamaki, K., Suzuki, K.-I., Yamada, Y. 1998. Intra-specific variability of the tandem repeats in *Nicotiana* putrescine N-methyltransferases. *Plant Mol. Biol.* 37: 25-37.

Hashimoto, T., and Yamada, Y. 1994. Alkaloid biogenesis: molecular aspects. *Ann. Rev. Plant Physiol. Plant Mol. Biol.* 45: 257-285.

Heby, O. and Persson, L. 1990. Molecular genetics of polyamine synthesis in eukaryotic cells. *Trends Biochem. Sci.* 15: 153-158.

Hiatt, A.C., McIndoo, J., Malmberg, R.L. 1986. Regulation of polyamine biosynthesis in tobacco. Effects of inhibitors and exogenous polyamines on arginine decarboxylase, ornithine decarboxylase and S-adenosylmethionine synthase. *J. Biol. Chem.* 261(3): 1293

Hibi, N., Higashiguchi, S., Hashimoto, T., and Yamada, Y. 1994 Gene expression in tobacco low-nicotine mutants. *Plant Cell* 6: 723-735.

Imanishi, S., Hashizumi, K., Nakakita, M., Kojima, H., Matsubayashi, Y., Hashimoto, T., Sakagami, Y., Nakamura, K. 1998a. Differential induction by methyl jasmonate of genes encoding ornithine decarboxylase and other enzymes involved in nicotine biosynthesis in tobacco cell cultures. *Plant Mol. Biol.* 38: 1101-1111.

Imanishi, S., Hashizumi, K., Kojima, H., Ichihara, A., Nakamura, K. 1998b. An mRNA of tobacco cell that is rapidly inducible by methyl jasmonate in the presence of cycloheximide codes for a putative glycosyltransferase. *Plant Cell Physiol.* 39: 202-211.

Ito, T., Kito, K., Adati, N., Mitsui, Y., Hagiwara, H., Sakaki, Y. 1994. Fluorescent differential display: arbitrarily primed RT-PCR fingerprinting on an automated DNA sequencer. *FEBS Letters* 351: 231-236.

Kuno, N., Furuya, M. 2000. Phytochrome regulation of nuclear gene expression in plants. *Sem. Cell Devel. Biol.* 11(6): 485-493.

Kutchan, T.M. 1995. Alkaloid biosynthesis—the basis for metabolic engineering of medicinal plants. *Plant Cell* 7: 1059-1070.

Kutchan, T.M. 1998. Molecular genetics of plant alkaloid biosynthesis. In: *Alkaloids*, vol. 50, G.A. Cordell, ed., Academic Press, Inc. San Diego, California, USA; London, England, U.K., 257-316.

Kutchan, T.M. 2001. Ecological arsenal and developmental dispatcher. The paradigm of secondary metabolism. *Plant Physiol.* 125: 58-60.

Latunde-Dada, A.O., Cabello-Hurtado, F., Czittrich, N., Didierjean, L., Schopfer, C., Hertkorn, N. et al. 2001. Flavonoid 6-hydroxylase from soybean (*Glycine max* L.) a novel plant P-450 monooxygenase. *J. Biol. Chem.* 276: 1688-1695.

- Leete, E. 1967. Biosynthesis of the *Nicotiana* alkaloids XI. Investigation of tautomerism in N-methyl-D-pyrrolinium chloride and its incorporation into nicotine. *J. Am. Chem. Soc.* 89: 7081.
- Leete, E. 1977. The incorporation of (5,6-<sup>13</sup>C<sub>2</sub>) nicotinic acid into the tobacco alkaloids examined by the use of <sup>13</sup>C nuclear magnetic resonance. *Bioorg. Chem.* 6: 273.
- Leete, E. 1980. Alkaloids derived from ornithine, lysine, and nicotinic acid. In *Encyclopedia of Plant Physiology, New Series 8*, E.A. Bell and B.V. Charlwood, eds (Berlin: Springer-Verlag), pp. 65-91.
- Leete, E. 1983. Biosynthesis and metabolism of the tobacco alkaloids. In: *Alkaloids: Chemical and Biological Perspectives*, S.W. Pelletier, ed. John Wiley & Sons. New York. pp. 85-151.
- Legg, P.D. and Collins, G.B. 1971. Inheritance of percent total alkaloids in *Nicotiana tabacum* L.II. genetic effects of two loci in Burley 21 X LA Burley 21 populations. *Can. J. Cytol.* 13: 287-291.
- Legg, P.D., Collins, G.B., Litton, C.C. 1970. Registration of LA Burley 21 tobacco germplasm. *Crop Sci.* 10:212.
- Liang, P., Pardee, A.B. 1992. Differential display of eukaryotic messenger RNA by means of the polymerase chain reaction. *Science* 257: 967-971.
- Lukacin R, Schreiner S, and Matern U. 2001. Transformation of acridone synthase to chalcone synthase. *FEBS Lett.* 508(3): 413-7.
- Malmberg, R.L., Smith, K.E., Bell, E., Cellino, M.L. 1992. Arginine decarboxylase of oats is clipped from a precursor into two polypeptides found in the soluble enzyme. *Plant Physiol.* 100: 146-152.
- Malmberg, R.L., Watson, M.B., Galloway, G.L., Yu, W. 1998. Molecular genetics of plant polyamines. *Crit. Rev. Plant Sci.* 17: 199-224.
- Mann, D.F., Byerrum, R.U. 1974. Activation of the de novo pathway for pyridine nucleotide biosynthesis prior to ricinine synthesis in castor beans. *Plant Physiol.* 53: 603-609.
- Memelink, J., Verpoorte, R., and Kijne, J.W. 2001. ORCAization of jasmonate-responsive gene expression in alkaloid metabolism. *Trends Plant Sci.* 6(5): 212-219.
- Menke, F.L.H., Champion, A., Kijne, J.W., Memelink, J. 1999. A novel jasmonate- and elicitor-responsive element in the periwinkle secondary metabolite biosynthetic gene *Str* interacts with a jasmonate- and elicitor-inducible AP2-domain transcription factor, ORCA2. *EMBO J.* 18: 4455-4463.
- Michael, A.J., Furze, J.M., Rhodes, M.J.C., Burtin, D. 1996. Molecular cloning and functional identification of a plant ornithine decarboxylase cDNA. *Biochem. J.* 314: 241-248.

- Misuzaki, S., Kisaki, T., Tamaki, E. 1968. Phytochemical studies on tobacco alkaloids. XII. Identification of  $\gamma$ -methylaminobutyraldehyde and its precursor role in nicotine synthesis. *Plant Physiol.* 43: 93.
- Misuzaki, S., Tanabe, Y., Noguchi, M., Tamaki, E. 1971. Phytochemical studies on tobacco alkaloids. XIV. The occurrence and properties of putrescine N-methyltransferase in tobacco roots. *Plant Cell Physiol.* 12: 633-640.
- Misuzaki, S., Tanabe, Y., Noguchi, M., Tamaki, E. 1972. N-methylputrescine oxidase from tobacco roots. *Phytochemistry* 11: 2757-2762.
- Misuzaki, S., Tanabe, Y., Noguchi, M., Tamaki, E. 1973. Changes in the activities of ornithine decarboxylase, putrescine N-methyltransferase and N-methylputrescine oxidase in tobacco roots in relation to nicotine biosynthesis. *Plant Cell Physiol.* 14: 103-110.
- Mizukami, H., Tabira, Y., Ellis, E.E. 1993. Methyl jasmonate-induced rosmarinic acid biosynthesis in *Lithospermum erythrorhizon* cell suspension cultures. *Plant Cell Rep.* 12: 706-709.
- Nam, K.H., Lee, S.H., Lee, J.H. 1997. Differential expression of ADC mRNA during development and upon acid stress in soybean (*Glycine max*) hypocotyls. *Plant Cell Physiol.* 38: 1156-1166.
- Ohnmeiss, T.E., McCloud, E.S., Lynds, G.Y., Baldwin, I.T. 1997. Within-plant relationships among wounding, jasmonic acid, and nicotine: implications for defense in *Nicotiana sylvestris*. *New Phytol.* 137: 441-452.
- Pegg, A.E. 1986. Recent advances in the biochemistry of polyamines in eukaryotes. *Biochem J.* 234: 249-262.
- Peña-Cortés, H., Fisahn, J., Willmitzer, L. 1995. Signals involved in wound-induced proteinase inhibitor II gene expression in tomato and potato plants. *Proc. Natl. Acad. Sci. USA* 92: 4106-4113.
- Philips, I.D.J. 1975. Apical dominance. *Annu. Rev. Plant Physiol.* 26: 341-367.
- Reichers, D.E. and Timko, M.P. 1999. Structure and expression of the gene family encoding putrescine N-methyltransferase in *Nicotiana tabacum*: new clues to the evolutionary origin of cultivated tobacco. *Plant Mol. Biol.* 41: 387-401.
- Reichmann, J.L. and Meyerowitz, E.M. 1998. The AP2/EREBP family of plant transcription factors. *Biol. Chem.* 379: 633-646.
- Rostogi, R., Dulson, J., Rothstein, S.J. 1993. Cloning of tomato (*Lycopersicon esculentum* Mill.) arginine decarboxylase and its expression during fruit ripening. *Plant Physiol.* 103: 829-834.

- Sato, F., Hashimoto, T., Hachiya, A., Tamura, K., Choi, K., Morishigi, T., Fujimoto, H., Yamada, Y. 2000. Metabolic engineering of plant alkaloid biosynthesis. *Proc. of the Natl. Acad. Sci. USA* 98(1): 367-372.
- Saunders, J.W., and Bush, L.P. 1979. Nicotine biosynthetic enzyme activities in *Nicotiana tabacum* L. genotypes with different alkaloid levels. *Plant Physiology* 64: 236-240.
- Schoendorf, A., Rithner, C.D., Williams, R.M., Croteau, R.B. 2001. Molecular cloning of a cytochrome P450 taxane 10 beta-hydroxylase cDNA from *Taxus* and functional expression in yeast. *Proc. Natl. Acad. Sci.* 98: 1501-1506.
- Schopfer, C.R., Ebel, J. 1998. Identification of elicitor-induced cytochrome P450s of soybean (*Glycine max* L.) using differential display of mRNA. *Mol. Plant Microbe Interact.* 9: 658-663.
- Sembdner, G. and Parthier, B. 1993. The biochemistry and the physiological and molecular actions of jasmonates. *Annu. Rev. Plant Physiol Plant Mol. Biol.* 44: 569-589.
- Shinshi, H., Mohnen, D., Meins, J.R. 1987. Regulation of a plant pathogenesis-related enzyme: Inhibition of chitinases and chitinases mRNA accumulation in cultured tobacco tissues by auxin and cytokinin. *Proc. Natl. Acad. Sci. USA.* 84: 89-93.
- Sinclair, S.J. Murphy, K.J. Birch, C.D., Hamill, J.D. 2000. Molecular characterization of quinolinate phosphoribosyltransferase (*QPRTase*) in *Nicotiana*. *Plant Mol. Biol.* 44: 603-617.
- Sisson, V.A., and Severson, R.F. 1984. Alkaloid composition of the *Nicotiana* species. *Tobacco Chem. Res. Conf. Abst. No. 24.*
- Smith, T.A. and Garraway, J.L. 1964. *Phytochemistry* 3: 23-26.
- Smith, T.A. 1981. Amines. In: *The Biochemistry of Plants, Vol. 7*, P.K. Stumpf and E.E. Conn, eds, London: Academic Press, pp. 249-268.
- Smith, T.A. 1985. Polyamines. *Annu. Rev. Plant Physiol.* 36: 117-143.
- Stockigt, J. 1995. *The Alkaloids*, G.A. Cordell, ed., Vol. 47, p. 115. Academic Press, San Diego.
- Tabor, C.W. and Tabor, H. 1984. Polyamines. *Annu. Rev. Biochem.* 53: 749-790.
- Takahashi, M. and Yamada, Y. 1972. Regulation of nicotine production by auxins in tobacco cultured cells in vitro. *Agr. Biol. Chem.* 37(7): 1755-1757.
- Tiburcio, A.F., Kaur-Sawhney, R., Ingersoll, R., Galston, A.W. 1985. Correlation between polyamines and pyrrolidine alkaloids in developing tobacco callus *Plant Physiol.* 78: 323.
- Tiburcio, A.F., and Galston, A.W. 1986. Arginine decarboxylase as the source of putrescine for tobacco alkaloids. *Phytochemistry* 25: 107-110.

- Tso, T.C. 1990. Organic metabolism- alkaloids. In: Production, Physiology, and Biochemistry of Tobacco Plant. IDEALS. Beltsville, Md. pp. 427-486.
- Uchida, K., Muramatsu, T., Jamet, E., Furuya, M. 1998. Control of expression of a gene encoding an extensin by phytochrome and a blue light receptor in spores of *Adiantum capillus-veneris*. L. Plant J. 15: 813-819.
- Valleau, W.D. 1949. Breeding low-nicotine tobacco. Agric. Res. 78: 171-181.
- van der Fits, L. and Memelink, J. 2000. ORCA3, a jasmonate-responsive transcriptional regulator of plant primary and secondary metabolism. Science 289: 295-297.
- Vepraskas, M.J., Miner, J.S. 1987. Tillage effects on alkaloid production in tobacco as influenced by soil texture, root abundance and rainfall. Tob. Sci. 31: 52-56.
- Wagner, R. Feth, F., Wagner, K.G. 1986. The regulation of enzyme activities of the nicotine pathway in tobacco. Physiol Plant. 68: 667-672.
- Wang, J., Sheehan, M., Brookman, H., Timko, M. 2000. Characterization of cDNAs differentially expressed in roots of tobacco (*Nicotiana tabacum* cv Burley 21) during the early stages of alkaloid biosynthesis. Plant Sci. 158: 19-32.
- Waterman, P.M. 1998. Chemical taxonomy of alkaloids. In: Alkaloids: Biochemistry, Ecology and Medicinal Applications. Roberts, M.F., Wink, M. eds. Plenum Press, New York, pp. 87-107.
- Watson, M.B., Yu, W., Galloway, G., Malmberg, R.L. 1997. Isolation and characterization of a second arginine decarboxylase cDNA from Arabidopsis (Accession No. AF009647 (PGR97-114)). Plant Physiol. 114: 1569.
- Weeks, W.W., Bush, L.P. 1974. Alkaloid changes in tobacco seeds during germination. Plant Physiol. 53: 73-75.
- Wildon, D.C., Thain, J.F., Minchin, P.E.H., Gubb, I.R., Reilly, A.J., Skipper, Y.D., Doherty, H.M., O'Donell, P.J., Bowles, D.J. 1992. Electrical signaling and systemic proteinase inhibitor induction in the wounded plant. Nature 360: 62-65.
- Wink, M. 1998. Modes of action of alkaloids. In: Alkaloids. M.F. Roberts and M. Wink, eds, Plenum Press, New York, pp. 301-326.
- Wolf, F.A., Bates, W.W. 1964. Extent of tobacco root development as related to nicotine content of the plants parts. Tobacco Science 12: 226-228.
- Yasumatsu, N. 1967. Studies on the chemical regulation of alkaloid biosynthesis in tobacco plants II. Inhibition of alkaloid biosynthesis by exogenous auxins. Agr. Biol. Chem. 81: 1441-1447.

## Chapter III. MATERIALS AND METHODS

### III.1 Root tissue preparation for FDD screen and Northern, QRT-PCR and HPLC analyses

Tobacco seeds from three near isogenic lines that were derived from introgressing the *a* and *b* mutations into the Burley 21 background (*Nicotiana tabacum* cv Burley 21, *AABB*; HI21, *AAbb*; LI21, *aaBB*; and LA21, *aabb*) were obtained from the USDA Tobacco Germplasm Stock Center, UNCS, Raleigh, NC. Seeds were surface sterilized with 10 ml 50% sodium hypochlorite and 0.05% Tween-20 solution and grown in continuous light at room temperature in 0.5X Gamborg's auxin-free B-5 media (GIBCO-BRL, Grand Island, NY; Gamborg et al. 1968) containing 1.5% sucrose and 0.2% phytoagar (Gibco-BRL, Grand Island, NY). After 14 days of growth, the cotyledons and hypocotyls were removed and sterile roots transferred to 250 ml flasks containing 50 ml of HF media (Mano et al. 1989) with 3% (w/v) sucrose, 0.0001% (w/v) thiamine, (SIGMA, St. Louis, MO) and 3  $\mu$ M indolebutyric acid (IBA) (Gibco-BRL, Grand Island, NY). The flasks were wrapped in aluminum foil to reduce light and the root cultures were grown at room temperature in the dark, on a rotary shaker at 90 rpm, for 12-14 days. Induction of root cultures for alkaloid biosynthesis by removal of auxin was performed as follows. Roots were rinsed three times in HF media lacking IBA and then incubated for 1-8 hours at room temperature in 50 ml IBA-free HF media with shaking at 90 rpm. Control root cultures (i.e., not induced for alkaloid synthesis) were rinsed with IBA-free HF media (as above), but were incubated 1-8 hours in 50 ml HF media with 3  $\mu$ M IBA. The root material was harvested by blotting the roots dry with Kimwipes® tissues (Kimberly-Clark, Roswell, GA), cutting the root mass into 0.5 cm pieces, and immediately freezing the tissue in 50 ml polypropylene sterile centrifuge tubes (Fisher Scientific, Pittsburgh, PA) in liquid nitrogen, then storing at -80°C. Frozen root tissue was subsequently ground to a powder using a mortar and pestle cooled with liquid nitrogen and subsequently stored at -80°C. For tissue samples used to isolate total RNA for Northern, QRT-PCR and HPLC analyses, the root cultures were grown for 12 days as described above, and induced for eight hours in IBA-free HF media, in order to increase nicotine synthesis and measurable steady-state mRNA levels in response to induction treatment.

### III.2 mRNA isolation for FDD screen and Northern and QRT RT-PCR analyses

Total RNA was extracted from ground tissue using either TRI reagent (Sigma-Aldrich, Inc., St. Louis, MO) or a modified phenol/chloroform isolation method (Ausubel et al. 2002). The phenol/chloroform extraction procedure was modified by (1) using 1/3 volumes (of root tissue and reagents), (2) omitting heating the homogenized root tissue/grinding buffer/phenol/chloroform mixture at 50°C, and (3) combining the selective precipitation of RNA by LiCl with ethanol precipitation as follows. After the final extraction of the aqueous nucleic acid phase with chloroform, the aqueous phase was brought to a concentration of 2 M LiCl, then combined with 2.5 volumes 100% ethanol, and incubated overnight at -20°C. The pellet was collected by centrifugation for 20 minutes at 10,000 rpm, rinsed with five ml of 2 M LiCl and resuspended in 1 ml DEPC-treated water. The RNA/DNA was then reprecipitated by adding 0.1 ml 3 M sodium acetate, pH 5.8 and 2.25 ml 100% ethanol for 20 minutes at -80°C and centrifuging for 15 minutes at 10,000 rpm. The RNA pellet was rinsed in 5 ml 70% ethanol, dried under vacuum and stored at room temperature or resuspended in DEPC-treated water to a concentration of approximately 1 µg/µl (determined by measuring absorbance at 260 nm with extinction coefficient (E) = 0.025 (µg/ml)<sup>-1</sup>cm<sup>-1</sup> and stored at -20°C. Table 1 shows genotypes, induction period, and RNA isolation procedure used for each lot of total RNA.

**TABLE 3.1: DESCRIPTION OF ROOT CULTURE LOTS AND RESULTING TOTAL RNA ISOLATION**

Lot #	Root culture growth period	Genotypes	Induction period	RNA isolation method	Application
6	14 days	<b>AABB, aabb</b>	1 hour	Phe/chl	FDD screen
8	14 days	<i>AABB, aabb</i>	1 hour	TRI reagent	FDD screen
13	12 days	<i>AABB, aabb</i>	8 hours	Phe/chl	QRT RT-PCR
15	12 days	<i>AABB, AAbb, aaBB, aabb</i>	8 hours	Phe/chl	Northern blots, QRT RT-PCR, HPLC
16	12 days	<i>AAbb, aaBB, aabb</i>	8 hours	Phe/chl	QRT RT-PCR
18	12 days	<i>AABB, AAbb, aaBB, aabb</i>	8 hours	Phe/chl	Northern blots, QRT RT-PCR

### III.3 FDD screen to isolate gene fragments coordinately regulated by the A/B loci.

The FDD procedure (Uchida et al., 1998 and Kuno et al., 2000) used in this study was performed in Professor Masaki Furuya's laboratory at Hitachi Advanced Research Laboratories (Saitama, Japan) as part of a collaboration with the Jelesko laboratory at Virginia Tech. The procedure was modified from the original FDD procedure (Ito et al. 1994). Two lots (Lot 6 and Lot 8) of *N. tabacum* cv B21 (induced and uninduced) and LA21 RNA (induced and uninduced) isolated from root tissue cultures were subjected to FDD analysis as follows.

#### III.3.1 FDD reactions: cDNA synthesis and PCR amplification

Total RNA (25 µg) from each sample (B21 induced and noninduced, LA21 induced and noninduced) was DNase-treated with 2 units of RQ1 DNase in 1X DNase buffer (Promega, Madison, WI) and 5 units of RNasin (Promega, Madison, WI) in a 50 µl reaction volume for 60 minutes. The reaction was diluted to 100 µl with DEPC-treated water, extracted with an equal volume 25:24:1 (v/v/v) phenol/chloroform/isoamyl alcohol, precipitated with ethanol and resuspended in DEPC-treated water to a concentration of approximately 1 µg/µl. The concentration of the resulting RNA solution was determined spectrophotometrically by measuring absorbance at 260 nm with  $E = 0.025 (\mu\text{g/ml})^{-1}\text{cm}^{-1}$ . First-strand cDNA was synthesized from 2.5 µg total RNA with 50 pmol TexasRed-labeled 5'-dG(dT)<sub>15</sub>dC primer and Superscript II First-Strand Synthesis System (Gibco BRL, Rockville, MD) reaction components in a 20 µl volume: 2.5 units Superscript II reverse transcriptase, 0.5 mM deoxynucleoside triphosphates (dNTPs), 10 mM dithiothreitol (DTT), and 0.4 units RNasin, in 1X RT buffer. The RT reaction conditions were as follows: 25°C, 10 min; 42°C, 50 min; 70°C, 15 min. The resulting first-strand cDNA solution was diluted with water by 10 fold to 200 µl, and 2 µl of the diluted cDNA solution were amplified by PCR in a 96-well thermal cycler (GeneAmp PCR System 9600, Perkin Elmer, Norwalk, CT), using a mixture (in a 20 µl volume of 1X Gene *Taq* buffer) of 1 nmol of dNTPs, 5 pmol Texas Red-labeled 5'-dG(dT)<sub>15</sub>dC primer and 10 pmol of an arbitrary 10-mer primer (kits A:1-20, B:1-20, D:1-20, F:1-20, X:1-20, Y:1-20, and Z:1-20; Operon Technologies, Alameda, CA), and 0.5 units Gene *Taq* polymerase (Nippon Gene, Japan) and 0.5 units Ampli-*Taq* polymerase (Perkin-Elmer Applied Biosystems, Foster City, CA). This combination of Gene *Taq* and Ampli-*Taq* polymerases facilitated the amplification of a range of sizes of PCR products. The PCR reactions were overlaid with a drop of mineral oil, mixed by

shaking, and spun down by centrifuging one minute at 6,000 rpm. The thermocycling conditions were: one cycle of 94°C, 3 min; 40°C, 5 min; and 72°C, 5 min; then 24 cycles of 94°C, 15 sec, 40°C, 2 min; 72°C, 1 min; and a final extension at 72°C, 5 min.

### III.3.2 FDD screening: gel analysis and band excision

A portion (15 µl) of the PCR products was mixed with an equal volume of 2X loading dye contained in the Thermo Sequenase Primer Cycle Sequencing Kit (Amersham Bioscience). and 4.5 µl of the PCR reaction/dye mixture was transferred to a 96-well PCR plate and evaporated at 60°C for 25 min to approximately 2.0 µl. A 27 cm 6% Long Ranger gel (FMC BioProducts, Rockland, ME) containing 6.1 M urea and 1.2X TBE (0.11 M Tris-HCl, pH 8.3; 0.11 M boric acid, and 2.4 mM EDTA) was pre-run at 600 V for 30 min at 40°C in 0.6X TBE. Samples were loaded onto the pre-run gel and run at 800 V for 4 hours. Loading dye was added to empty wells to maintain a uniform ionic strength and even band front across the gel. The labeled PCR fragments were visualized by an automated SQ-5500 DNA sequencer (Hitachi Ltd., Tokyo, Japan). Scanned images were saved as FM data files and converted to TIF files with FRAGLIS software. The TIF files were opened in Adobe Photoshop 6.0 with a resolution of 200 pixels/inch and transformed to a canvas size of 25 cm x 35 cm. The image brightness, saturation and contrast levels were adjusted to optimize detection of differentially expressed band patterns and the images were printed on A3 paper.

### III.3.3 FDD screening: band excision from preparative gel

The FDD gel images were visually scored for relative band intensity, and target bands (representing FDD fragments with the desired differential expression pattern) were separated on longer preparative gels. Eight µl of the original PCR/dye mixture (from both induced and noninduced samples) were evaporated at 60°C for 60 min to approximately 4.0 µl. The samples were denatured at 80°C for 5 min, loaded on a 37 cm 5.5% acrylamide/7 M urea/1.2X TBE gel (pre-run 60 min at 1000V) and run at 1400 V. Induced and non-induced samples were loaded on preparative gels to both confirm differential expression and isolate target bands. After 6 hours, the bands representing PCR fragments less than 520 bp were well-separated; after 10 hours, bands of 520-620 bp were well-separated; and after 11 hours, bands larger than 620 bp were well-separated. The bands showing desired differential expression were prioritized for cloning

according to the size of bands, differential pattern reproducibility, and intensity of differential expression. After removing the notched glass plate on top of the gel, the preparative gels were scanned using an FMBIO 100 fluorescent image analyzer (TaKaRa Schuzo, Tokyo, Japan). Target bands of induced samples were excised from the gel with a razor blade by overlaying the glass plate with the gel (gel side up) on a transparency film printed with the actual size fluorescent image of the scanned gel. The gel was rescanned following band excision to verify that the target bands were removed.

#### III.3.4 FDD screening: band confirmation

The size of the reamplified gel excised PCR product and original FDD reaction products were compared on a 6% Long Ranger gel as described below. The excised gel slice was suspended in 50  $\mu$ l of water and heated 10 min at 90°C with intermittent vortexing to elute the FDD fragments. The FDD fragments were reamplified from one  $\mu$ l of eluted gel solution in a final PCR reaction volume of 50  $\mu$ l (PCR conditions were as described for FDD reactions in III.3.2). Five  $\mu$ l of the reamplified PCR product were diluted 10-fold with water to 50  $\mu$ l and 2  $\mu$ l of the diluted reamplification product was combined with an equal volume of loading dye. Sample evaporation and gel running conditions were as described in III.3.2. The reamplification products were loaded in adjacent lanes to the original FDD reaction products and the sizes of reamplified bands were compared to the original FDD bands. If at least one reamplified band matched the original FDD band, the eluted band solution used to reamplify the band was reserved for cloning and the remaining 45  $\mu$ l of undiluted PCR reamplification product was reserved to screen subcloned FDD fragments by DNA fingerprinting analysis (see III.3.7 below).

#### III.3.5 FDD: cloning

To clone target FDD fragments, 1  $\mu$ l of eluted band solution (generated as described in III.3.4) was PCR amplified with 15 pmol *EcoRI* linker primer 5'-GAATTC(T)<sub>15</sub>C and 15 pmol of the original arbitrary primer in a 50  $\mu$ l reaction volume. The *EcoRI* linker primer provided a more efficient template for TA cloning, because *Taq* polymerase is most efficient at adding a non-template 3'A next to a C. PCR conditions were as described in III.3.1 for FDD reactions. The PCR product was diluted with water to a volume of 100  $\mu$ l, then extracted with an equal volume phenol/chloroform/isoamyl alcohol and precipitated with 0.1 volume 3 M sodium acetate and

2.25 volumes 100% ethanol. The dried pellet was resuspended in 5  $\mu$ l of water. TA cloning was performed according to the Promega Technical Manual for pGEM-T and pGEM-T Easy Vector Systems (Promega Corp., Madison, WI) as follows. One  $\mu$ l of the resuspended PCR product was ligated to 0.5  $\mu$ l (50 ng) of the pGEM-T vector (Promega Corp., Madison, WI) in a 10  $\mu$ l reaction volume containing 3 units T4 DNA Ligase and 1X Rapid Ligation Buffer (Promega Corp., Madison, WI), at 4°C overnight. Five  $\mu$ l of the ligation reaction was used to transform 50  $\mu$ l XL1Blue (Stratagene) high efficiency chemically competent cells, which were then plated on LB plates containing 50  $\mu$ g/ml ampicillin (AMP), 0.5 mM isopropyl-1-thio- $\beta$ -D-galactoside (IPTG), and 80  $\mu$ g/ml 5-bromo-4-chloro-3-indolyl- $\beta$ -D-galactoside (X-Gal). Twelve white colonies from each plate were inoculated into 100  $\mu$ l Luria Bertani broth (LB) with 50  $\mu$ g/ml AMP in a covered sterile 96-well plate and incubated with shaking at 250 rpm at 37°C.

#### III.3.6 Preliminary screen of FDD clones by agarose gel electrophoresis

After 4-5 hours of growth, 1  $\mu$ l of cells from each colony were used for PCR amplification with 1 pmol M13 Forward (F) and 1 pmol M13 Reverse (R) primer in a 20  $\mu$ l reaction volume. PCR conditions were as described in III.3.1 for FDD reactions. The size of the PCR products (including 236 bp with multiple cloning site DNA sequences, added to the insert by using F and R primers) was checked on a 1.5% agarose gel in 1X TAE buffer (40 mM Tris-acetate, pH 8.5 and 2 mM EDTA) and clones with approximately the correct size insert (after correcting for the 236 added bp) were selected for further analysis. The remaining 99  $\mu$ l of cells were grown for 16 hours and stored in 15% glycerol at -80°C.

#### III.3.7 Fingerprinting analysis of FDD clones

Since some FDD clones may contain inserts consisting of non-target contaminating PCR products (present in the excised gel slice) that were fortuitously the same size as the differentially expressed target PCR product, a restriction enzyme fingerprinting procedure to distinguish plasmids with target FDD fragments from plasmids containing identical-size cloned PCR products that are not the differentially expressed genes was performed. Frequent cutter restriction enzyme digests of PCR products derived from cloned FDD fragments were compared to the similarly digested original FDD reaction products. Restriction digest band patterns from

cloned FDD fragments most closely resembling the restricted original FDD reaction product were selected for further analysis. This is explained in more detail below.

To regenerate the original FDD fragment insert from the FDD clones, 0.5 µl of the PCR product amplified with F and R primers from cloned FDD fragments (generated as described in III.3.6) was reamplified with 3.8 pmol Texas Red-labeled 5'-G(T)<sub>15</sub>C primer and 2.5 pmol of the arbitrary primer used in the original FDD reactions, in a 50 µl reaction volume. The size of the cloned insert was compared to the original FDD reaction products by running 2 µl of the reamplified PCR product (containing the regenerated FDD fragment insert) and the original FDD reaction products on a 6% Long Ranger gel (sample preparation and gel running conditions as described in III.3.2). FDD clones that contained inserts the same size as the original FDD reaction products were further analyzed by restriction enzyme fingerprinting. For the restriction enzyme digest, the remaining 48 µl of the reamplified FDD fragment (derived from FDD clones) and the remaining 45 µl of the reamplified PCR product of the original gel-eluted FDD fragment (generated as described in III.3.3.) were precipitated with 0.1 volume 3 M sodium acetate and 2.25 volumes 100% ethanol, and the dried pellets were resuspended in 10 µl of water. Restriction enzyme digests of the PCR products were performed by combining 8 µl of template with 5 units of *Hae*III and 5 units of *Msp*I in 1X reaction buffer in a 10 µl total reaction volume for one hour at 37°C. Four µl of the restriction enzyme digest reactions were combined with equal volumes of loading dye and the band patterns were visualized on 6% Long Ranger gels (as per III.3.2). Banding patterns resulting from restriction digests of the reamplified excised FDD bands were complicated by contaminating (non-target) FDD fragments present in the gel slice, so a comparison of restriction digest pattern of original FDD fragments and FDD clones containing inserts did not show identical patterns. Therefore, FDD clones that produced restriction digest band patterns (i.e. major bands) most similar to the reamplified excised FDD bands were sequenced.

### III.3.8 Sequencing of FDD clones

Plasmid containing cloned FDD fragments was isolated using a QIAprep® Spin Mini-prep kit (Qiagen, Valencia, CA). Consensus sequence information was obtained for cloned FDD fragments longer than 300 bp by mutagenizing these clones with Mu transposon using the GeneJumper™ Primer Insertion Kit (Invitrogen, Carlsbad, CA), in order to introduce additional

primer binding sites for sequencing. Cloned FDD fragments were sequenced in both directions with 3.2 pmol M13 Forward and M13 Reverse primers and *Mu* end primer (for cloned FDD fragments longer than 300 bp) using automated cycle sequencing with Big Dye Terminator™ v 3.0 chemistry (P-E Applied Biosystems, Foster City, CA) on ABI 377 or 3100 sequencing machines (P-E Applied Biosystems, Foster City, CA) by the Virginia Tech DNA Sequencing Facility. Lasergene SeqMan software was used to analyze sequence information and generate contigs. Nucleotide and deduced protein sequence homology was determined using the BLAST-N and BLAST-X programs that utilized non-redundant Genbank databases (NCBI).

#### III.4 Northern blot analysis

To confirm differential expression during conditions inducing alkaloid biosynthesis, Northern blots of known nicotine biosynthetic genes and of FDD gene fragments were performed using total RNA from cultured root tissue induced for alkaloid biosynthesis and chemiluminescent deoxyuridine triphosphate-dioxygenin (DIG)-labeled probes.

##### III.4.1 DIG probe synthesis

Primers for DIG probe synthesis were originally designed for QRT-PCR analysis, using Lasergene PrimerSelect software, based on sequence information of inserts of FDD clones (generated as described in III.3.5) and known cDNA sequences of nicotine biosynthetic genes: *ODC3* (D89984), *ADC1* (AF127239), *QPRT* (AJ243437) and *PMT3* (AF126811) and constitutive gene *β-ATPase* (U96496). Sequence information used to design primers, primer sequences, annealing temperatures for DIG-probe synthesis and QRT-PCR (III.5.3), and location and length of the PCR product are described in Tables 2-5. Plasmid template for the DIG-labeling PCR reactions was isolated using a QIAprep® Spin Mini-prep kit (Qiagen, Valencia, CA). PCR-based probe synthesis using dioxygenin-dUTP was performed with 1 µl plasmid template DNA, 0.5 µM each primer, 0.2 mM dNTP's, 0.033 mM DIG-dUTP (Roche Molecular Biochemicals), and 0.5 mM MgCl<sub>2</sub> in a 50 µl reaction volume (as described in the Boehringer-Mannheim Genius manual, p. 55). Thermocycling conditions were as follows: one cycle of 94°C, 2 min; then 40 cycles of 94°C, 45 sec; 47°C, 1 min.; 72°C, 90 sec; and a final extension at 72°C, 7 min.

TABLE 3.2. REED-GENERATED FDD CLONES

GENE	UPSTREAM SEQUENCE	DOWNSTREAM SEQUENCE	PROBE SIZE	SOURCE
Tumor-related protein (y2-6)	5'GCCGCATCCTGGAAACTCTA (oDGR21)	5'CTGCTCCATATAACCTCCTCATTG (oDGR22)	408 bp	pDGR33
Glucosyltransferase (a11-7)	5'CAATCGCCGTCAGAGCACACT (oDGR38)	5'TATGGCATCAGGAAAGGGAAAGAC (oDGR39)	394 bp	pDGR1
Anionic peroxidase (y18a-9)	5'ATCGGCATGCATCTTCTCTG (oDGR19)	5'GCCGCTCTTGCATCTCTTC (oDGR20)	363 bp	pDGR38

TABLE 3.3. JELESKO-GENERATED FDD CLONES

GENE	UPSTREAM SEQUENCE	DOWNSTREAM SEQUENCE	Probe Size	SOURCE
Subtilisin protease	5'CATGGCCCGGGATTCAAAC (oDGR58)	5'GGTCACTCGGTATGTCAACTTCTG (oDGR59)	143 bp	pJGJ331
Purine permease	5' TCAGACAAAACAAAGAAGCAGAAGA (oWGH1)	5'TGAAAGTAGCAATGAAAAGGAAAAC (oWGH2)	162 bp	pJGJ332
Lipoxygenase	5'GATTGGGGGACTCACAG (oDGR56)	5'GATTTGGGGGACTCACAG (oDGR57)	211 bp	pJGJ334

TABLE 3.4. NICOTINE BIOSYNTHETIC GENES

GENE	UPSTREAM SEQUENCE (PRIMER LOCATION)	DOWNSTREAM SEQUENCE (PRIMER LOCATION)	PROBE SIZE	SOURCE: GENBANK ACCESSION #
<i>QPRT</i>	5'GGCACGAGAGCTCCCAAAAAC (oDGR36)  outside coding region	5'CCGCGAATATCATCTCAGCAAGTG (oDGR37)  inside coding region	376 bp	AJ243437  (Sinclair 2000)
<i>ADC1</i>	5' CTCGGCCTCGGCGGGTTTTA (oDGR50)  outside coding region	5' CGGCGGCGGAGTTTGTAGGAG (oDGR51)  inside coding region	265 bp	AF127239  (Wang and Timko, 1999, unpublished)
<i>PMT3</i>	5' GTAAAGCCGCACAAGCAGGATA (oDGR40)  inside coding region	5' GTAAAGCCGCACAAGCAGGATA (oDGR41)  inside coding region	413 bp	AF126811  (Reichers and Timko, 2000)
<i>ODC3</i>	5' GTAAAGCCGCACAAGCAGGATA (oDGR48)  inside coding region	5' GTAAAGCCGCACAAGCAGGATA (oDGR49)  inside coding region	449 bp	D89984  (Imanishi et al. 1998)

TABLE 3.5. CONTROL PRIMERS (primers designed by Reichers and Timko, 1999)

CONSTITUTIVE GENE	UPSTREAM SEQUENCE (PRIMER LOCATION)	DOWNSTREAM SEQUENCE (PRIMER LOCATION)	PROBE SIZE	SOURCE: GENBANK ACCESSION #
<i>β-ATPase</i>  (control)	5' GTATATGGTCAAATGAATGAGCC (5')  inside coding region	5' GGATCGACAGCAGGATAGATACC (3' INT)  inside coding region	400 bp	U96496  (Boutry and Chua 1985; Lalanne et al. 1998)

### III.4.2 Northern blot analysis

Formaldehyde agarose gel and RNA sample preparation was performed according to Gerard and Miller (1986). Total RNA (isolated as described in III.2) from Lots 15 and 18 of B21 and LA21 root tissue was used for Northern blot analysis of known alkaloid biosynthetic genes and of FDD gene fragments. Twenty  $\mu\text{g}$  of each RNA sample (B21 induced, B21 uninduced, LA21 induced, LA21 uninduced) was dried under vacuum and resuspended in 2  $\mu\text{l}$  10X 3-(N-morpholino) propanesulfonic acid (MOPS) buffer (0.2 M MOPS, pH 7.0, 5 mM sodium acetate, 10 mM EDTA, pH 8.0), 3.5  $\mu\text{l}$  37% formaldehyde, 10  $\mu\text{l}$  deionized formamide, 0.5 mg/ml ethidium bromide and 2  $\mu\text{l}$  loading buffer (50% glycerol, 1 mM EDTA, 0.4% bromophenol blue, 0.4% xylene cyanol). The samples were denatured at 68°C for 10 minutes and loaded on a 1% agarose formaldehyde gel. The gel was run in 1X MOPS buffer at 60 V for three hours, soaked in water to remove formaldehyde, and photographed by illumination with UV light using a BioRad Gel Doc 2K Transilluminating System for MAC (RS-170) running TDS Quantity One software (BioRad, Hercules, CA). The RNA was transferred and UV cross-linked to a 0.45  $\mu\text{m}$  Magnacharge positively charged nylon membrane (Osmonics, Inc., Westborough, MA) in 25 mM sodium phosphate buffer, pH 6.5, and the gel was re-photographed to confirm RNA transfer. Hybridization of DIG-labeled probes to the membrane blots was performed using a procedure by Dr. Winkel-Shirley's laboratory at Virginia Tech (<http://main.biol.vt.edu/Department/faculty/Winkel/southern.htm>). Membrane blots were pre-hybridized in 15 ml Church buffer (Church and Gilbert, 1984), consisting of 1 % BSA fraction 5; 1 mM EDTA, pH 8; 0.5 M NaHPO<sub>4</sub>, pH 7.2; and 7% SDS at 65°C for one hour, then hybridized with 30  $\mu\text{l}$  (approximately 60 ng) denatured probe (generated as described in III.4.1) in 15 ml fresh Church buffer at 65°C overnight. The membranes were rinsed twice for 20 minutes in 200 ml pre-heated (to 65°C) Wash/SDS buffer (1 mM EDTA, pH 8; 40 mM NaHPO<sub>4</sub>, pH 7.2; 1% SDS), with shaking at 75 rpm and then rinsed in 500 ml Wash buffer (1 mM EDTA, pH 8; 40 mM NaHPO<sub>4</sub>, pH 7.2) at room temperature. Membranes were equilibrated in Na-maleate buffer (100 mM maleic acid; 150 mM NaCl, pH 7.5) at room temperature for one minute prior to blocking in 1% w/v blocking reagent in Na-maleate buffer (Roche Molecular Biochemicals, Indianapolis, IN) for 30 minutes at RT. To perform chemiluminescent detection of DIG-labeled probes, membranes were incubated for 30 minutes in 50 ml blocking solution with anti-DIG antibody (Roche Molecular Biochemicals) diluted 1:15,000 (to 50 mU/ml), then washed twice

with 100 ml Na-maleate wash buffer (Roche Molecular Biochemicals) with 3% Tween 20 (v/v). The membranes were equilibrated five minutes in 20 ml detection buffer (100 mM Tris, pH 9.5; 150 mM NaCl) which was replaced with 10 ml detection buffer containing 100  $\mu$ l of ready-to-use CDP-Star (Roche Molecular Biochemicals). The membranes were enclosed in clear polypropylene sheet protectors (C-Line Products, Inc., Mt. Prospect, IL) and exposure of BioMax MR film (Kodak, Rochester, NY) to membranes was performed for various time intervals to optimize image quality. Following hybridization and detection of FDD gene and nicotine biosynthetic gene probes, the membranes were stripped by twice incubating membranes in a stripping solution composed of 50% formamide, 5% SDS, and 50 mM Tris-HCl, pH 7.5, at 80°C for one hour (as described in the Boehringer-Mannheim Genius manual, p. 31).  *$\beta$ -ATPase* is expressed constitutively, and stripped membranes were re-hybridized (using the same hybridization conditions as described above) with DIG-labeled  *$\beta$ -ATPase* probe, in order to provide a loading control.

### III.5 Quantitative Real Time Polymerase Chain Reaction (QRT-PCR) analysis

The Applied Biosystems ABI Prism 7700 Sequence Detection System (Applied Biosystems, Perkin-Elmer) consists of a PCR machine, fluorescence detector, and detection and analysis software. This technology allows PCR product quantification after each extension step of a PCR cycle, by measuring increased fluorescence associated with the incorporation of an intercalating fluorescent dye, SYBER Green I, into double stranded (ds) PCR products. The number of PCR cycles required for the fluorescence associated with SYBER Green I-labeled ds PCR products to first increase above background is termed the threshold cycle ( $C_T$ ), and is inversely proportional to the initial template concentration. Since ds DNA artifacts of PCR, including primer dimers, can contribute to increased fluorescence and a shifted  $C_T$ , non-specific PCR products are detected by performing a melt-curve analysis to discriminate between different sequences of ds DNA. Melt curves are generated by raising the temperature of the PCR product from RT to 95°C to separate ds DNA, while measuring the fluorescence decrease (as SYBER Green I is released) every 0.2°C. Since the melting temperature of ds DNA is dependent on its GC content and length, the rate at which the fluorescence (F) decreases with temperature (T), plotted as  $-dF/dT$  vs. T, is a function of the sequence and length of the PCR products. In this study, differential expression and absolute levels of cDNA of nicotine biosynthetic genes and genes represented by

FDD clones were quantified by QRT-PCR with the ABI Prism 7700 Sequence Detection System and Sequence Detector v. 1.7a software (P-E Applied Biosystems). The production of a single target PCR product was confirmed by melt curve analysis using Dissociation Curves v. 1.0 software (P-E Applied Biosystems).

### III.5.1 cDNA synthesis by RT

Lots 13, 15, 16, and 18 of total RNA extracted from induced and noninduced B21, HI21, LI21 and LA21 root tissue (Table 3.1) were used to synthesize cDNA for QRT-PCR analysis. Total RNA 2(5 µg) from each sample was DNase-treated as described in III.3.1, extracted with phenol/chloroform, precipitated with 0.1 volume 3 M sodium acetate and 2.25 volumes 100% ethanol, and resuspended in DEPC-treated water to a concentration of 1 µg/µl, based on spectrophotometric determination at 260 nm ( $E = 0.025 (\mu\text{g/ml})^{-1}\text{cm}^{-1}$ ). First-strand cDNA was synthesized using the Omniscript Reverse Transcriptase kit (Qiagen, Valencia, CA). Two µg total RNA was reverse-transcribed in a 20 µl reaction volume containing 2 mM dNTPs, 1 µM oligo-dT primer, 10 units RNasin (Promega, Madison, WI), 1X Omniscript RT buffer and 4 units Omniscript Reverse Transcriptase. The RT reaction was incubated at 37°C for one hour and the resulting cDNA mixture was stored at -20°C prior to QRT-PCR analysis.

### III.5.2 TA cloning to generate plasmid for standard curves

In order to obtain cloned fragments of alkaloid biosynthetic and  $\beta$ -ATPase genes suitable for standard curves in QRT-PCR reactions, cDNA was subjected to gene-specific PCR and resulting fragments were TA cloned (Table 3.6). The nicotine biosynthetic gene primers (Table 3.4) and  $\beta$ -ATPase gene (Table 3.5) were used to amplify B21 noninduced cDNA (generated in III.5.1) to produce PCR products for TA cloning. PCR thermocycling conditions were: one cycle of 94°C, 2 min; then 30 cycles of 94°C, 45 sec; 50°C, 1 min; 72°C, 90 sec; and a final extension at 72°C, 7 min. PCR products were precipitated with 0.1 volume 3 M sodium acetate and 2.25 volumes 100% ethanol, dried and resuspended in water to a concentration of 1 µg/µl. The PCR products were TA cloned as directed in the Invitrogen TOPO TA Cloning® (Version K2) Manual (Invitrogen Corp., Carlsbad, CA), into pCR®2.1-TOPO® vectors (Invitrogen Corp., Carlsbad, CA) and the resulting plasmids were used to transform *E. coli* TOP10F' One Shot® Chemically Competent cells (Invitrogen Corp., Carlsbad, CA). Transformants containing PCR product

inserts were detected as light blue or white colonies, which were selected for plasmid isolation. Plasmid was isolated with a QIAprep® Spin Mini-prep kit (Qiagen, Valencia, CA) and resuspended in water to a concentration of 1 µg/µl, which was determined spectrophotometrically by measuring absorbance at 260 nm ( $E = 0.02 (\mu\text{g/ml})^{-1} \text{cm}^{-1}$ ). The cloned PCR products were sequenced in both directions as described in III.3.8 and nucleotide sequence homology was determined using the BLAST-N program to confirm plasmid identity. The quantities of plasmid template for QRT-PCR reactions that would provide a  $C_T$  range for a standard curve were determined experimentally. The number of plasmid cDNA equivalents was derived from the quantity (in µg) and size (in bp) of plasmid cDNA used as starting template. A standard curve plotting the log of number of plasmid cDNA equivalents vs.  $C_T$  (average of three replications of identical QRT-PCR reactions for each concentration of plasmid template) was drawn in Excel 2000 (Microsoft Corp., Santa Rosa, CA). The  $C_T$  value (average of 3 replications of identical QRT-PCR reactions for each lot of RNA) for each gene-specific QRT-PCR reaction was used to extrapolate cDNA equivalents of the nicotine biosynthetic genes, FDD genes and constitutive  $\beta$ -ATPase gene from the standard curves.

TABLE 3.6. PLASMID FOR QRT-PCR STANDARD CURVE

NICOTINE BIOSYNTHETIC GENE	PRIMERS	PLASMID FOR STD CURVE	FDD CLONE/ $\beta$ -ATPASE CONTROL	PRIMERS	PLASMID FOR STD CURVE
<i>QPRT</i>	oDGR36,37 (Table 4)	pDGR54	A11-7	oDGR38,39 (Table 2)	pDGR49
<i>ADC1</i>	oDGR50,52 (Table 4)	pDGR55	Y18a-9	oDGR19,20 (Table2)	pDGR53
<i>PMT3</i>	oDGR40,41 (Table 4)	pDGR60	Y2-6	oDGR21,22 (Table2)	pDGR52
<i>ODC3</i>	oDGR48,49 (Table 4)	pDGR58	$\beta$ -ATPase	5', 3'INT (Table 5)	pDGR61

### III.5.3 Quantitative Real-Time PCR

For each gene analyzed, identical QRT-PCR reactions with induced and noninduced cDNA samples from Lots 13, 15, 16 and 18 of B21, HI21, LI21 and LA21 root tissue (prepared in III.5.1) were prepared in triplicate on separate 96-well PCR plates. All the QRT-PCR reactions on a single 96-well PCR plate therefore contained the same gene-specific primers; and, for each induced and uninduced genotype of root tissue (B21, HI21, LI21 and LA21) in Lots 13, 15, 16 and 18, three identical QRT-PCR reactions were performed. Each QRT-PCR reaction contained

2 µl of sample cDNA (generated as described in III.5.1) or known quantities of the standard curve plasmid (generated as described in III.5.2), 0.5 µM concentrations of each primer (Tables 2-5), and 23 µl of Syber Green 1 Master Mix (P-E Applied Biosystems), which was 0.5X the volume recommended in the P-E Applied Biosystems ABI Prism 7700 Sequence Detection System manual. PCR conditions were modified from the P-E Applied Biosystems manual to optimize primer annealing and to perform fluorescence detection at an elevated temperature (a more accurate fluorescence signal was obtained by measuring fluorescence at a temperature high enough to melt the non-specific PCR products without denaturing target PCR products). As a positive control, 2 µl of a genomic DNA preparation (provided by Amanda Mellilo) isolated from B21 leaf tissue was amplified with each gene-specific primer set, and a no-template negative control was also included. Since QRT-PCR is very sensitive to small variations in starting template concentration, a QRT-PCR reaction with *β-ATPase* primers (Table 5) was performed as a constitutive control to ensure that pipetting errors did not contribute to perceived C<sub>T</sub> values for differentially expressed genes. PCR thermocycling conditions were: one cycle of 95°C, 10 min to activate Hot-Start *Taq* DNA polymerase; and 40 cycles of: 95°C, 0.5 min; 55°C, 0.5 min; 72°C, 1 min; and 85°C, 0.5 min (detection).

#### III.5.4 QRT-PCR data analysis

The number of cDNA equivalents for any given gene in each lot of RNA was determined by using the observed C<sub>T</sub> value to extrapolate the cDNA equivalents from the respective cDNA equivalent vs. C<sub>T</sub> value standard curve (described in II.5.2) generated on the same PCR plate. The lot average of cDNA equivalents for each gene was then determined and graphed using Excel 2000 (Microsoft Corp., Santa Rosa CA) plotting the average cDNA equivalents with standard error = [standard deviation (lot average<sub>1</sub>, lot average<sub>n-1</sub>, lot average<sub>n</sub>)]/(n)<sup>-3</sup> versus RNA sample genotype. A statistical analysis was performed in Excel 2000 (Microsoft Corp., Santa Rosa CA) that consisted of a student's t-test to compare cDNA equivalents from induced versus noninduced samples within each genotype to assess genotype inducibility. To determine whether relative levels of cDNA corresponded to expected alkaloid content of each genotype in the order: B21 > HI21 > LI21 > LA21, student's t-tests were used to compare cDNA equivalents from 1. induced B21 samples to induced HI21, LI21, and LA21 samples and 2. non-induced B21 samples to non-induced HI21, LI21, and LA21 samples.

### III.6 HPLC analysis of nicotine content

Nicotine extraction from ground root tissue and quantitation by HPLC were performed according to a modified procedure of Saunders and Blume (1981). To quantify nicotine content in B21, HI21, LI21 and LA21 root tissue, 50 mg of lyophilized Lot 15 root tissue (prepared and ground as described in III.1) was extracted with 10 ml of 25 mM sodium phosphate buffer, pH 7.8 at RT for 24 hours with shaking. Duplicate extractions were performed with addition of 7 mg of an external standard, atropine (Sigma-Aldrich) to lyophilized tissue prior to extraction. The aqueous extract was filtered under reduced pressure through a Whatman No. 2 filter-paper and the undiluted filtrate was re-filtered through a 0.2  $\mu\text{m}$  nylon membrane filter (VWR Scientific Products, West Chester, PA). A portion (100  $\mu\text{l}$ ) of twice-filtered extract was loaded into glass screw-top vials to permit injection of a 20  $\mu\text{l}$  aliquot for HPLC analysis. The HPLC system consisted of a Waters 2690 separations module and Waters 996 photodiode detector. Absorbance was detected at 254 nm. Sample extracts were quantitatively separated on a Waters Resolve C18 90  $\text{\AA}$  5 $\mu\text{m}$  reversed-phase column (3.9 mm x 150 mm) with matrix eluted with an isocratic mobile phase of 40% (v/v) methanol containing 0.2% (v/v) phosphoric acid adjusted to pH 7.25 with triethylamine at a flow rate of 0.5 ml/min. Chromatographic solvents were HPLC grade (Fisher Scientific, Pittsburgh, PA) and were filtered through an 0.45  $\mu\text{m}$  Whatman nylon membrane filter prior to use. To confirm nicotine peak identity, a 50 mg sample of B21 (induced) lyophilized tissue was spiked prior to extraction with 7 mg of nicotine (Sigma Aldrich). Nicotine standards were prepared in 25 mM sodium phosphate buffer, pH 7.8, in a concentration range (0.7  $\mu\text{g}$ , 1.75  $\mu\text{g}$ , 3.5  $\mu\text{g}$ , 5.25  $\mu\text{g}$ , and 7.0  $\mu\text{g}$  nicotine in a 20  $\mu\text{l}$  injection volume). To calibrate HPLC peak area to nicotine content ( $\mu\text{g}$ ), a standard curve of peak area vs.  $\mu\text{g}$  nicotine was generated in Excel 2000. Nicotine content in each tissue sample was extrapolated by referencing sample peak integrations to the standard curve and was reported as % nicotine/dry weight of roots.

### III.7 Bibliography

Ausubel, F.M., Brent, R., Kingston, R.E, Moore, D.D., Seidman, J.G., Smith, J.A., Struhl, K., eds. 2002. Phenol/SDS method for plant RNA preparation. In: Current Protocols in Molecular Biology. John Wiley & Sons, Inc., New York, NY pp. 4.3.1-4.3.3.

Boutry, M. and Chua, N.H. 1985. A nuclear gene encoding the beta subunit of the mitochondrial ATP synthase in *Nicotiana plumbaginifolia*. EMBO J. 4: 2159-2165.

Church GM, and Gilbert W. 1984. Genomic sequencing. Proc. Natl. Acad. Sci USA 81(7):1991-1995.

Gamborg, O.L. et al. 1968. Nutrient requirements of suspension cultures of soybean root cells. Exp. Cell Resarch 50: 151-158.

Gerard, G.F. and Miller, K. 1986. Comparison of glyoxal and formaldehyde gels for sizing rRNAs. Focus 8(3): 5-7.

Imanishi, S., Hashizume, K., Nakakita, M., Kojima, H., Matsubayashi, Y., Hashimoto, T., Sakagami, Y., Yamada, Y. and Nakamura, K. 1998. Differential induction by methyl jasmonate of genes encoding ornithine decarboxylase and other enzymes involved in nicotine biosynthesis in tobacco cell cultures. Plant Mol. Biol. 38 (6): 1101-1111.

Ito, T., Kito, K., Adati, N., Mitsui, Y., Hagiwara, H., Sakai, Y. 1994. Fluorescent differential display: arbitrarily primed RT-PCR fingerprinting on an automated DNA sequencer. FEBS Lett 351: 231-236.

Kuno, N., Muramatsu, T., Hamazato, F. and Furuya, M. 2000. Identification by large-scale screening of phytochrome-regulated genes in etiolated seedlings of *Arabidopsis* using a fluorescent differential display technique. Plant Phys. 122: 15-24.

Lalanne, E., Mathieu, C., Vedel, F., De Paepe, R. 1998. Tissue-specific expression of genes encoding isoforms of the the mitochondrial ATPase  $\beta$  subunit in *Nicotiana sylvestris*. Plant Mol. Biol. 38: 885-888.

IV. Ligations using the pGEM®-T and pGEM®-T Easy Vectors and the 2X Rapid Ligation Buffer. V. Transformations using the pGEM®-T and pGEM®-T Easy Vector ligation reactions. In: Promega Corp. Technical Manual No. 042: pGEM®-T and pGEM®-T Easy Vector Systems Rev. 6/1999.

Mano et al. 1989. Production of alkaloids by hairy root cultures of *Duboisia leinchhardtii* Transformed by *Agrobacterium rhizogenes*. Plant Sci. 59: 19102001

Palmiter, R.D. 1974. Magnesium precipitation of ribonucleoprotein complexes: Expedient techniques for the isolation of ungraded polysomes and messenger ribonucleic acid. Biochemistry 13: 3606.

Riechers, D.E. and Timko, M.P. 1999. Structure and expression of the gene family encoding putrescine N-methyltransferase  $\mu$ l new clues to the evolutionary origin of cultivated tobacco. *Plant Mol. Biol.* 41 (3): 387-401.

Saunders, J.A. and Blume, D.E. 1981. Quantitation of major tobacco alkaloids by high-performance liquid chromatography. *J. Chromatogr.* 205: 147-154.

TOPO TA Cloning®: Five minute cloning of Taq polymerase-amplified PCR products. In: Invitrogen Cop. Instruction Manual No. 000808: TOPO TA Cloning® Version K2.

Uchida, K. Muramatsu, T., Jamet, E., and Furuya, M. 1998. Control of expression of a gene encoding an extensin by phytochrome and a blue light receptor in spores of *Adiantum capillus-veneris* L. *Plant J.* 15(6): 813-819.

## Chapter IV. RESULTS

### IV.1 FDD screening

The *A* and *B* loci in *Nicotiana tabacum* control the majority of nicotine accumulation in tobacco (Legg et al. 1971) and are thought to encode regulatory proteins that coordinate alkaloid biosynthetic enzyme expression (Saunders and Bush 1979, Hibi et al. 1994). The nicotine biosynthetic gene, *PMT*, is coordinately regulated by *A* and/or *B*, and is inducible in the wild-type tobacco cultivar Burley 21 (*AABB*) by removal of auxin from root culture media, but expressed at greatly reduced levels in the low alkaloid mutant LA21 (*aabb*) (Hibi et al. (1994). It is therefore expected that other genes which are coordinately up-regulated by alkaloid-inducing conditions in Burley 21 but not in LA21 are likely to be regulated by *A* and/or *B* and perhaps involved in alkaloid biosynthesis. To find novel genes in the *A/B* regulon, mRNA from root cultures of Burley 21 and LA21 were screened for differential expression using the transcriptional profiling technique, fluorescent differential display (FDD). FDD is particularly well suited for gene discovery because multiple samples can be compared simultaneously for differential expression and a large population of mRNA species can be screened very efficiently.

For FDD analysis, RNA was isolated from Lot 6 and Lot 8 root tissue of Burley 21 (*AABB*) and LA21 mutant (*aabb*) tobacco grown under both alkaloid-inducing and non-inducing conditions for 1 hour. Each RNA sample was reverse transcribed and the resulting cDNA was used as template in FDD using a fluorescent labeled C-anchored oligo(dT) primer and an arbitrary primer. Fluorescent-labeled PCR products (Burley 21, non-induced; Burley 21, induced; LA21, non-induced; and LA21, induced) were separated in adjacent lanes on automated DNA sequencing machines. On average, about 150 bands per FDD reaction were visualized per primer pair. Therefore, the combination of C-anchored oligo(dT) primer with 120 different arbitrary primers sampled as many as 12,000 to 18,000 mRNA transcripts for differential expression, assuming each FDD band was derived from a separate mRNA molecule.

Figure 4.1 shows a typical gel image of FDD fragments from PCR reactions using C-anchored oligo(dT) primer with 10 different arbitrary primers. Constitutively expressed mRNA molecules showed FDD fragments with the same band intensity in all four samples. The majority of

screened FDD bands did not show differential intensity and were therefore constitutively expressed. In contrast, steady state mRNA levels that increased following alkaloid induction were visualized as darker FDD bands in the induced samples relative to identical-size FDD bands in the non-induced samples. Steady state mRNA levels that decreased following alkaloid induction were visualized as lighter FDD bands. Figure 4.1 shows that the Y18 and Y19 arbitrary primers, in combination with the C-anchored oligo(dT) primer, produced FDD bands at about 520 and 530 bp that appeared to show a pattern of differential expression predicted for genes regulated by the *A* and/or *B* loci.

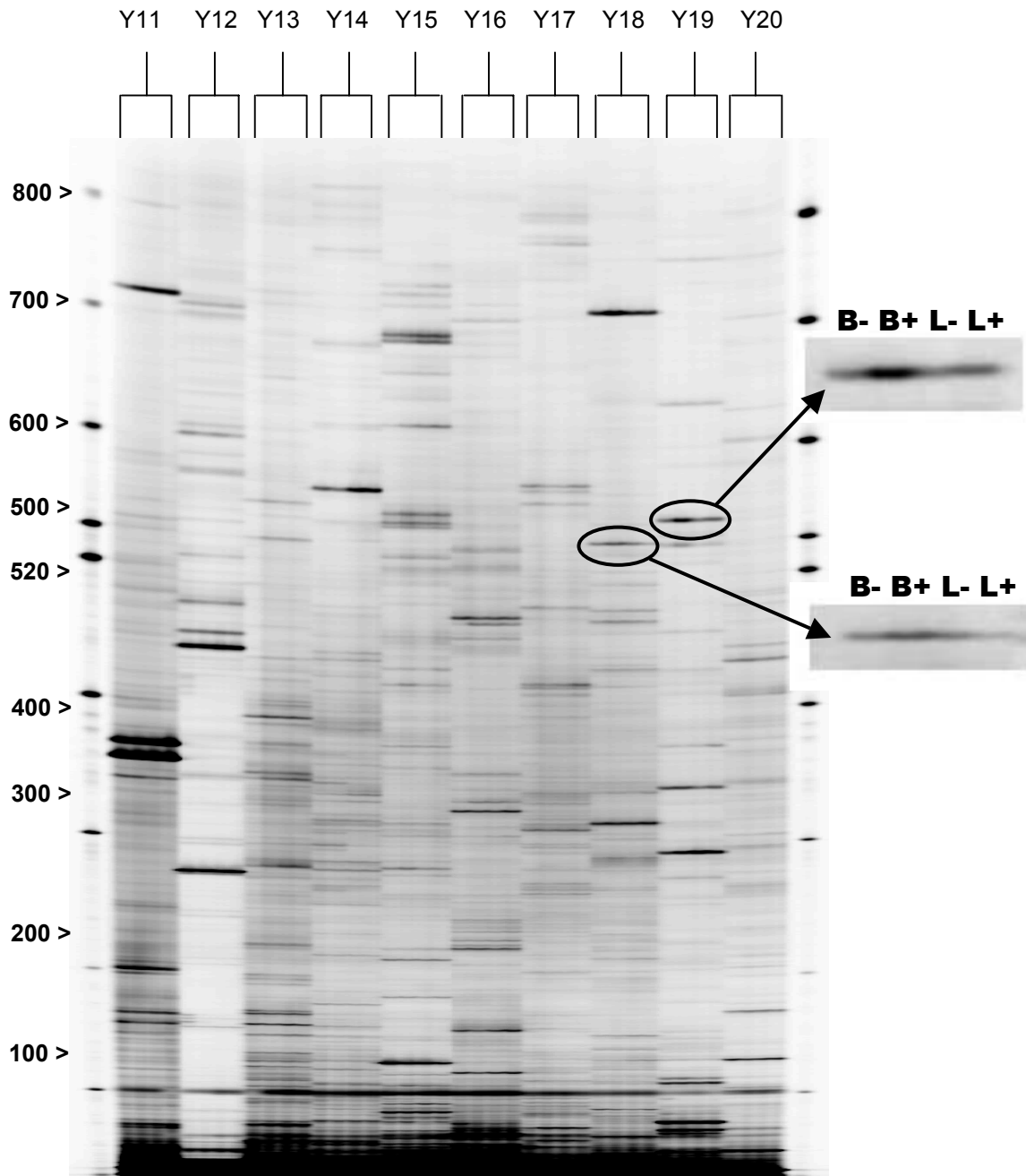


**Figure 4.1. Image of a typical FDD gel .**

Each set of four lanes consists of FDD reactions with different cDNA template: B21 uninduced (B-); B21 induced (B+); LA21 uninduced (L-); LA21 induced (L+). FDD reactions were performed using C-anchored oligo(dT) primer and an arbitrary primer (Y11-Y20). Enlarged views show bands with target differential expression pattern 1 (Figure 2).

Types of differentially expressed band patterns that were observed during FDD screening are shown in cartoon form in Figure 4.2. Pattern 1 was the primary target for FDD band selection because this band pattern corresponds to an expressed gene that is inducible in Burley 21, and either not inducible or weakly inducible in LA21. FDD bands represented by pattern 1 were therefore targeted because they are most likely to correspond to genes regulated by A and/or B, which are known to regulate alkaloid biosynthesis. Lower priority band patterns that were targeted for selection included 2, 3, 4, 5, 6 and 7 (Table 4.1). FDD band patterns 2, 3, 6, and 7 represented complex expression regulation patterns that were potentially related to genotype or alkaloid induction. Genes represented by FDD band pattern 4 are expressed constitutively at higher levels in LA21 and genes represented by FDD band pattern 5 are expressed constitutively at higher levels in Burley 21. These FDD gene fragments do not show differential expression in response to alkaloid-inducing conditions. FDD bands were selected for isolation primarily based on pattern of differential expression, and excised FDD bands were subsequently evaluated for cloning based on the intensity of the band pattern and its reproducibility in a second lot of RNA. Although FDD bands corresponding to all patterns 1-7 (Figure 4.2) were excised, only bands corresponding to patterns 1, 3, 5 and 7 met the criteria for cloning and sequencing. A total of 26 FDD fragment bands that were differentially expressed between Burley 21 and LA21 were excised (Figure 4.2). The majority (20) of the excised bands were classified as pattern 1, with increased FDD band intensity following alkaloid induction in Burley 21 but not in LA21. One representative band of each of the other six patterns (2, 3, 4, 5, 6, and 7) was also excised.

Cultivar/ alkaloid induction treatment <sup>a</sup>					Number of candidate bands <sup>b</sup>	Predicted regulation of B21/ LA21
Pattern of expression	B21 --	B21 +	LA21 --	LA21 +		
1					20	induction/ weak or no induction
2					1	complex
3					1	complex
4					1	non-inducible / increased basal level, non-inducible
5					1	increased basal level, non-inducible/ non-inducible
6					1	complex
7					1	complex

**Figure 4.2. Differentially expressed band patterns observed in FDD screening for A and/or B regulated genes in Burley 21 and LA21 root tissue induced and not induced for alkaloid synthesis.**

<sup>a</sup> Cultivars: Burley 21 (B21) and LA21. Alkaloid induction (+), no alkaloid induction (-). <sup>b</sup>FDD bands selected for excision after screening C-anchored oligo(dT) primer with 120 arbitrary primers.

#### IV.1.1 Cloning of FDD fragments

To clone FDD fragments from target bands, selected band-containing regions were cut from preparative acrylamide gels, the DNA was eluted, and FDD fragments were reamplified with *EcoRI* oligo(dT) linker primer and the original arbitrary primer, ligated into pGEM-T and transformed into *E. coli* XL1 Blue competent cells. As many as 12 bacterial transformants from each excised FDD band were analyzed for the presence of inserts corresponding approximately to the expected size of the excised band. This size analysis was performed by PCR amplification of inserted FDD fragments using M13 forward and reverse primers, and estimating the size of the cloned FDD fragments from the resulting PCR products separated on 1.5% agarose gels. The size of FDD fragments was approximated after subtracting the length of sequence corresponding to the multiple cloning site. A more precise size comparison was then performed on automated sequencing gels with cloned FDD fragment insert that was reamplified using fluorescent-labeled anchored-C oligo(dT) primer and the arbitrary primer used in the original FDD reactions. Several subclones containing appropriately-sized FDD fragment inserts were recovered for each of the excised bands (Table 1).

#### IV.1.2 Confirmation of differentially expressed FDD fragments in FDD clones

FDD clones may have contained inserts consisting of non-target contaminating PCR products (present in the excised gel slice) that were fortuitously the same size as the differentially expressed target PCR product. To distinguish cloned target FDD fragments from identical-size cloned PCR products that are not derived from the differentially expressed genes, a restriction enzyme fingerprinting procedure was performed. FDD fragments from excised bands and from FDD fragment subclones were digested with frequent cutter restriction enzymes *HaeIII* and *MspI* and the resulting restriction digest band patterns (i.e., fingerprints) of the FDD fragments were then compared. Restriction digest band patterns from cloned FDD fragments that most closely resembled the restricted original FDD reaction product were selected for further analysis.

Differences in minor restriction digest band patterns between cloned FDD fragments and excised FDD bands were expected, since excised bands may have contained non-differentially expressed FDD fragments as well as target FDD fragments. Therefore, minor band patterns were ignored when evaluating differences between band patterns and only the major restriction digest band

patterns were compared. A sample gel comparing fingerprints of gel excised FDD fragments with derived FDD transformants is shown in Figure 4.3.

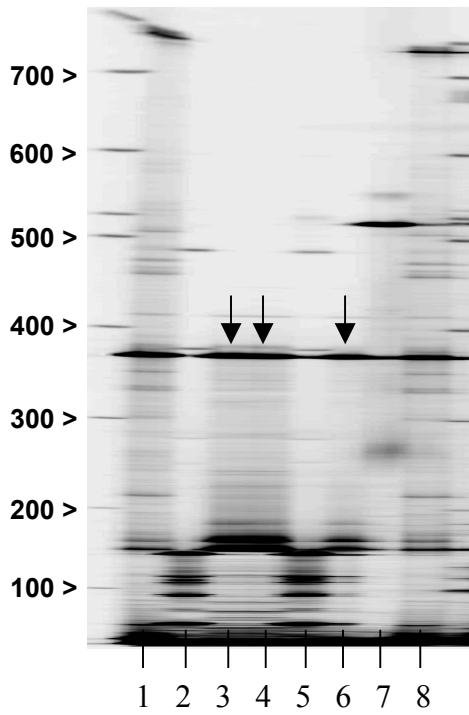


**Figure 4.3. Example of fingerprint comparison of cloned FDD fragments and gel excised FDD fragments.** Cloned FDD fragments and gel excised FDD fragments were digested with *Hae*III and *Msp*I and the major bands were compared to confirm cloned FDD fragment identity. In this example, the 360 bp band is compared. Lanes 1,8: gel excised FDD fragments. Lanes 2-7: cloned FDD fragments. Fingerprints of FDD subclones in lanes 3, 4 and 6 match excised FDD bands, based on comparison of 360 bp band.

### IV.1.3 Sequencing of cloned FDD fragments

After fingerprint analysis to confirm that FDD subclones contained differential FDD fragment inserts, representative subclones were subjected to DNA sequencing. Twenty-six differentially expressed bands were originally excised (Figure 4.2); however, only 12 were finally cloned because many FDD bands were precluded due to either a lack of pattern reproducibility in a duplicate gel or a second RNA lot. Sequenced subclones are listed in Table 4.1.

**Table 4.1. FDD bands cloned and sequenced**

FDD band pattern <sup>a</sup>	arbitrary primer	FDD fragment size (bp)	Number of clones confirmed by fingerprinting	Number and identity of clones sequenced
1	A11	610	2	2 (A11-7, -11)
1	A19	450	10	3 (A19-4, -6, -11)
1	D2	570	4	3 (D2-8, -10, -11)
1	X7	775	3	3 (X7-2, -3, -10)
1	Y2	675	7	2 (Y2a-5, -6)
1	Y18	520	7	3 (Y18a-1, -5, -9)
1	Y18	720	2	2 (Y18-1, -2)
1	Y19	520	8	4 (Y19a-3, -5, -6, -7)
1	Y19	530	8	4 (Y19-8, -9, -10, -11)
3	X4	620	1	3 (x4-3)
5	D15	370	6	5 (D15-2,-6,-7,-9,-11,-12)
7	Y2	750	7	4 (Y2-2,-6,-8,-10)

<sup>a</sup>differential expression patterns described in Figure 4.2

### IV.1.4 Sequences of FDD clones

Several independent subclones corresponding to each target FDD band were sequenced and analyzed for protein homology using a BLASTX search of EMBL/Genbank non-redundant protein databases. Nine cloned FDD fragments selected for sequencing (A11, A19, D2, X7, Y2a, Y18a, Y18, Y19a, and Y19) appeared to be up-regulated in Burley 21 following alkaloid induction (pattern 1, Figure 4.2). FDD fragment X4 appeared to be down-regulated in Burley 21 with higher constitutive levels in LA21 (pattern 3, Figure 4.2). Levels of FDD fragment D15 appeared to be constitutively higher in Burley 21 than in LA21 (pattern 5, Figure 4.2), and FDD fragment Y2 appeared to be down-regulated in Burley 21, but up-regulated in LA21 (pattern 7, Figure 4.2). Consensus sequence information for a representative subclone of each of the 12 cloned FDD fragments is included in Appendix 1. With the exception of D15 subclones, the nucleotide sequences of all subclones of an FDD fragment generated identical BLASTN search

results; therefore, the deduced protein sequence of one representative subclone of each cloned FDD fragment was analyzed using BLASTX to determine protein homology.

#### IV.1.5 Low priority FDD clones

Nucleotide sequence homology information indicated that subclones of eight FDD fragments (A19, D2, D15, X4, X7, Y2a, Y18, Y19a, and Y19) corresponded to a ribosomal RNA (rRNA), a ribosomal protein, or did not show significant BLASTN or BLASTX homology to previously identified genes or proteins (Table 4.2). These FDD gene fragments were determined not to represent structural genes relevant to alkaloid biosynthesis and were therefore not characterized further.

**Table 4.2. BLASTN homology of low priority cloned FDD fragments**

FDD Clone	Fragment Size	Pattern of differential expression <sup>a</sup>	BlastN homology: Accession No.	BlastN score
A19-11 Y19a-3 Y19-9	436 bp 532 bp 551 bp	1 1 1	<b>25S rRNA</b> <i>N. tabacum</i> (GBPLN: 19919613)	0
D15-9	373 bp	5	<b>60S ribosomal protein</b> <i>N. tabacum TSC40-4</i> (GBPLN: 436031)	0
D15-11	375 bp	5	<b>no significant BLASTN or BLASTX homology</b>	> 0.01
X4-3 X7-10 D2-10, Y18-1 Y2a-6	618 bp 787 bp 572 bp 726 bp 688 bp	3 1 1 1 1	<b>mitochondrial 25S rRNA</b> <i>Oenothera berteriana</i> (GBPLN: 13185)	0

<sup>a</sup>differential expression patterns described in Figure 4.2

FDD fragments A19, Y19, and Y19a were amplified from the same anchored-C oligod(T) primer site but different arbitrary primer sites, and corresponded with 98% nucleotide identity to a 25S ribosomal RNA gene in *N. tabacum* (GBPLN: 19919613). FDD fragments D2, X4, X7, and Y2a were amplified from the same anchored-C oligo(dT) primer site and different arbitrary primer sites, and corresponded with 97% to 98% nucleotide identity to the middle region of a gene for mitochondrial 26S rRNA, in *Oenothera berteriana* (GBPLN: 13185). Clone Y18-1 corresponded with 98% identity to the 3' region of the same *O. berteriana* 26S rRNA gene. Clone D15-9

corresponded with 98% nucleotide identity to a gene for 60S ribosomal protein from *N. tabacum* (GBPLN: 436031).

#### IV.1.6 Cloned FDD fragments selected for further investigation

Four FDD subclones (Y18A-9, A11-7, Y2-6, and D15-12) had significant BLASTX homology scores to previously identified proteins (Table 4.3). Alignments of deduced amino acid sequences of FDD subclones to homologous protein sequences are shown in Figures 4.4, 4.5, 4.6, and 4.7.

**Table 4.3. BLASTX homology of cloned FDD fragments**

FDD Clone	Fragment Size	Pattern of differential expression <sup>a</sup>	BLASTX homology: Accession No.	BLAST X score
Y18a-9	529 bp	1	<b>suberization-associated anionic peroxidase</b> <i>Solanum tuberosum</i> (GBPLN: 169554)	2e <sup>-60</sup>
A11-7	623 bp	1	<b>glucosyltransferase-like protein</b> <i>A. thaliana</i> (GBPLN: 5832736)	2e <sup>-87</sup>
D15-12	372 bp	5	<b>disease resistance gene homolog Mi-copy1</b> <i>Lycopersicon esculentum</i> (GBPLN: 3426259)	5e <sup>-11</sup>
Y2-6	763 bp	7	<b>Tobacco tumor-related protein</b> <i>Nicotiana glauca</i> x <i>N. langsdorfii</i> (GBPLN: 454193)	7e <sup>-87</sup>

<sup>a</sup>differential expression patterns described in Figure 4.2

##### IV.1.6.1 FDD clone Y18a-9

Clone Y18a-9 contained an open reading frame (ORF) encoding 176 amino acids with deduced amino acid sequence homology to plant stress and/or wounding inducible peroxidases, including 72% identity and 77% similarity to the middle region of a suberization-associated anionic peroxidase of potato (GBPLN: 169554) (Figure 4.4). Homology to previously identified peroxidases in tobacco was less significant: 56% deduced amino acid sequence identity and 68% similarity to *Nicotiana sylvestris* anionic peroxidase (GBPLN: 170202), and 42% identity and 60% similarity to *N. tabacum* anionic peroxidase (GBPLN: 170299). Two conserved motifs were found in the ORF of clone Y18a-9: a consensus sequence for peroxidases and a highly conserved vacuolar targeting sequence. A peroxidase consensus sequence, [SGATV]-X(3)-[LIVMA]-R-[LIVMA]-X-[FW]-H-X-[SAC] (Kimura and Ikeda-Saito 1988), containing an active site histidine residue, was found from position 52-63 (GASLIRLHFHDC). A vacuolar targeting

sequence, which consists of three hydrophobic amino acids followed by an acidic amino acid (Nakamura and Matsuoka 1993), was found from position 72-75 (VLLD). Due to the use of anchored-C oligo(dT) primers in FDD screening, FDD clones were expected to contain the 3' untranslated region of the mRNAs. However, the position of Y18a-9 in the middle of coding sequence for anionic peroxidase (Figure 4.4) suggests that the oligo(dT) primer bound internally to the mRNA transcript instead of the 3' polyadenylated region so that Y18a-9 was amplified from the middle of the gene.

```

peroxidase      1 SFVALALAGVAIYRNTYEAIIMNNGSLQNASPHFDSLESSGVASILTLNKK--KRNSDMY
Y18a_9_frame2  1 -----VESA-ASILTLNNNNAEQNSDSK

peroxidase      59 LRQQITFEACVFSVAVRGVVDSSAIDAETRMGASLIRLHFHDCFVDGCDGGILLDDTNGTFT
Y18a_9_frame2  23 LTQPLSPSACIFSAVRRVVNRAIDRRRMGASLIRLHFHDCFVDGCDGGVLLDDIPGSEQ

peroxidase     119 GEQNSPPNANSARGYEVIQAQKQSVIDTCPNISVSCADILAIAARDSVAKLGGQTYNVAL
Y18a_9_frame2  83 GEKTSPPNNNSARGFEVIEQAQKQSVKDTCPNTPVSCADILAIAARDSVVKLGGQGYNVAL

peroxidase     179 GRSDARTANFTGALTQLPAPFDNLTVQIQKFNDKNFTLREMVALAGAHTVGFARCTVCT
Y18a_9_frame2  143 GRRDARAANFTGALTQLPAPFDNLTVQI-----

peroxidase     239 SGNVNPAAQLQCNCSATLTDSDLQQLDTPTMFDKVYYDNLNNNQGIMFSDQVLTGDATT
Y18a_9_frame2  -----

peroxidase     299 AGFVTDYSNDVSVFLGDFAAAMIKMGDLPPSAGAQLEIRDVCSRVNFTSVASM
Y18a_9_frame2  -----

```

**Figure 4.4. Deduced amino acid sequence alignment of FDD gene fragment Y18a-9 (anionic peroxidase-like protein).**

Amino acid sequence alignment of FDD clone Y18a-9 with anionic peroxidase-like protein (GBPLN: 169554). Dark gray background indicates conserved sequences and light gray background indicates similar sequences. Outlined boxes indicate the conserved amino acids sharing a peroxidase consensus sequence, [SGATV]-X(3)-[LIVMA]-R-[LIVMA]-X-[FW]-H-X-[SAC], and a vacuolar targeting sequence, three hydrophobic amino acids followed by an acidic amino acid.

#### IV.1.6.2 FDD clone A11-7

Clone A11-7 contained an open reading frame (ORF) encoding 207 amino acids with a deduced amino acid sequence homologous to putative glucosyltransferase/cellulose synthase-like (CSL) proteins previously found in Arabidopsis, rice, and chickpea. Members of the CSL gene superfamily are related to cellulose synthase (CESA) genes. The putative glycosyltransferase/CSL proteins are predicted to be integral membrane proteins that function to synthesize glucose polymers such as hemicellulose, as opposed to glucosyltransferases that are responsible for conjugating glucose to secondary metabolites. The ORF of clone A11-7 showed 70% deduced amino acid identity and 83% deduced amino acid similarity to a region near the C terminus of a glucosyltransferase-like protein in Arabidopsis (GBPLN: 5832736) (Figure 4.5). A Q-X-X-R-W motif characteristic of processive glycosyltransferases (Saxena and Brown 1995), was found from position 35-39 in the ORF of clone A11-7 (QQHRW). Hydrophobicity analyses performed with Biology Workbench v. 3.2 THMM v.2 (Sonnhammer et al. 1998) predicted two membrane-spanning domains from amino acid positions 71-93 and 103-120 on the ORF of clone A11-7, supporting the classification of clone A11-7 as an integral membrane protein. Two of the five membrane-spanning domains predicted for the glucosyltransferase-like protein of Arabidopsis were located in the region with homology to clone A11-7. The position of alignment of A11-7 with putative glucosyltransferase (Figure 4.5) suggests that the oligo(dT) primer bound internally and that clone A11-7 contained an internal region of the gene.

```

A11_7_frame2      1  -----
glucosyltransf.  1  MAPNSVAVTMEKPDNFSLLEINGSDPSSFPDKRKSISPKQPSWFLLKARHLISCLSWLV

A11_7_frame2      1  -----
glucosyltransf.  61  SSVKKRIAPSAKNINEEEDPKSRGKQMYRPIKACLVISIIALSIEIVAHFKKWNLDLINR

A11_7_frame2      1  -----
glucosyltransf. 121  PSWEVYGLVEWSYMAWLSFRSDYIAPLVISLSRFCTVLFPLIQSLDRLVLCGLGCPWIKPKK

A11_7_frame2      1  -----
glucosyltransf. 181  IEPKLTEESIDLEDPSSPPMVLIQIPMCNEREVYEQSIGAASQLDWPKDRILIQVLDSDS

A11_7_frame2      1  -----
glucosyltransf. 241  DPNLQLLKEEVSVWAEKGVNIYRHLRIRTYKAGNLKSAMTCDYVKDYEFTVTFDADF

A11_7_frame2      1  -----
glucosyltransf. 301  TPNDPFLKKTVPHPFKGNPELGLVQARWSFVNKDENLLTRLQINLCPHFEVEQQVNGVPL

A11_7_frame2      1  -----S IAVRAHICGWKFIYVD DVRALCPELPS
glucosyltransf. 361  NFFGFNGTAGVWRKALEESGGWLERTTVEDMD IAVRAHINGWKFIYLN DVEVTCPELPS

A11_7_frame2      29  -----
glucosyltransf. 421  YEAYKKQHRWISGPMQLPRLCLPSILKSKISVWKKANLIFLFFLLRKLILPFYSPTLPC
YEAYKKQHRWISGPMQLPRLCLPSILKSKISVWKKANLIFLFFLLRKLILPFYSPTLPC

A11_7_frame2      89  -----
glucosyltransf. 481  IILPLTMFIPAEELPPVICYIFIVMSILNLILSPKSPFPFLMPYLLFENTMSVTKFNAMV
IILPLTMFIPAEELPLWIIICYVPIPIELNLILSPKSPFPFLVPYLLFENTMSITKFNAMI

A11_7_frame2      149  -----
glucosyltransf. 541  SGLPQLGSAYEWVVTKKTGRASESDLVLAERE SKNMNEEKISRELSSEGLELFE----
SGLPQFGSAYEWVVTKKTGRSSESDLVLAERKE-----EKLHRENSSEGLEL LSKLKEQ

A11_7_frame2      595  -----
glucosyltransf. 595  ETNLVQGQETVKKSLGGLMRPKNKKKTNMVFKKELGLAFLLLTAAARSFLSAHGLHFYPLL

A11_7_frame2      -----
glucosyltransf. 655  FQGLSFLVVGLDLIGEQIS

```

**Figure 4.5. Deduced amino acid sequence alignment of FDD gene fragment A11-7 (glucosyltransferase/cellulose synthase-like protein).**

Amino acid sequence alignment of FDD clone A11-7 with Arabidopsis glucosyltransferase-like protein (GBPLN: 5832736). Dark gray background indicates conserved sequences and light gray background indicates similar sequences. An outlined box indicates the conserved amino acids sharing a consensus sequence Q-X-X-R-W for processive glucosyltransferases. Filled boxes above the sequences indicate the positions of potential transmembrane domains (TM) found only in the Arabidopsis sequence as predicted by TMHMM version 2.0. Stippled boxes indicate the positions of TM domains that are also shared by clone A11-7.

#### IV.1.6.3 FDD clone D15-12

Clone D15-12 contained an ORF encoding 65 amino acids with 55% deduced amino acid identity and 74% deduced amino acid sequence similarity to the C-terminus of a disease resistance protein Mi-1.1 in tomato (GBPLN: 3426259). The position of D15-12 in the alignment with protein Mi-1.1 (Figure 4.6) suggests that the anchored-C oligo(dT) primer bound at the polyadenylated tail of the mRNA transcript as expected, and that D15-12 contained the 3' untranslated region of the mRNA. The D15-12 ORF was followed by an untranslated region of 162 bp.

```

disease_res. 1081 ELETLSVGFKSSNTNDSGSSVATNRPWDFHFPFNLKILWLREFPLTSDSLSTIARLPNLE
D15-12_frame1 1 -----
disease_res. 1141 ELSLYHTIIHGEEWNMGEDTFENLKFLNPNQVSIKWEVGEESFPNLEKIKLRGCHKLE
D15-12_frame1 1 -----SSV-----LEELQILXCTELM
disease_res. 1201 EIEPSPFGDIYSLNSIKIVKSPQLEDSALKIKEYAEDMRGGEELQILGQKNIPLPK
D15-12_frame1 17 EIRDSPFGDIFSLKYISLLGSGQLEVSA TRIKEYVADMTGEKLEVKCNW-----

```

**Figure 4.6. Deduced amino acid sequence alignment of FDD gene fragment D15-7 (disease resistance-like protein).**

Amino acid sequence alignment of FDD clone D15-12 with the C terminus of a *Lycopersicon esculentum* disease resistance protein Mi-copy 1 (GBPLN: 3426259). Dark gray background indicates conserved sequences and light gray background indicates similar sequences. To most effectively illustrate the region of homology, only the last 173 amino acids of the tomato disease resistance protein are shown.

#### IV.1.6.4 FDD clone Y2-6

Clone Y2-6 contained an ORF encoding 118 amino acids with 94% deduced amino acid identity and 97% similarity to the N-terminus of a tobacco tumor-related protein isolated from a hybrid produced from a cross between *N. glauca* and *N. langsdorfii* (GBPLN: 454193). The ORF of clone Y2-6 also showed 80% identity and 86% similarity with the N terminus of the tumor-related protein HR2 from *N. tabacum* (GBPLN: 2852374). The position of alignment of Y2-6 with a tumor-related protein (Figure 4.7) suggests that the oligo(dT) primer bound internally to the cDNA and that clone Y2-6 contained an internal region of the message.

```

Y2-6_frame3      1  IAASWKLYKNGVGCACVQVRCKDKALCS DVGVKVKVTDSGEGPGTDFIILSSDAFAKMAK
tumor-related   1  -----GLCDVGVKVKVTDSGEGPGTDFIILSSDAFAKMAK

Y2-6_frame3     61  HPKLAHMLFPKGVVDVDYKRVSCYGNLIK VNEHSNYNGYLAILLLNNGGYADILAVEI
tumor-related   36  HPKLAHMLFPKGVVDVDYKRVSCYGNLIK VNEHSNYNGYLAILLLNNGGYADILAVQI

Y2-6_frame3     121 YEEKSHKWIAMRRLYGAVPDLNPPKGNLKLKIQIKEDGKTRKWVQSDKTVIPDHWKAGSA
tumor-related   96  SEEKSHKWLAMRRLYGAVPDLNPPKGNLKLKIQIKEDGKTRKWVQSDKTVIPDHWKAGDA

Y2-6_frame3     181 YETDIQIP TSIYNSLVCNFSVMVWSQMKFVVISHCGLTKCLFVNNKAEIRVLLREYEIKH
tumor-related   156 YETDVQIP -----

Y2-6_frame3     241 CRILC
tumor-related   -----

```

**Figure 4.7. Deduced amino acid sequence alignment of FDD gene fragment Y2-6 (tumor related-like protein).**

Amino acid sequence alignment of FDD clone Y2-6 with a *Nicotiana glauca* x *Nicotiana langsdorffii* tumor-related protein (GBPLN: 454193). Dark gray background indicates conserved sequences and light gray background indicates similar sequences.

#### IV.1.7 Previously isolated FDD clones selected for further investigation

In addition to the FDD gene fragments identified by the present study, a number of FDD gene fragments were isolated and sequenced during an FDD screen previously performed by Dr. John Jelesko with an anchored-A oligo(dT) primer. BLASTX homology analyses of cloned FDD fragments pJGJ331, pJGJ332, and pJGJ334 are summarized in Table 4.4. Nucleotide sequences of pJGJ331, pJGJ332 and pJGJ334 are listed in Appendix 1 and alignments of deduced amino acid sequences of these FDD clones to homologous protein sequences are shown in Figures 4.8, 4.9, and 4.10.

**Table 4.4. Previously isolated FDD clones (Dr. John Jelesko)**

<b>FDD Clone</b>	<b>Arbitrary/ Anchored primers</b>	<b>Fragment size</b>	<b>Pattern of differential expression</b>	<b>BlastX homology: Accession No.</b>	<b>BlastX score</b>
pJGJ331	A19/anchored A	374 bp	<b>1</b>	<b>subtilisin protease</b> <i>Lycopersicon esculentum</i> (GBPLN: 3413480)	6e <sup>-19</sup>
pJGJ332	A19/anchored A	511 bp	<b>1</b>	<b>purine permease</b> <i>A. thaliana</i> (GBPLN:7620006)	5e <sup>-27</sup>
pJGJ334	B9/anchored A	327 bp	<b>1</b>	<b>lipoygenase</b> <i>Solanum tuberosum</i> (GBPLN: 765202)	8.8

<sup>a</sup>differential expression patterns described in Table 2

#### IV.1.7.1 FDD clone pJGJ331

FDD clone pJGJ331 contained an ORF encoding 84 amino acids with deduced amino acid homology of 56% identity and 72% similarity to the C terminus of the P69D subtilisin protease of tomato cultivar VFW8 (GBPLN: 3413480) (Figure 4.8). The P69D subtilisin protease is a member of the subtilase serine protease superfamily. Five distinct subtilase subfamilies have been found in tomato, with six genes comprising the P69 subfamily (Meichtry et al. 1999). The position of pJGJ331 in the alignment with serine protease (Figure 4.8) suggests that the anchored-C oligo(dT) primer bound at the polyadenylated sequence of the mRNA transcript, and that FDD fragment JGJ331 was amplified from the 3' end of the gene. The pJGJ331 ORF was followed by an untranslated region of 105 bp.

```

JGJ331_frame3      1 M-----
serine_protease   1 MGPLKILLVFIPGSPWPPTIQSNLETYLVHVESPELISTQSSLTDLDSYLSFLPKTTT

JGJ331_frame3      2 -----
serine_protease   61 AISSSGNEEAATMIYSYHNVMTGFAARLTAEQVKEMEKIHGFVSAQKQRTLSLDTHTSS

JGJ331_frame3      2 -----
serine_protease   121 FLGLQQNMGVWKDSNYGKGVIIIGVIDTGILPDHPSFSDVGMPPPPAKWKGVCSNPTNKC

JGJ331_frame3      2 -----AAG-----
serine_protease   181 NNKLI GARSYQLGHGSPIDDDGHGHTTASTAAGAFVNGANVFGNANGTAAGVAPFAHIAV

JGJ331_frame3      5 FX-----RRG---
serine_protease   241 YKVCNSDGCADTDVLAAMDAIDDDVDILSISLGGGSSDFYSNPIALGAYSATERGILV

JGJ331_frame3      10 -----
serine_protease   301 SCSAGNNGPSTGSGVNEAPWILTVGASTQDRKLNKATVVKLGNGEFEGESAYRPKISNSTF

JGJ331_frame3      10 -----GKILL-----
serine_protease   361 FALPDAGKNASDEFETPYCRSGLTDPVIRGKIVICLAGGGVPRVDKQAVKDAGGVGMI

JGJ331_frame3      15 -----
serine_protease   421 IINQQRSGVTKSADAHVLPALDISDADGTKILAYMNSTSNPVATITFQGTIIGDKNAPIV

JGJ331_frame3      15 -----
serine_protease   481 AAPSSRGPSPGASIGILKPDIIIGPGVNILAAWPTSVDDNKNKTKSTFNIIISGTSMSCPHLSG

JGJ331_frame3      15 -----
serine_protease   541 VAALLKSTHPDWSPAAIKSAMTTADTLNLANSPIILDERLLPADIIYAIAGHVNPSTRAND

JGJ331_frame3      15 -----
serine_protease   601 PGLVYDTPFEDYVPLYCGLNYTNRQVGNLLQQRKVNCSSEVKSILEAQLNYPSFSIYDLGST

JGJ331_frame3      15 -----XRVIVSFRSXSVVKKFXXTLKTKLNQKLTFRVFXFSATNI
serine_protease   661 PQT YTRTVTNVGDAKSSYKVEVASPEGVAIEVEFSE-LNFSSELNQLTYQVT-FSKTANS

JGJ331_frame3      58 TNMEVVHAYXXKWSNRHFPVRSPIAVIIXQESETPED
serine_protease   719 SNTQVIEQFL-KWTSNRHSVRSPIALLLIQ-----

```

**Figure 4.8. Deduced amino acid sequence alignment of FDD gene fragment JGJ331 (serine protease-like protein).**

Amino acid sequence alignment of FDD clone pJGJ331 with *Lycopersicon esculentum* serine protease (GBPLN: 3413480). Dark gray background indicates conserved sequences and light gray background indicates similar sequences.

#### IV.1.7.2 FDD clone pJGJ332

FDD clone pJGJ332 contained an ORF encoding 107 amino acids with deduced amino acid homology of 59% identity and 73% similarity to the C terminus of *Arabidopsis thaliana* purine permease (AtPUP1) (GBPLN: 26450404) (Figure 4.9). AtPUP1, which is able to transport adenine and structural analogs of adenine (including the alkaloids caffeine and nicotine), is a member of a family of small, highly hydrophobic PUP proteins. PUP proteins are predicted to be membrane transporter proteins, containing from 9 to 10 membrane-spanning domains. Hydrophobicity analyses performed with Biology Workbench v. 3.2 THMM v.2 (Sonnhammer et al. 1998) predicted three membrane-spanning domains from position 7-29, 33-55, and 64-81 of the ORF of clone pJGJ332, supporting the classification of clone pJGJ332 as a membrane protein. Three of the ten membrane-spanning domains predicted for the purine permease protein of *Arabidopsis* were located in the region with homology to clone pJGJ332. The position of pJGJ332 in the alignment with purine permease (Figure 4.9) suggests that the anchored-C oligo(dT) primer bound at the polyadenylated sequence of the mRNA transcript, and that FDD fragment JGJ332 was amplified from the 3' end of the cDNA. The pJGJ332 ORF was followed by a 3' untranslated region of 161 bp.

```

JGJ332_frame3      1 -----
purine_permease    1  MNKGLIIINCIILTIGTCGGPLLRLLYPTNGGKRIWPMFSLSTAGPPIILIPLLVSFLSR

JGJ332_frame3      1 -----
purine_permease    61  RRGNRNPNNNAENKRRKTKLFLMETPLFIASIVIGLLTGLDNYLSYGLAYLPVSTSSLIIG

JGJ332_frame3      1 -----NVG-----
purine_permease    121 TQLAPNALFAFLLVKQKPTFFSINAVVLLTVGIGILALHSDGDKPAKESKREYVVGFLMT

JGJ332_frame3      4 -----
purine_permease    181 VVAALLYAFILPLVELTYKKARQEITFPLVLEIQMVMCLAATFFFCVIGMFI VGDPKVIAR

JGJ332_frame3      4  EAR-----YVTVICTAAIWQXFFVGIIGVIYRSSSLMSGVMTAVLLPVTEVLAVI
purine_permease    241  EAREPKIGGSVFFYVALIVITGIITWQGFPLGATGIVFCASSLASGVLISVLLPVTEVFAVV

JGJ332_frame3      55  FPKENSGEKGLAFLSLWGFVSYFYGEFRQTKK--QNTSPHAEMTITHTESVPTING
purine_permease    301  CEREKQAQEKGVSLLSLWGFVSYFYGEFKSGKKVVDLPQPPETELP-----

```

**Figure 4.9. Deduced amino acid sequence alignment of FDD gene fragment JGJ332 (purine permease-like protein).**

Amino acid sequence alignment of FDD clone pJGJ332 with AtPUP1 (GBPLN: 7620006). Dark gray background indicates conserved sequences and light gray background indicates similar sequences. Stippled boxes above the sequences indicate the positions of potential transmembrane domains (TM) in both AtPUP1 and clone pJGJ332.

#### IV.1.7.3 FDD clone pJGJ334

FDD clone pJGJ334 contained an ORF of 14 amino acids with deduced amino acid homology of 92% identity and 92% similarity to the C terminus of a lipoxygenase (LOX) of potato (GBPLN: 765202) (Figure 4.10). Strong homology to the lipoxygenase in potato (GBPLN: 765202) and to a lipoxygenase in tomato (GBPLN: 534845) was confirmed by BLASTN scores ( $3e^{-6}$  and  $8e^{-10}$ , respectively). Plant LOXs are members of a class of nonheme iron-containing dioxygenases that are inducible by wounding and are involved in MeJA synthesis. LOX is encoded by a multigene family of at least two genes in potato (Geerts et al. 1994). The position of pJGJ334 in the alignment with lipoxygenase (Figure 4.10) suggests that the anchored-C oligo(dT) primer bound at the polyadenylated sequence of the mRNA transcript, and that the arbitrary primer bound very close to the 3' end of the cDNA, so that FDD fragment JGJ334 contained only a very small portion of the 3' end of the lipoxygenase coding sequence. The pJGJ334 ORF was followed by a 3' untranslated region of 279 bp.

```

lipoxxygenase      1 QIVGGLIGGHDSKVKVKTVMKKNALDFTDLAGSLTDKIFEALGQKVSFQLISSVQSD
JGJ334_frame2     1 -----
lipoxxygenase     61 PANGLQGKHSNPAYLENPLFTLTPLAAGETAFGVTPDWNEEFGVPGAFIKNTHINEFFL
JGJ334_frame2     1 -----
lipoxxygenase    121 KSLTLEDVPNHGKVFVCSWSVYPSFRYKSDRIFPANQPYPSPETPELLRKYRENELLTL
JGJ334_frame2     1 -----
lipoxxygenase    181 RGDGTGKREAWDRIYDYDVYNDLGNPDQGEQNVRTTLGGSADYPYPRRGRTGRPFRTDP
JGJ334_frame2     1 -----
lipoxxygenase    241 KSESRIPLILSLDIYVPRDERFGHLKMSDFLTALYSIVQFILPELHALFDGTPNEPDSF
JGJ334_frame2     1 -----
lipoxxygenase    301 EDVLRLYEGGKIKLPQGPLFKALTAIPEMMKELLRTDGEGLRFPPTPLVIKDSKTAWRT
JGJ334_frame2     1 -----
lipoxxygenase    361 DEEFAREMLAGVNPPIIISRLQEFPPKSKLDPEAYGNQNSTITAHHIEDKLDGLTVDEAMN
JGJ334_frame2     1 -----
lipoxxygenase    421 NNKLPILNHHDLVLIPLYLRRINTTTTKTYASRTLLPLQDNGSLKPLAIELSLPHPDGDQFG
JGJ334_frame2     1 -----
lipoxxygenase    481 VISKVTTPSDQGVESISWQLAKAYVAVNDSGVHQLISHWLNTHAVIEFPVIATNRQLSVL
JGJ334_frame2     1 -----
lipoxxygenase    541 HPIHKLLYPHPRDTMNINAMARQILINAGGVLESTVPPSKPAMEMSAVVYKDWVPPDQAL
JGJ334_frame2     1 -----
lipoxxygenase    601 PADLVKRGVAVEDSSSPHGVRLIEDYPYAVDGLEIWSAISKSWVTDYCSPYYGSDEEILK
JGJ334_frame2     1 -----
lipoxxygenase    661 DNELQAWWKELEEVGHGDKKNEPWFEMETPQELIDSCTTIWIASALHAAVNFGQYPYA
JGJ334_frame2     1 -----
lipoxxygenase    721 GYLPNRPTVSRRFMPPEPGTPEYEELKKNPKAPLKTITATLQTLGVSLEIILSRHTDE
JGJ334_frame2     1 -----
lipoxxygenase    781 IYLGQRESPEWTKDKEPLAAPDKFGKLTLDIEKQIIQRNGDNILNRSQPVNAPYTLTLP
JGJ334_frame2     1 -----
lipoxxygenase    841 TSEGGLTCKGIPNSV-SI
JGJ334_frame2     1 ---GGLTAKGIPNSVVS-

```

**Figure 4.10. Deduced amino acid sequence alignment of FDD gene fragment JGJ334 (lipoxxygenase-like protein).**

Amino acid sequence alignment of FDD clone pJGJ334 with a potato lipoxxygenase (GBPLN: 765202). Dark gray background indicates conserved sequences and light gray background indicates similar sequences.

## IV.2 Independent confirmation of differential expression of FDD gene fragments

Differential expression of genes identified by FDD was independently confirmed using Northern blot and Quantitative Real Time Polymerase Chain Reaction (QRT-PCR) analysis of steady state mRNA levels. FDD involves PCR amplification of small amounts of cDNA template and reproducibility of FDD results may be significantly affected by experimental factors (i.e. errors in pipetting or inaccurate RNA quantification prior to reverse transcription). Northern blot analysis does not involve reverse transcription of mRNA and PCR amplification, and is therefore not subject to the same types of experimental error as FDD. Northern blots were prepared from independent lots of RNA to confirm that differential expression of genes identified by FDD was reproduced in multiple samples. QRT-PCR was also used to independently confirm differential expression of FDD genes in separately isolated lots of RNA. QRT-PCR involves the monitoring of PCR product synthesis during the PCR reaction in order to determine the relative initial cDNA template concentration in samples. Although QRT-PCR is a PCR-based technique and is therefore subject to the same experimental error as FDD, QRT-PCR analysis provides better quantification of differential expression than Northern blot analysis, and is therefore useful both to confirm and quantify relative differential expression of endogenous genes represented by cloned FDD fragments.

Northern blot and QRT-PCR analysis was also used to confirm that the differential expression pattern used to screen FDD fragments is characteristic of known alkaloid biosynthetic genes. Differential expression of endogenous genes represented by FDD gene fragments was compared with the differential expression of known nicotine biosynthetic genes (i.e. *PMT3*, *ODC3*, *ADC1* and *QPRT*). A pattern of differential expression of endogenous genes represented by FDD gene fragments that is similar to the differential expression of known nicotine biosynthetic genes suggests at least coordinate regulation and possibly a role in alkaloid biosynthesis.

### IV.2.1 Northern blot analysis

Seven cloned FDD gene fragments were selected by FDD screening as putatively differentially expressed in Burley 21 and LA21 in response to alkaloid induction: A11-7, Y18a-9, D15-12, and Y2-6 (identified by the present study) and JGJ331, JGJ332, and JGJ334 (previously identified by Dr. John Jelesko). To confirm differential expression of endogenous genes represented by cloned

FDD fragments, Northern blot analysis was performed on total RNA isolated from root cultures subjected to alkaloid inducing and non-inducing conditions. Likewise, Northern blot analysis was also performed using probes to known nicotine biosynthetic genes *PMT3*, *ODC3*, *ADC1* and *QPRT* to confirm their expression patterns during the same conditions. For Northern blot analysis, total RNA was probed with DIG-labeled probes specific for nicotine biosynthetic genes (Figures 4.11A-D) and cloned FDD gene fragments (Figures 4.12A-F): A11-7 (glucosyltransferase-like protein), Y18a-9 (anionic peroxidase-like), Y2-6 (tumor-related-like protein), JGJ331 (serine protease-like protein), JGJ332 (purine permease-like protein), and JGJ334 (lipoxygenase-like protein). Although D15-12 (disease-resistance protein) was determined to merit further investigation, suitable primers for PCR-based probe synthesis specific for D15-12 could not be designed. All Northern blots were stripped and then re-hybridized with a probe specific for a constitutive gene,  $\beta$ -*ATPase*, as a loading control.

#### IV.2.1.1 Northern blot analysis of nicotine biosynthetic genes

A pattern of differential expression similar to FDD target pattern 1 (Table 4.2) was expected to be observed with Northern blot analysis of nicotine biosynthetic genes because previous investigations of the inducibility of nicotine biosynthetic genes have shown that *PMT* (Hibi et al. 1994, Reichers and Timko 1999, Sinclair et al. 2000), *ADC* (Wang et al. 2000), *ODC* (Imanishi et al. 1998, Wang et al. 2000) and *QPRT* (Imanishi et al. 1998, Sinclair et al. 2000) are inducible in tobacco by alkaloid-inducing conditions. Northern blot analysis results for *PMT3* (Figure 4.11A), *ODC3* (Figure 4.11B), *QPRT* (Figure 4.11C) and *ADC1* (Figure 4.11D) are shown below.

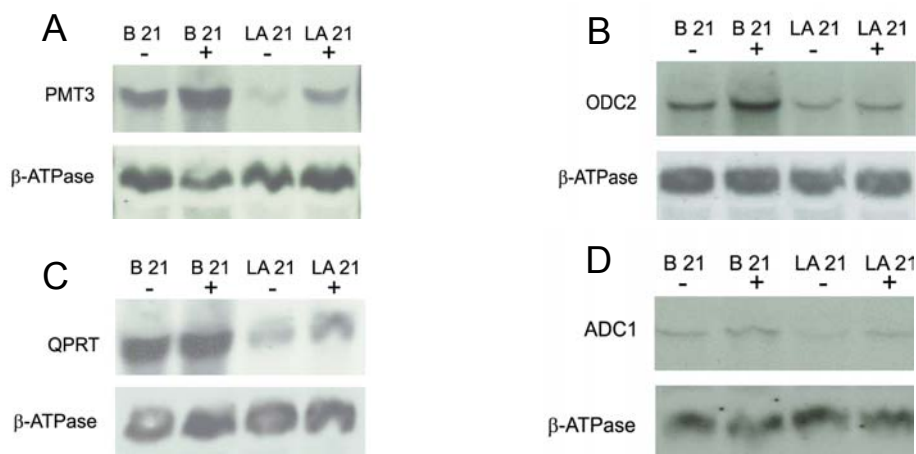


**Figure 4.11. Nicotine biosynthetic genes**

RNA gel blots of steady state mRNA levels of A. *PMT3*, B. *ODC2*, C. *QPRT*, and D. *ADC1* in cultivars Burley 21 (B21) and LA21 with no alkaloid induction (-), or with alkaloid induction (+) by removal of auxin (IBA) from root culture media for 8 hours. Blots containing 20 ug of RNA per lane were subjected to hybridization with the indicated nicotine biosynthetic gene probes and were stripped and re-probed with  $\beta$ -ATPase as a loading control

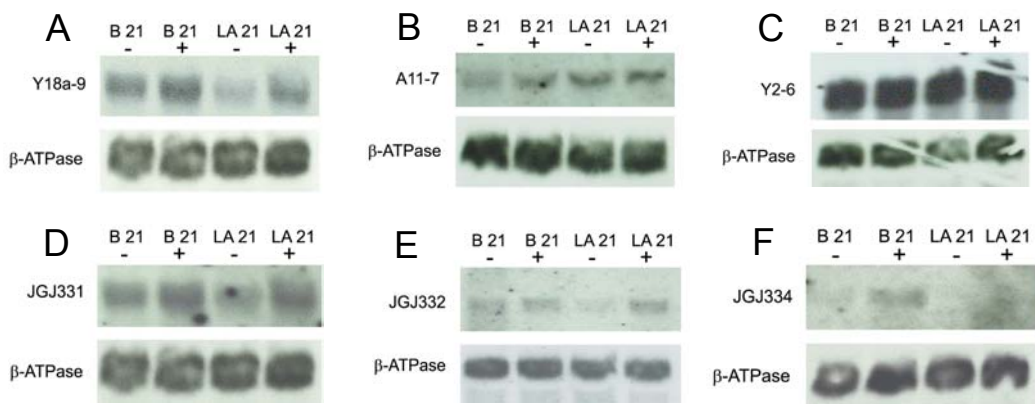


**Figure 4.12. Cloned FDD gene fragments**

RNA gel blots of steady state mRNA levels of genes represented by A. Y18a-9 (anionic peroxidase-like protein), B. A11-7 (glycosyltransferase-like protein), C. Y2-6 (tumor-related-like protein), D. JGJ331 (lipoxygenase-like protein), E. JGJ332 (purine permease-like protein), and F. JGJ334 (serine protease-like protein), in cultivars Burley 21 (B21) and LA21 with no alkaloid induction (-), or with alkaloid induction (+) by removal of auxin (IBA) from root culture media for 8 hours. Blots containing 20 ug of RNA per lane were subjected to hybridization with the indicated nicotine biosynthetic gene probes and were stripped and re-probed with  $\beta$ -ATPase as a loading control.

Differential expression is clearly observed for *PMT3*, with steady state mRNA levels of *PMT3* highest in root tissue of Burley 21 induced for alkaloid synthesis, next highest in uninduced Burley 21, lower in induced LA21, and lowest in uninduced LA21 (Figure 4.11A). *PMT3* is inducible in both Burley 21 and LA21 by alkaloid induction. This pattern of differential expression varies from the expected pattern 1 (Table 4.2) in that *PMT3* mRNA levels in LA21 showed a weak but demonstrable degree of induction in the LA21 induced samples. Differential expression of *ODC3* (Figure 4.11B) and *QPRT* (Figure 4.11C) clearly corresponds to the pattern observed for *PMT3*. Due to a weak signal, *ADC1* expression levels were less definitive (Figure 4.11D). However, *ADC1* was slightly higher in Burley 21 than in LA21 and was weakly inducible in both Burley 21 and LA21. The pattern of differential expression that was observed for all four nicotine biosynthetic genes suggests that these genes are expressed at a higher basal level in B21 than in LA21, and that gene expression is inducible in both B21 and LA21.

#### IV.2.1.2 Northern blot analysis of FDD clones

The pattern of differential expression observed in screening FDD gene fragments was expected to be reproduced with Northern blot analysis of the cloned FDD gene fragments. FDD clones Y18a-9, A11-7, D15-2, pJGJ331, pJGJ332, and pJGJ334 were selected by FDD screening for differential expression corresponding to pattern 1 (Figure 4.2) and clone Y2-6 was selected for differential expression corresponding to pattern 7 (Figure 4.2).

Northern analysis of clone Y18a-9 (anionic peroxidase-like protein) (Figure 4.12A), clone pJGJ331 (subtilisin protease-like protein) (Figure 4.12D), and pJGJ332 (purine permease-like protein) (Figure 4.12E) showed differential expression represented by pattern 1 (Figure 4.2), which was also observed for nicotine biosynthetic genes *PMT*, *ODC*, *ADC* and *QPRT* (Figures 4.11A-D), thus confirming FDD screening results for these clones. Clone pJGJ334 (lipoxygenase-like protein) produced a weak signal (Figure 4.12F); however, the Northern analysis appears to corroborate FDD screening results, with induced wild type mRNA levels higher than uninduced levels and mutant mRNA levels not detected.

Conversely, Northern analysis of clone A11-7 (glucosyltransferase-like protein) and Y2-6 (tumor-related-like protein) did not corroborate FDD screening results. Clone A11-7 showed an

anomalous expression pattern (Figure 4.12B), with the mutant induced mRNA levels higher than both wild type induced and uninduced. Clone Y2-6 was expected to show differential expression representative of pattern 7 (Figure 4.2); however, Northern analysis appeared to show constitutive expression for this clone (Figure 4.12C).

#### IV.2.2 QRT-PCR analysis

QRT-PCR was performed in order to more accurately quantify absolute levels of nicotine biosynthetic genes and endogenous genes represented by cloned FDD gene fragments than was possible by Northern analysis, and to quantify the fold-induction of gene expression due to genotype and/or alkaloid induction effects. For QRT-PCR analysis, total RNA was isolated from Lot 13, 15, 16 and 18 root tissue of Burley 21, HI21, LI21 and LA21 that was grown under both alkaloid-inducing and non-inducing conditions. Total RNA was DNase-treated to remove DNA contamination and then reverse transcribed with oligo(dT) to generate a population of cDNAs that were subsequently used as template for the QRT-PCR reactions. QRT-PCR was performed with this cDNA using gene-specific primers (Table 3.2, 3.3, 3.4; Materials and Methods) for FDD clones Y18a-9, A11-7, and Y2-6 and nicotine biosynthetic genes *PMT3*, *ODC3*, *QPRT* and *ADCI*. For *QPRT* and *ADCI*, it was possible to design gene-specific primers that amplified outside the coding region in non-conserved regions, in order to limit amplification of multi-gene family members. Gene-specific primers for *PMT3* and *ODC3* were designed within the coding region, however, since primers outside the coding region could not be designed. *PMT3* and *ODC3* primers could therefore potentially amplify additional *PMT* (Reichers and Timko 1999) and *ODC* (Wang et al. 2000) genes.

For each QRT-PCR reaction, the amount of PCR product is a function of the amount of starting template cDNA (Higuchi et al. 1992). In this study, PCR product synthesis was monitored by measuring the increase in fluorescence units due to intercalation of Syber Green fluorescent dye in double stranded PCR products. Increasing quantities of double stranded DNA produced in the PCR reaction generated a proportional increase in fluorescence, which was recorded as a curve that was linear over a number of PCR cycles before a saturation point was reached (where the amount of PCR product was no longer a function of the original starting amount of template). To quantify the amount of cDNA starting material, a threshold fluorescence level was selected that

was above background, but within the linear portion of the fluorescence curve for each QRT-PCR run, and the PCR cycle corresponding to that threshold level ( $C_T$ ) was determined.

Constitutively expressed genes were expected to show approximately the same  $C_T$  values for all samples.  *$\beta$ -ATPase*, a constitutively expressed gene that did not show genotype or alkaloid induction effects on PCR cycle threshold, was used as a control for pipetting and/or RNA quantification error. An example of fluorescence curves for  *$\beta$ -ATPase* in cDNA samples of Burley 21 and LA21 that were either induced for alkaloid synthesis or uninduced is given in Figure 4.13.

With increasing amounts of starting template, fewer PCR cycles were required to reach the  $C_T$ , and the fluorescence curves of up-regulated nicotine biosynthetic genes and FDD gene fragments in induced samples were expected to be shifted to the left of non-induced samples. Figure 4.14 shows an example of the shift in fluorescence curves observed with alkaloid induction of *PMT3* in cDNA samples of Burley 21.

To confirm that fluorescently-labeled double-stranded (ds) PCR product detected by QRT-PCR analysis consisted of a single sequence, a “melt curve analysis” was performed following completion of the amplification cycles. To generate melt curves, the rate of decrease of fluorescence was measured over a temperature range at which the ds PCR product became single stranded. The negative derivative of fluorescence (F) with respect to temperature (T) was plotted as  $-dF/dT$  versus T using TM software (P-E Applied Biosystems) in order to convert fluorescence data into melting peaks. Each melting peak corresponded to a unique sequence of ds PCR product, so the presence of only single peaks in a melt curve analysis confirmed the presence of a single species of PCR product. Figure 4.15 shows an example of melt curve analysis.

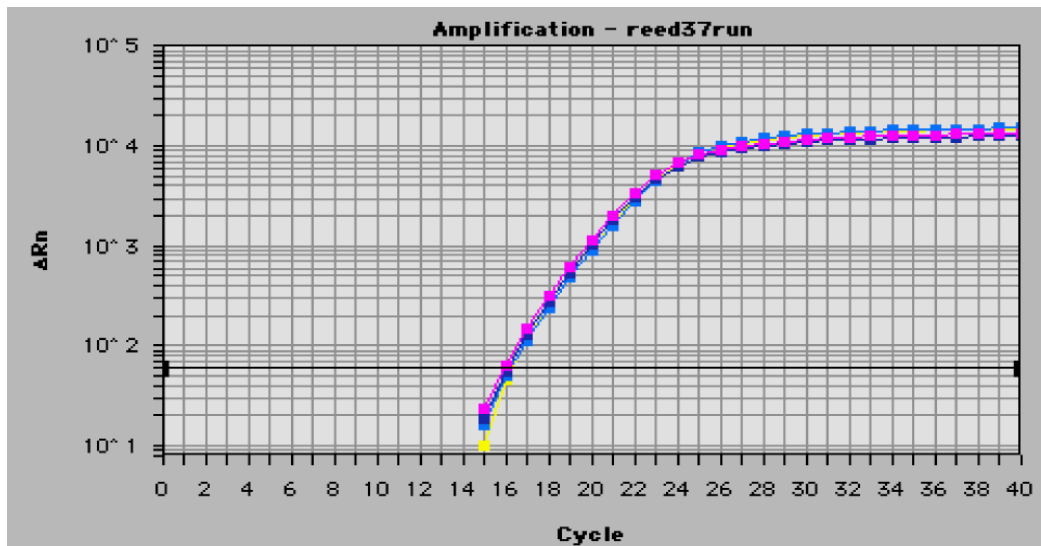


**Figure 4.13. Fluorescence curves:  $\beta$ -ATPase**

Example of fluorescence curves generated by QRT-PCR analysis of  $\beta$ -ATPase in samples of Burley 21 with no alkaloid induction (pink), Burley 21 induced for alkaloid synthesis (royal blue), LA21 uninduced (yellow) and LA21 induced (light blue).

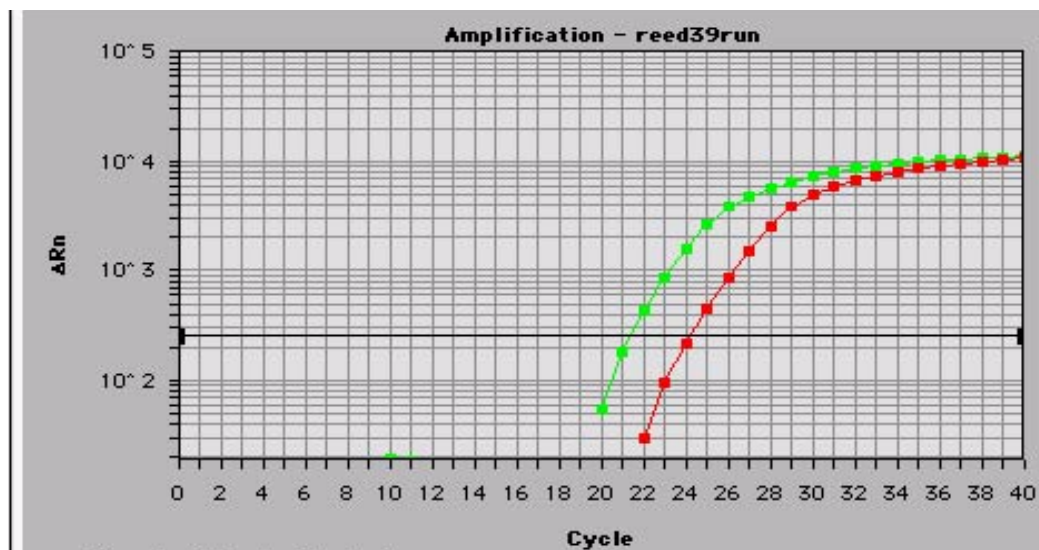


**Figure 14. Fluorescence curves:  $PMT3$**

Example of fluorescence curves generated by QRT-PCR analysis of  $PMT3$  in samples of Burley 21 with no alkaloid induction (red) and Burley 21 with alkaloid induction by auxin removal for 8 hours (green).

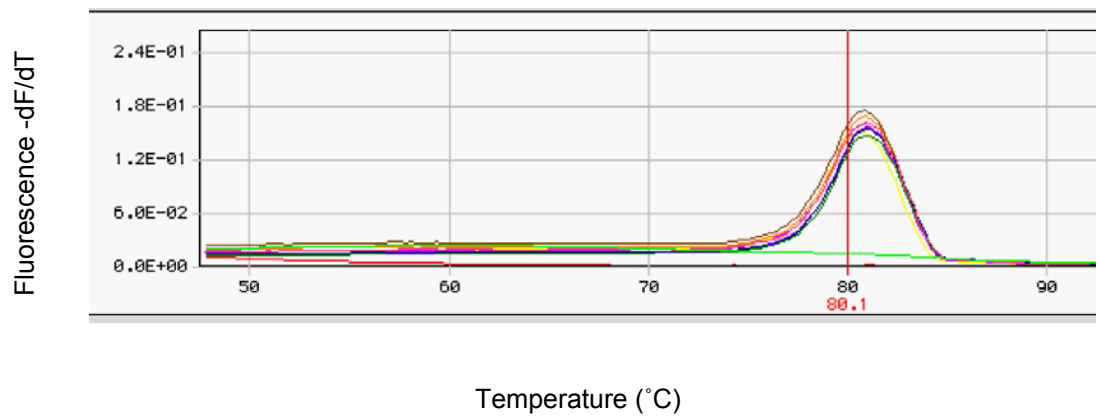


**Figure 4.15. Fluorescence melt curves: *PMT3***

Example of superimposed fluorescent melt curves generated by melt curve analysis of *PMT3* in samples of Burley 21, HI21, LI21 and LA21 with and without alkaloid induction.

QRT-PCR analysis was performed in triplicate for *β-ATPase*, *PMT3*, *ODC3*, *QPRT* and *ADCI* and Y18a-9, A11-7, and Y2-6 with induced and noninduced cDNA samples from Lots 13, 15, 16 and 18 of B21, HI21, LI21 and LA21 root tissue. In order to generate standard curves, triplicate QRT-PCR assays were also performed with a ten-fold serial dilution series of plasmid containing *β-ATPase*, nicotine biosynthetic gene or FDD gene fragment inserts (plasmids described in Table 3.6, Materials and Methods). The average  $C_T$  for each nicotine biosynthetic gene and FDD gene fragment was determined and the number of "cDNA equivalents" (representative of the number of copies of a particular DNA template) was extrapolated from QRT-PCR standard curves. An example of fluorescence curves showing a ten-fold serial dilution series of pDGR55 (containing a cloned region of *ADCI*) and the corresponding standard curve are shown below (Figure 4.16a, Figure 4.16b). The number of cDNA equivalents of each gene (per 200 ng total RNA) as a function of alkaloid induction and genotype is given in Figures 4.17-4.22, and fold-induction due to treatment and genotype is shown in Tables 4.5-4.12. Paired t-test analyses between treatments were performed for each gene to determine if there were significant transcript copy number differences between uninduced and induced samples of each genotype, and two-sample t-test analyses were performed to determine if there were significant transcript copy number differences between genotypes (Tables 4.5-4.12).

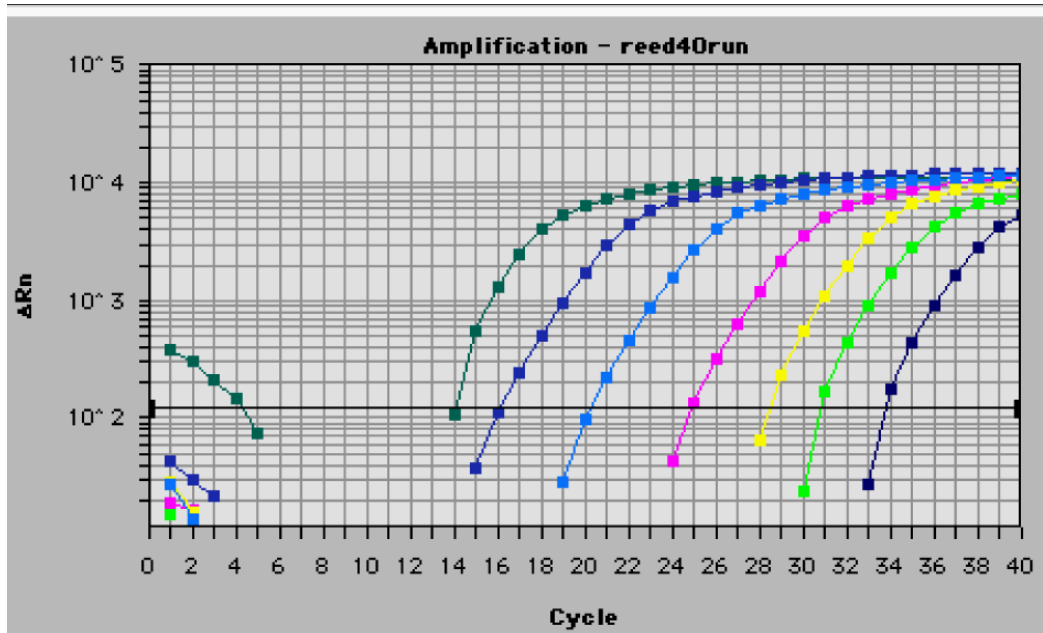


**Figure 4.16a. Amplification plot showing serial dilutions of pDGR55.**

Initial template copy number was 10<sup>8</sup> and was diluted 10-fold in subsequent wells. 10<sup>8</sup> copies = dark green, 10<sup>7</sup> copies = royal blue, 10<sup>6</sup> copies = light blue, 10<sup>5</sup> copies = pink, 10<sup>4</sup> copies = yellow, 10<sup>3</sup> copies = light green, 10<sup>2</sup> copies = dark blue.

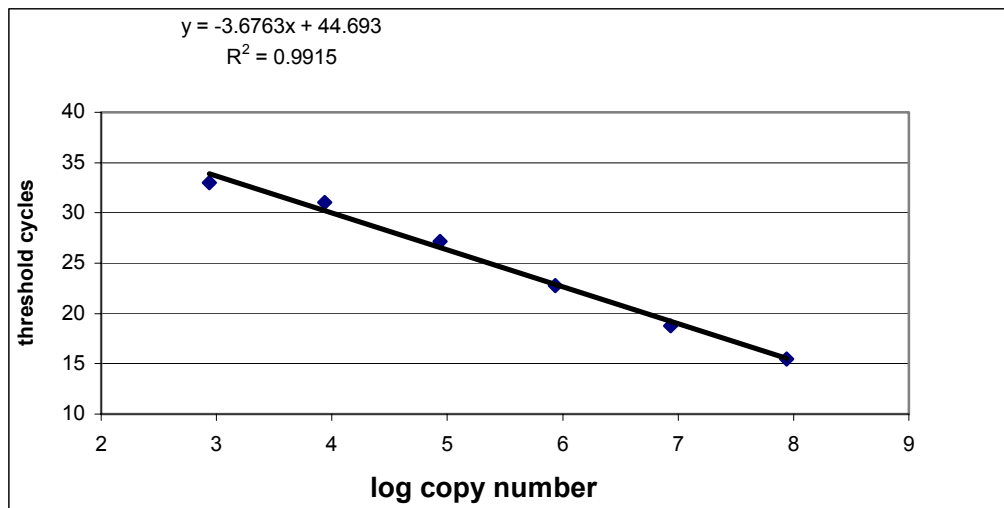


**Figure 4.16b. pDGR55 standard curve.**

QRT-PCR threshold cycles corresponding to 10-fold serial dilutions of pDGR55 over a range of 10<sup>3</sup> to 10<sup>8</sup> copies.

#### IV.2.2.1 $\beta$ -ATPase

The  $\beta$ -ATPase gene was selected as a constitutively expressed gene under the conditions utilized in this study. Northern blot analysis of  $\beta$ -ATPase showed comparable hybridization levels consistent with constitutive expression (Figure 4.11A-D, Figure 4.12A-F). Likewise, QRT-PCR measurements (Figure 4.17 and Table 4.5) indicated that no significant differences were observed between treatments of B21, HI21, and LI21.  $\beta$ -ATPase mRNA accumulation levels varied between genotypes by as much as 30%; however, these differences were not statistically significant ( $0.23 < P < .50$ ). A difference of 27% between treatments of LA21 that was significant at the  $P = 0.03$  level was attributed to a Type I error. The number of cDNA equivalents of  $\beta$ -ATPase ranged from 4 to 7 million per ng of total RNA. Overall, the QRT-PCR results confirmed earlier Northern blot results showing constitutive expression of  $\beta$ -ATPase during alkaloid induction in B21, HI21, LI21, and LA21.

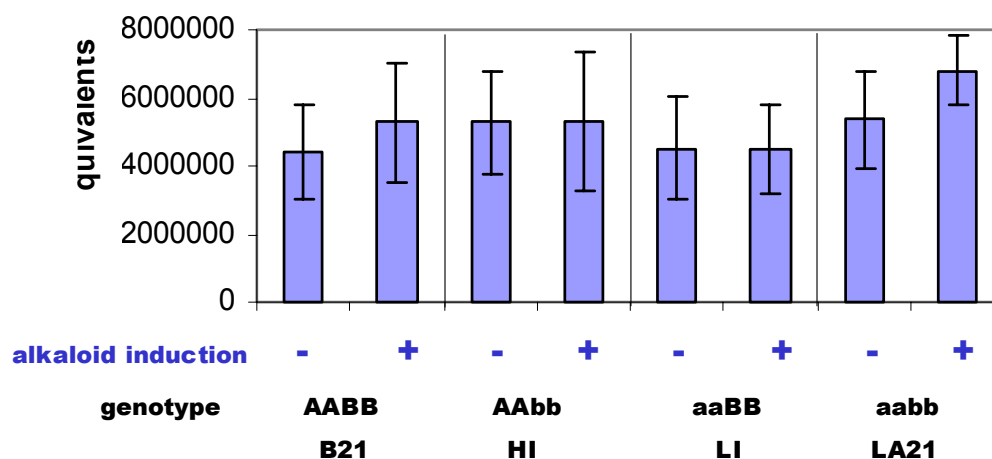


**Figure 4.17. QRT-PCR analysis of  $\beta$ -ATPase expression.**

Levels of  $\beta$ -ATPase expression in wild type Burley 21 (AABB), single mutants HI (AAbb) and double mutant LA21 (aaBB) with (+) and without (-) alkaloid induction. The y-axis represents transcript copy number (in cDNA equivalents) per 200 ng of total RNA and the x-axis represents induction treatment for each genotype.

**Table 4.5. Fold-increase of  $\beta$ -ATPase due to genotype and/or alkaloid induction**

	B21 +	HI21 -	HI21 +	LI21 -	LI21 +	LA21-	LA21 +
B21 -	1.20 (P=0.10)	1.20 (P=0.34)		1.00 (P=0.48)		1.20 (P=0.33)	
B21 +			1.00 (P=0.50)		.84 (P=0.36)		1.30 (P=0.23)
HI21 -			1.00 (P=0.50)				
LI21 -					.99 (P=0.45)		
LA21 -							1.27 (P=0.03)

#### IV.2.2.2 *PMT3*

Saunders and Bush (1979) showed that PMT activity levels are comparable to leaf nicotine levels in four genotypes: B21, HI21, LI21 and LA21, and that PMT activity levels increase following alkaloid induction treatment in all four genotypes. Therefore, *PMT3* expression was chosen to be a benchmark for genotype effects and induction by conditions that induce alkaloid biosynthesis. QRT-PCR analysis of *PMT3* mRNA accumulation levels (Figure 4.18 and Table 4.6) supported Northern blot analysis results indicating that steady state mRNA levels of *PMT3* were highest in root tissue of Burley 21 induced for alkaloid synthesis and lowest in uninduced LA21, with *PMT3* inducible in both B21 and LA21 (Figure 4.11A).

*PMT3* expression appeared to be correlated to both alkaloid induction and genotype according to two primary trends.

- 1) mRNA levels were inducible in all genotypes tested; however, B21 showed the greatest induction, LA21 showed the least induction and HI21 and LI21 showed induction levels intermediate between B21 and LA21.
- 2) mRNA levels in both uninduced and induced HI21 were comparable to levels in similarly treated B21. Uninduced/induced LA21 showed lowest levels and uninduced/induced LI21 showed levels of expression intermediate between LA21 and HI21/B21.

More specifically, alkaloid induction caused significant ( $P < 0.05$ ) differential *PMT3* mRNA accumulation levels of B21 (3.57-fold induction), HI21 (2.81-fold induction) and LI21 (2.46-fold induction). Although LA21 showed a 2.08-fold induction following alkaloid induction, the lack of significance of this induction ( $P = 0.12$ ) was likely due to increased variance due to lower overall levels of LA21.

Comparisons of *PMT3* mRNA levels showed no significant difference between B21 and HI21, during all conditions tested (Table 4.6). *PMT3* mRNA levels in the uninduced single mutant LI21 were found to be 63% of levels in uninduced B21, although increased variance due to lower overall levels of LI21 decreased the significance ( $P = 0.19$ ) of this result. *PMT3* mRNA levels in induced LI21 were found to be 43% of levels in induced B21 ( $P = 0.08$ ). *PMT3* mRNA levels in

the uninduced double mutant LA21 were found to be 30% of levels in uninduced B21 ( $P = 0.08$ ), and levels in induced LA21 were found to be 18% of levels in induced B21 ( $P = 0.04$ ).

Overall, numbers of cDNA equivalents of *PMT3* were calculated to range from 1.7 to 20 million per 200 ng of total RNA.

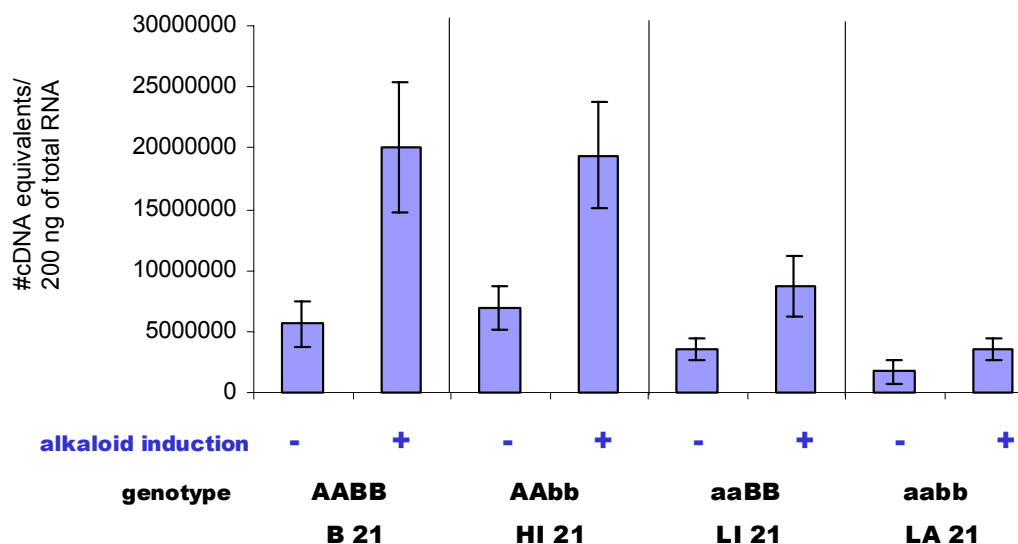


**Figure 4.18. QRT-PCR analysis of *PMT3* expression.**

Levels of *PMT3* expression in wild type Burley 21 (AABB), single mutants HI (AAbb) and double mutant LA21 (aaBB) with (+) and without (-) alkaloid induction. The y-axis represents transcript copy number (in cDNA equivalents) per 200 ng total RNA and the x-axis represents induction treatment for each genotype.

**Table 4.6. Fold-increase of *PMT3* due to genotype and/or alkaloid induction**

	B21 +	HI21 -	HI21 +	LI21 -	LI21 +	LA21-	LA21 +
B21 -	3.57 (P=0.04)	1.23 (P=0.32)		0.63 (P=0.19)		0.30 (P=0.08)	
B21 +			0.97 (P=0.47)		0.43 (P=0.08)		0.18 (P=0.04)
HI21 -			2.81 (P=0.03)				
LI21 -					2.46 (P=0.05)		
LA21 -							2.08 (P=0.12)

#### IV. 2.2.3 *ODC3*

Wagner et al. (1986) showed that ODC activity levels are correlated to nicotine levels in cultivars with high (BaN+), low (BiN-), and intermediate (Samsun) nicotine content. ODC activity (Mizusaki et al 1973) and steady state mRNA levels (Imanishi et al. 1998) increase following alkaloid induction treatment. *ODC3* expression was therefore expected to be correlated to genotype and increased by conditions that induce alkaloid biosynthesis as observed with QRT-PCR results for *PMT3*.

QRT-PCR analysis of *ODC3* mRNA accumulation levels (Figure 4.19 and Table 4.7) supported previously described Northern blot analysis results (Figure 4.11B), in that differential *ODC3* mRNA accumulation levels were observed following alkaloid induction treatment of B21 and LA21. Levels of *ODC3* mRNA also increased following alkaloid induction of HI21 and LI21. Consistent with results for *PMT3*, comparisons of *ODC3* mRNA levels showed no significant difference between B21 and HI21, either induced or uninduced. *ODC3* mRNA levels in the uninduced single mutant LI21 were found to be 59% of levels in uninduced B21 and *ODC3* mRNA levels in induced LI21 were found to be 53% of levels in induced B21. *ODC3* mRNA levels of LA21 were reduced even further: mRNA levels in the uninduced double mutant LA21 were 55% of levels in uninduced B21 and levels in induced LA21 were 44% of levels in induced B21. The number of cDNA equivalents of *ODC3* ranged from 1 to 5 million per 200 ng of total RNA.

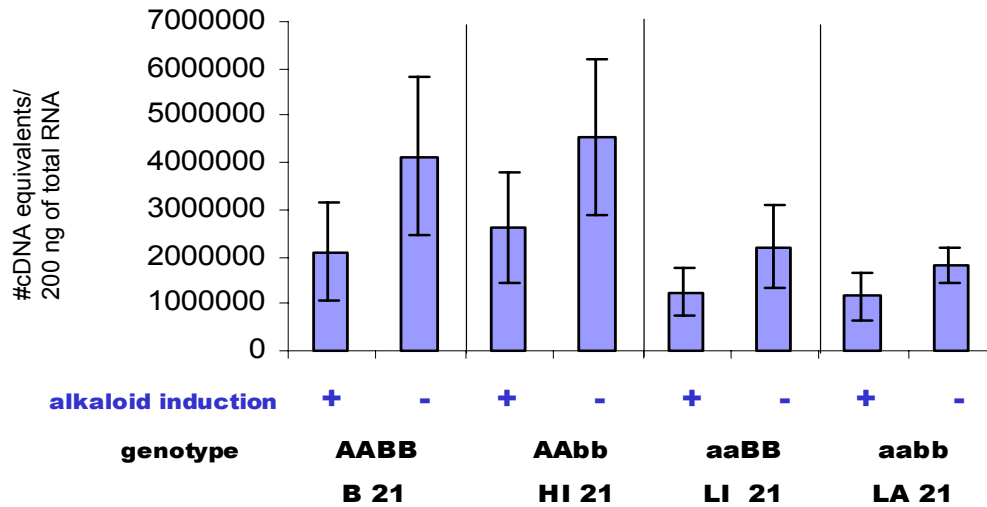


**Figure 4.19. QRT-PCR analysis of *ODC3* expression.**

Levels of *ODC3* expression in wild type Burley 21 (AABB), single mutants HI (AAbb) and double mutant LA21 (aaBB) with (+) and without (-) alkaloid induction. The y-axis represents transcript copy number (in cDNA equivalents) per 200 ng total RNA and the x-axis represents induction treatment for each genotype.

**Table 4.7. Fold-increase of *ODC3* due to genotype and/or alkaloid induction**

	B21 +	HI21 -	HI21 +	LI21 -	LI21 +	LA21-	LA21 +
<b>B21 -</b>	1.96 (P=0.05)	1.24 (P=0.38)		0.59 (P=0.25)		0.55 (P=0.24)	
<b>B21 +</b>			1.10 (P=0.44)		0.53 (P=0.19)		0.44 (P=0.15)
<b>HI21 -</b>			1.74 (P=0.095)				
<b>LI21 -</b>					1.77 (P=0.07)		
<b>LA21 -</b>							1.56 (P=0.06)

#### IV.2.2.4 QPRT

Saunders and Bush (1979) showed that QPRT activity levels are comparable to leaf nicotine levels in B21, HI21, LI21 and LA21, and that QPRT activity levels increase following alkaloid induction treatment in all four genotypes. Sinclair et al. (2000) showed that *QPRT* steady state mRNA levels are correlated to nicotine content in cultivars with high (NC95) or low (LAF53) levels of nicotine. *QPRT* expression was therefore expected to be correlated to genotype and increased by conditions that induce alkaloid biosynthesis as observed with QRT-PCR results for *PMT3* and *ODC3*.

QRT-PCR analysis of *QPRT* mRNA accumulation levels (Figure 4.20 and Table 4.8) supported previously described Northern blot analysis results (Figure 11C), except for inducibility of LA21 expression: no significant difference in mRNA levels of LA21 following alkaloid induction was observed. Levels of *QPRT* mRNA increased following alkaloid induction treatments of B21, HI21, and LI21. Despite large variances in QRT-PCR data, which reduced the significance of genotype differences, a similar correlation between gene expression and genotype that was observed for *PMT3* and *ODC3* was also observed for *QPRT*. Comparisons of *QPRT* mRNA levels showed no significant difference between B21 and HI21, either induced or uninduced. *QPRT* mRNA levels in induced LI21 were found to be 54% of levels in induced B21 and *QPRT* mRNA levels in induced LA21 were found to be 31% of levels in induced B21. The number of cDNA equivalents of *QPRT* ranged from 250,000 to 2 million per 200 ng of total RNA.

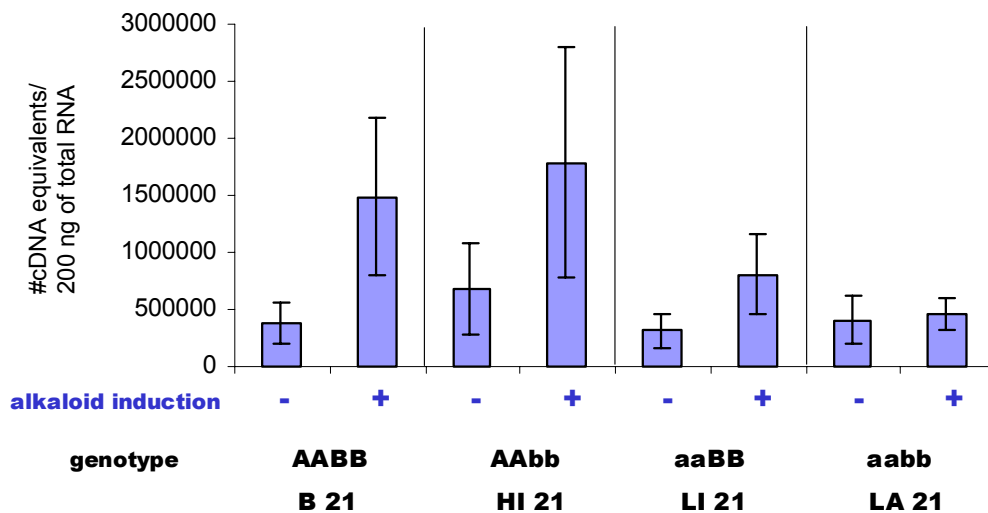


**Figure 4.20. QRT-PCR analysis of *QPRT* expression.**

Levels of *QPRT* expression in wild type Burley 21 (AABB), single mutants HI (AAbb) and double mutant LA21 (aaBB) with (+) and without (-) alkaloid induction. The y-axis represents transcript copy number (in cDNA equivalents) per 200 ng total RNA and the x-axis represents induction treatment for each genotype.

**Table 4.8. Fold-increase of *QPRT* due to genotype and/or alkaloid induction**

	B21 +	HI21 -	HI21 +	LI21 -	LI21 +	LA21-	LA21 +
<b>B21 -</b>	3.98 (P=0.08)	1.81 (P=0.27)		0.84 (P=0.40)		1.10 (P=0.45)	
<b>B21 +</b>			1.20 (P=0.41)		0.54 (P=0.22)		0.31 (P=0.14)
<b>HI21 -</b>			2.65 (P=0.19)				
<b>LI21 -</b>					2.57 (P=0.07)		
<b>LA21 -</b>							1.12 (P=0.39)

#### IV.2.2.5 ADC1

Wang et al. (2000) showed that levels of ADC mRNA increase following alkaloid induction. No previous studies have correlated ADC expression or ADC activity to nicotine content in tobacco, but QRT-PCR results were expected to support Northern blot analysis results (Figure 4.11D) showing *ADC1* expression correlated to genotype and increased by alkaloid induction.

QRT-PCR analysis of *ADC1* mRNA accumulation levels (Figure 4.21 and Table 4.9) did support Northern blot analysis results (Figure 4.11D), except for inducibility of LA21 expression: no significant difference in mRNA levels of LA21 following alkaloid induction was observed with QRT-PCR analysis. Levels of *ADC1* mRNA increased following alkaloid induction treatments of B21, HI21, and LI21. Correlation between gene expression and genotype that was observed for *PMT3*, *ODC3*, and *QPRT* was also observed for *ADC1*. Comparisons of *ADC1* mRNA showed no significant difference between B21 and HI21, either induced or uninduced. *ADC1* mRNA levels in induced LI21 were found to be 72% of levels in induced B21. *ADC1* mRNA levels in induced LA21 were found to be 57% of levels in induced B21. The number of cDNA equivalents of *ADC1* ranged from 500,000 to 1.3 million per 200 ng of total RNA.

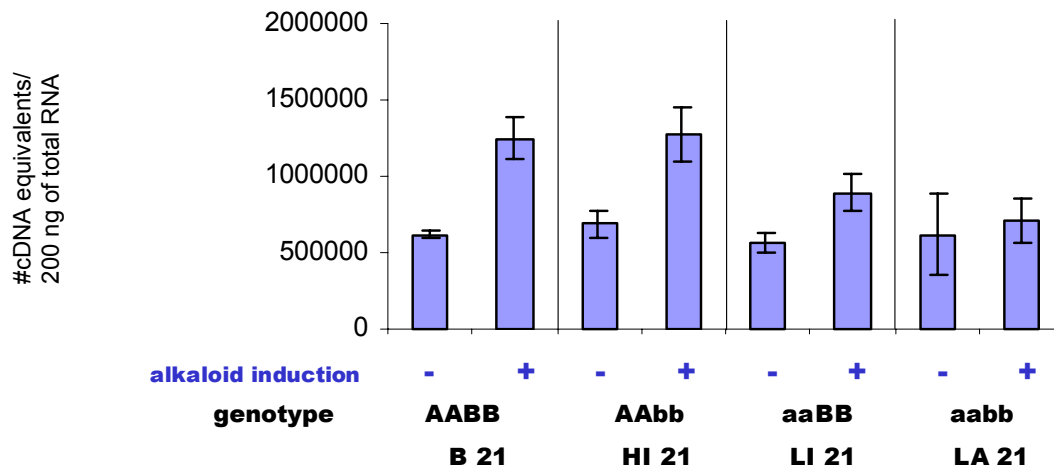


**Figure 4.21. QRT-PCR analysis of *ADC1* expression.**

Levels of *ADC1* expression in wild type Burley 21 (AABB), single mutants HI (AAbb) and double mutant LA21 (aaBB) with (+) and without (-) alkaloid induction. The y-axis represents transcript copy number (in cDNA equivalents) and the x-axis represents induction treatment for each genotype.

**Table 4.9 Fold-increase of *ADC1* due to genotype and/or alkaloid induction**

	B21 +	HI21 -	HI21 +	LI21 -	LI21 +	LA21-	LA21 +
<b>B21 -</b>	2.02 (P=0.02)	1.11 (P=0.25)		0.92 (P=0.27)		1.00 (P=0.50)	
<b>B21 +</b>			1.02 (P=0.46)		0.72 (P=0.06)		0.57 (P=0.02)
<b>HI21 -</b>			1.85 (P=0.07)				
<b>LI21 -</b>					1.57 (P=0.11)		
<b>LA21 -</b>							1.14 (P=0.33)

#### IV. 2.2.6 FDD clone Y18a-9

QRT-PCR results for the endogenous gene represented by the FDD clone Y18a-9 (anionic peroxidase homolog) were expected to support Northern blot analysis results (Figure 4.12A) showing gene expression to be correlated to genotype and increased by alkaloid induction. QRT-PCR analysis of endogenous *Y18a-9* mRNA accumulation levels (Figure 4.22 and Table 4.10) did support Northern blot analysis results (Figure 4.12A), except that the gene represented by *Y18a-9* was found to be more strongly inducible in LA21 than in B21, with levels of *Y18a-9* mRNA higher in induced LA21 than in induced B21.

Consistent with QRT-PCR results for *PMT3* and *ODC3*, levels of *Y18a-9* mRNA increased following alkaloid induction treatments of B21, HI21, LI21, and LA21. The correlation between gene expression and genotype that was observed during QRT-PCR of *PMT3*, *ODC3*, *QPRT*, and *ADC1* was not observed for *Y18a-9*. Although comparisons of *Y18a-9* mRNA levels between B21 and HI21 were consistent with QRT-PCR results for *PMT3*, *ODC3*, *QPRT*, and *ADC1*, no significant differences were found between B21 and LI21 or between B21 and LA21 (Table 4.10). The number of cDNA equivalents of the endogenous gene represented by FDD fragment Y18a-9 ranged from 600,000 to 1.6 million per 200 ng of total RNA.

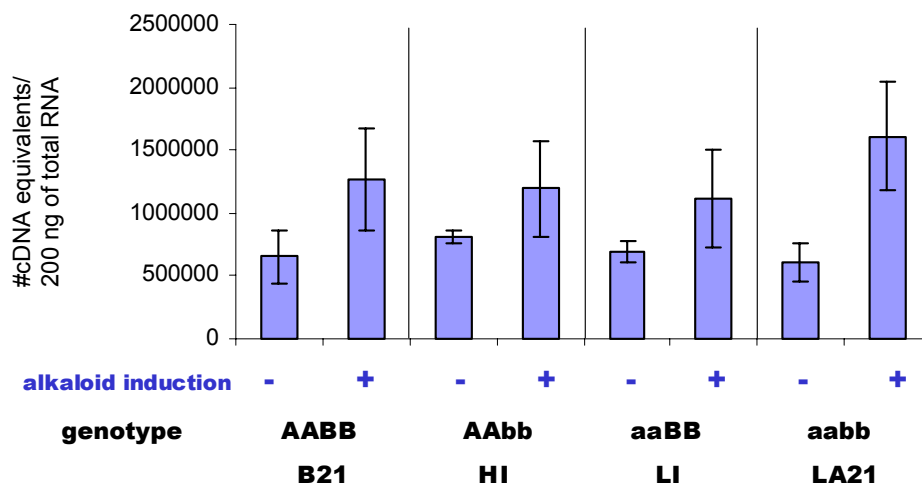


**Figure 4.22. QRT-PCR analysis of expression of endogenous gene represented by Y18a-9.**

Levels of endogenous *Y18a-9* gene expression in wild type Burley 21 (AABB), single mutants HI (AAbb) and double mutant LA21 (aaBB) with (+) and without (-) alkaloid induction. The y-axis represents transcript copy number (in cDNA equivalents) and the x-axis represents induction treatment for each genotype.

**Table 4.10. Fold-increase of endogenous Y18a-9 due to genotype and/or alkaloid induction**

	B21 +	HI21 -	HI21 +	LI21 -	LI21 +	LA21-	LA21 +
<b>B21 -</b>	1.95 (P=0.05)	1.24 (P=0.27)		1.06 (P=0.44)		0.93 (P=0.43)	
<b>B21 +</b>			0.94 (P=0.45)		0.88 (P=0.44)		1.27 (P=0.43)
<b>HI21 -</b>			1.48 (P=0.19)				
<b>LI21 -</b>					1.61 (P=0.15)		
<b>LA21 -</b>							2.66 (P=0.04)

#### IV.2.2.7 FDD clone A11-7

QRT-PCR results for FDD clone A11-7 (glucosyltransferase homolog) supported Northern blot analysis results (Figure 4.12B). However, unlike the benchmark *PMT3* gene, a statistically significant increase in *A11-7* gene expression following alkaloid induction was not observed for any of the genotypes analyzed. Less than 1.5-fold induction was observed for B21, HI21, LI21, and LA21.

Specifically, comparisons of *A11-7* mRNA levels showed no significant difference between B21 and HI21, or between B21 and LI21. Interestingly, *A11-7* mRNA levels in uninduced LA21 appeared to be 235% the levels in uninduced B21, and levels in uninduced LA21 appeared to be 170% the levels of uninduced B21. The latter result was consistent with increased hybridization signal in the Northern blot in the LA21 lanes (Figure 4.12B). The number of cDNA equivalents of the endogenous gene represented by FDD fragment A11-7 ranged from 15,000 to 40,000 per 200 ng of total RNA, a level significantly lower than that observed for the other genes analyzed.

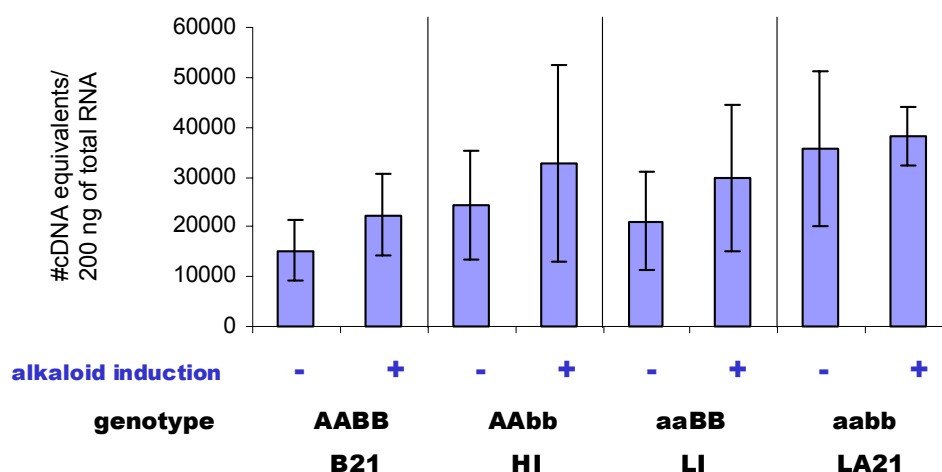


**Figure 4.23. QRT-PCR analysis of expression of endogenous gene represented by A11-7.** Levels of endogenous *A11-7* gene expression in wild type Burley 21 (AABB), single mutants HI (AAbb) and double mutant LA21 (aaBB) with (+) and without (-) alkaloid induction. The y-axis represents transcript copy number (in cDNA equivalents) and the x-axis represents induction treatment for each genotype.

**Table 4.11. Fold-increase of endogenous *A11-7* due to genotype and/or alkaloid induction**

	B21 +	HI21 -	HI21 +	LI21 -	LI21 +	LA21-	LA21 +
<b>B21 -</b>	1.47 (P=0.04)	1.60 (P=0.26)		1.39 (P=0.32)		2.35 (P=0.15)	
<b>B21 +</b>			1.46 (P=0.33)		1.33 (P=0.35)		1.70 (P=0.08)
<b>HI21 -</b>			1.34 (P=0.27)				
<b>LI21 -</b>					1.41 (P=0.15)		
<b>LA21 -</b>							1.07 (P=0.44)

#### IV.2.2.8 FDD clone Y2-6

QRT-PCR results for FDD clone Y2-6 (tumor-related protein homolog) supported Northern blot analysis results (Figure 4.12C). An increase in gene expression following alkaloid induction was not consistently observed for Y2-6. Alkaloid induction caused a 1.5-fold increase in Y2-6 mRNA expression in B21, a 2.22-fold increase in HI21, no significant difference in LI21, and a 1.59-fold increase in L A 21. Y2-6 did not show a correlation between gene expression and genotype. Comparisons of Y2-6 mRNA levels showed no significant difference between B21 and HI21 or between B21 and LI21 (Table 4.12). Y2-6 mRNA levels in uninduced LA21 were 179% the levels in uninduced B21, and levels in uninduced LA21 were 190% the levels of uninduced B21. In contrast, *PMT3* levels in the LA21 genotype were approximately half the levels in B21. The number of cDNA equivalents of the endogenous gene represented by FDD fragment Y2-6 ranged from 50,000 to 155,000 per 200 ng of total RNA.

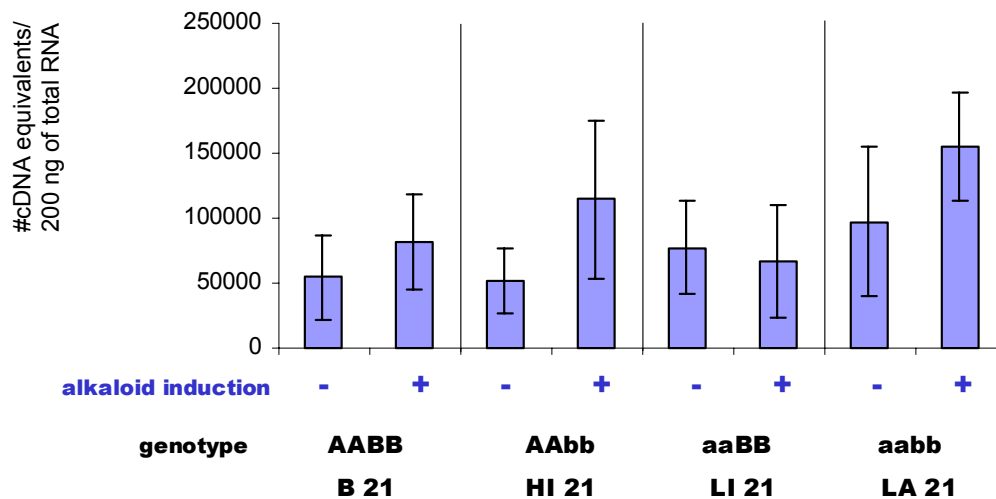


**Figure 4.24. QRT-PCR analysis of expression of endogenous gene represented by Y2-6.** Levels of endogenous *Y2-6* gene expression in wild type Burley 21 (AABB), single mutants HI (AAbb) and double mutant LA21 (aaBB) with (+) and without (-) alkaloid induction. The y-axis represents transcript copy number (in cDNA equivalents) and the x-axis represents induction treatment for each genotype.

**Table 4.12. Fold-increase of endogenous *Y2-6* due to genotype and/or alkaloid induction**

	B21 +	HI21 -	HI21 +	LI21 -	LI21 +	LA21-	LA21 +
<b>B21 -</b>	1.50 (P=0.06)	0.95 (P=0.47)		1.42 (P=0.33)		1.79 (P=0.27)	
<b>B21 +</b>			1.40 (P=0.33)		0.82 (P=0.40)		1.90 (P=0.13)
<b>HI21 -</b>			2.22 (P=0.11)				
<b>LI21 -</b>					0.86 (P=0.34)		
<b>LA21 -</b>							1.59 (P=0.18)

#### IV.2.2.9 Relative expression of genes analyzed by QRT-PCR

Numbers of cDNA equivalents of mRNA of  $\beta$ -*ATPase*, *PMT3*, *ODC3*, *ADC1*, and Y18a-9, A11-7, and Y2-6 endogenous genes were measured in B21, HI21, LI21 and LA21 with and without alkaloid induction. The number of cDNA equivalents per 200 ng of total RNA ranged from 15,000 to 20 million cDNA equivalents. The relative abundances of cDNA equivalents of  $\beta$ -*ATPase*, *PMT3*, *ODC3*, *ADC1*, and Y18a-9, A11-7, and Y2-6 endogenous genes were compared on a  $2.5 \times 10^7$  scale (Figure 4.25A-F). At this scale, the relatively low abundances of endogenous genes represented by A11-7 (Figure 4.25G) and Y2-6 (Figure 4.25H), which ranged from 15,000 to 155,000 cDNA equivalents per 200 ng total RNA, were negligible.

*PMT3* was the most abundant mRNA, with a range of 1.7 million to 20 million cDNA equivalents per 200 ng total RNA.  $\beta$ -*ATPase* was the next most abundant gene, with a range of 4 to 7 million cDNA equivalents. After *PMT3*, *ODC3* was the next most abundant nicotine biosynthetic mRNA, with a range of 1 to 5 million cDNA equivalents. *QPRT* and *ADC1* showed similar abundances, with ranges of 250,000 to 2 million and 500,000 to 1.3 million, respectively. The endogenous gene represented by Y18a-9, with a range of 600,000 to 1.6 million, showed a similar abundance to *ADC1*. The abundance of the endogenous gene represented by A11-7, which ranged from 15,000 to 40,000, was less than 1% of the most abundant nicotine biosynthetic gene, *PMT3*. The endogenous gene represented by Y2-6 was expressed at a level approximately 3 times higher than that of A11-7, and ranged from 50,000 to 155,000.

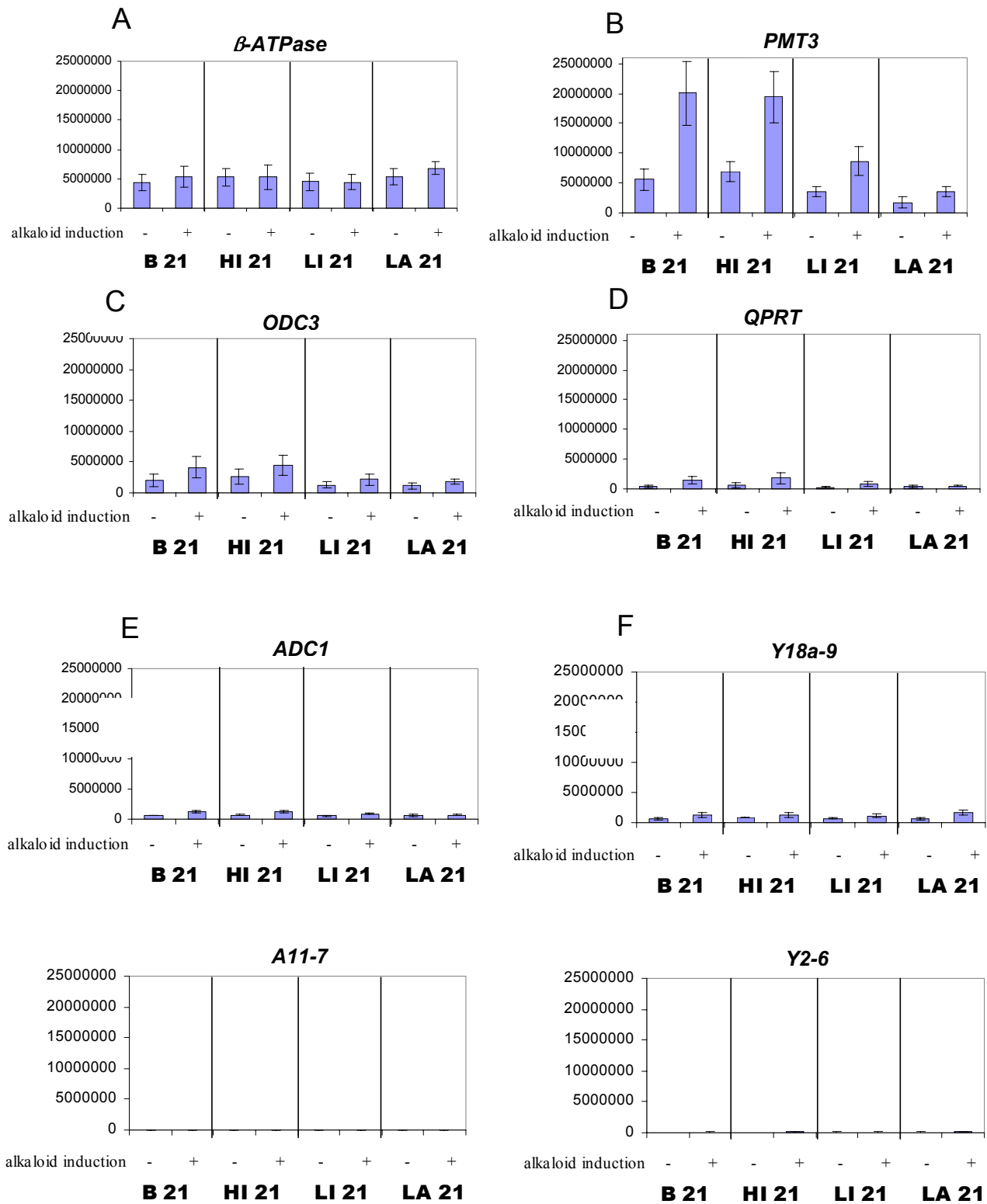


**Figure 25. Relative expression of genes analyzed by QRT-PCR**

### IV.3 HPLC analysis of root nicotine content

To determine whether gene induction that was observed during QRT-PCR analysis resulted in increased nicotine content in root tissue, HPLC was performed using extracts from root tissue of samples B21, HI21, LI21, and LA21 from Lot 15, harvested 8 hours after auxin removal from root culture media. Lot 15 was also used to derive RNA for Northern blot and QRT-PCR analysis. A previous study has shown that leaf nicotine content is correlated to genotype in the order B21 > HI21 > LI21 > LA21 following alkaloid induction (Saunders and Bush 1979). The time course of nicotine synthesis in root tissue has not been established; however, leaf nicotine content doubles by the fourth day following alkaloid induction (Saunders and Bush 1979). Under the conditions utilized for this study, nicotine content of extracted root tissue was expected to be correlated to genotype and to induction treatment.

To ensure that reproducible alkaloid peaks were obtained and that integration of peak area accurately measured alkaloid content, 70 µg of an independent alkaloid, atropine, was added to samples after extraction and filtering. Atropine peak integration areas were then compared to a standard atropine peak generated by adding 70.0 µg atropine to extract buffer. The standard atropine peak, with an integration value of 299,663, was detected at 5.4 minutes (Figure 4.26B). In root tissue extract from induced B21 root tissue culture (Figure 4.26D), the atropine peak integration value was 289,990, detected at 5.4 minutes. Consistent atropine content was measured in all root tissue samples.

To measure nicotine content in root tissue samples, a nicotine standard curve was prepared using nicotine standards within a concentration range of 0.7-7.0 µg in extract media (Table 4.13). A nicotine peak with an integration value of 1,069,227 was detected at 7.3 minutes in extract media containing 7.0 µg nicotine (Figure 4.26C). A nicotine peak with an integration value of 982,899 was detected at 7.3 minutes in root tissue extract from induced B21 root tissue culture (Figure 4.26D). Under the conditions of the HPLC assay, the nicotine peak eluted more slowly with decreasing concentration of nicotine standards, and this trend was also observed with decreasing concentration of nicotine in root tissue samples. Nicotine peak area and peak migration times for all genotypes and nicotine standards tested are shown in Table 4.13.

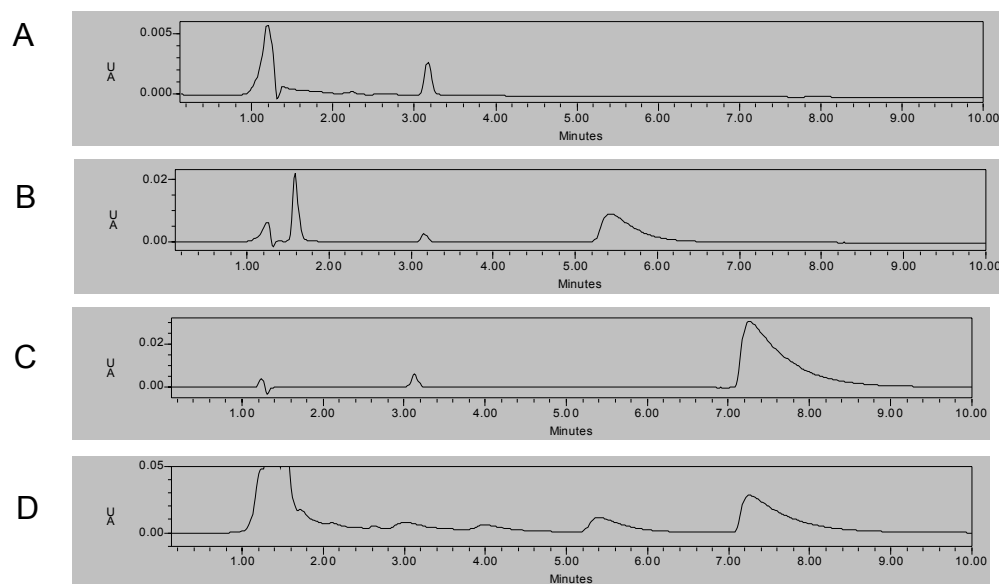


**Figure 4.26. HPLC analysis of root tissue nicotine content.**

- A. 100 µl extract buffer (25 mM sodium phosphate buffer).
- B. 100 µl extract buffer + 70 µg atropine standard.
- C. 100 µl extract buffer + 7 µg nicotine standard.
- D. 100 µl root tissue extract (from Lot 15 B21 root tissue culture induced for alkaloid synthesis)

**Table 4.13. HPLC nicotine analysis**

SAMPLE	MIGRATION TIME (MINUTES)	NICOTINE PEAK AREA	NICOTINE CONTENT MG/G EXTRACTED ROOT TISSUE (% DRY WEIGHT)	AVERAGE NICOTINE CONTENT FOR GENOTYPE (MG/G EXTRACTED ROOT TISSUE, % DRY WEIGHT)
7.0 µg std	7.26	1,069,227		
5.25 µg std	7.37	779,262		
3.5 µg std	7.50	532,520		
1.75 µg std	7.80	186,716		
0.7 µg std	8.03	64,975		
B21 -	7.24	1,021,933	14 mg/g (1.40%)	
B21 +	7.26	982,899	12 mg/g (1.20%)	13 mg/g (1.30%)
HI21 -	7.32	829,612	11 mg/g (1.10%)	
HI21 +	7.29	910,252	12 mg/g (1.20%)	11.5 mg/g (1.15%)
LI21 -	7.39	677,424	9.1 mg/g (0.91%)	
LI21 +	7.40	642,578	8.7 mg/g (0.87%)	8.9 mg/g (0.89%)
LA21 -	7.65	317,895	4.7 mg/g (0.47%)	
LA21 +	7.62	353,012	5.1 mg/g (0.51%)	4.9 mg/g (0.49%)

Nicotine content was reported as mg per gram of dry root tissue (percent dry weight). A comparison of the nicotine content of uninduced and induced root tissue of all tested genotypes is shown in Figure 4.27. As described previously, QRT-PCR analysis indicated that levels of nicotine biosynthetic gene mRNA in HI21 were comparable to levels in similarly treated B21, with lowest levels in LA21 and intermediate levels in LI21 (Figure 4.18, Table 4.7). A similar trend for nicotine content was observed during HPLC analysis, as follows. Nicotine content was highest in B21 (average of 1.30% nicotine/dry weight of roots), lower in HI21 (1.15%), lower still in LI21 (0.89%) and lowest in LA21 (0.49%). However, unlike the observed increased in mRNA accumulation levels of expression of nicotine biosynthetic genes during conditions that induce alkaloid biosynthesis, intracellular nicotine levels did not show a corresponding increase in these tissues.

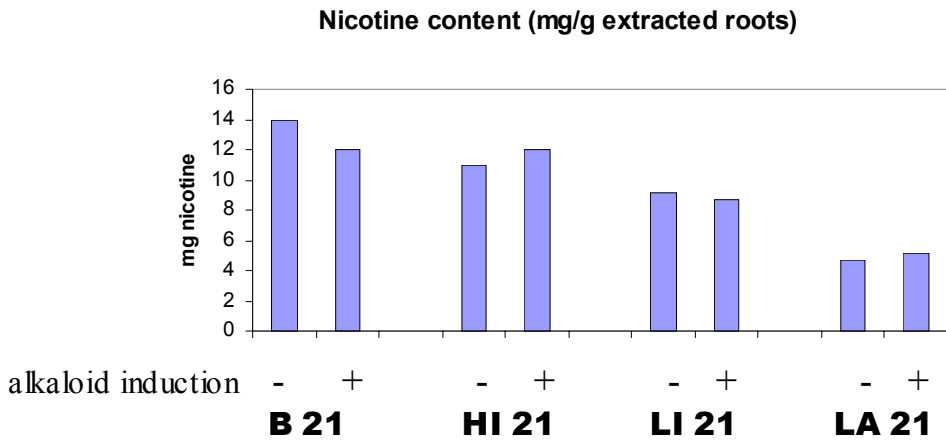


**Figure 4.27. Nicotine content of extracted root tissue**

#### IV.4 Bibliography

- Geerts, A., Feltkamp, D., Rosahl, S. 1994. Expression of lipoxygenase in wounded tubers of *Solanum tuberosum* L. *Plant Physiol.* 105(1): 269-77.
- Hibi, N., Higashiguchi, S., Hashimoto, T., and Yamada, Y. 1994. Gene expression in tobacco low-nicotine mutants. *Plant Cell* 6: 723-735.
- Higushi, R., Dollinger, G., Walsh, P.S. and Griffith, R. 1992. Simultaneous amplification and detection of specific DNA sequences. *Biotechnology (NY)* 10: 413-417.
- Imanishi, S., Hashizumi, K., Nakakita, M., Kojima, H., Matsubayashi, Y., Hashimoto, T., Sakagami, Y., Nakamura, K. 1998. Differential induction by methyl jasmonate of genes encoding ornithine decarboxylase and other enzymes involved in nicotine biosynthesis in tobacco cell cultures. *Plant Mol. Biol.* 38: 1101-1111.
- Kimura, S. and Ikeda-Saito, M. 1988. Human myeloperoxidase and thyroid peroxidase, two enzymes with separate and distinct physiological functions, are evolutionarily related members of the same gene family. *Proteins.* 3(2): 113-20.
- Legg, P.D. and Collins, G.B. 1971. Inheritance of percent total alkaloids in *Nicotiana tabacum* L.II. genetic effects of two loci in Burley 21 X LA Burley 21 populations. *Can. J. Cytol.* 13: 287-291.
- Meichtry, J., Amrhein, N., and Schaller, A. 1999. Characterization of the subtilase gene family in tomato (*Lycopersicon esculentum* Mill.). *Plant Mol. Biol.* 39: 749-760.
- Misuzaki, S., Tanabe, Y., Noguchi, M., Tamaki, E. 1973. Changes in the activities of ornithine decarboxylase, putrescine N-methyltransferase and N-methylputrescine oxidase in tobacco roots in relation to nicotine biosynthesis. *Plant Cell Physiol.* 14: 103-110.
- Nakamura, K. and Matsuoka, K. 1993. Protein targeting to the vacuole in plant cells. *Plant Physiol.* 101: 1-5.
- Reichers, D.E. and Timko, M.P. 1999. Structure and expression of the gene family encoding putrescine N-methyltransferase in *Nicotiana tabacum*: new clues to the evolutionary origin of cultivated tobacco. *Plant Mol. Biol.* 41: 387-401.
- Saunders, J.W., and Bush, L.P. 1979. Nicotine biosynthetic enzyme activities in *Nicotiana tabacum* L. genotypes with different alkaloid levels. *Plant Physiol.* 64: 236-240.
- Saxena, I.M. and Brown, R.M. Jr. 1995. Identification of a second cellulose synthase gene (acsAII) in *Acetobacter xylinum*. *J Bacteriol.* 177(18): 5276-83.

Sinclair, S.J. Murphy, K.J. Birch, C.D., Hamill, J.D. 2000. Molecular characterization of quinolinate phosphoribosyltransferase (*QPRTase*) in *Nicotiana*. *Plant Mol. Biol.* 44: 603-617.

Sonnhammer, E.L., von Heijne, G., and Krogh, A. 1998. A hidden Markov model for predicting transmembrane helices in protein sequences. *Proc. Intl. Conf. Intell. Syst. Mol. Biol.* 6: 175-82.

Wagner, R. Feth, F. and Wagner, K.G. 1986. The regulation of enzyme activities of the nicotine pathway in tobacco. *Physiol. Plant.* 68: 667-672.

## Chapter V. DISCUSSION

### V.1 Efficiency of FDD analysis and extent of transcriptome screened

In order to characterize the *A/B* regulon in tobacco, fluorescent differential display (FDD) was used to isolate 14 DNA PCR fragments representing potentially novel genes inducible by conditions effecting alkaloid biosynthesis. The degree to which the tobacco transcriptome was sampled by FDD analysis was estimated based on the number of genes expressed in tobacco. One approach used to estimate the size of the tobacco transcriptome utilized an estimation of the size of the tomato transcriptome, which has been better characterized than the tobacco transcriptome. By developing and analyzing an EST database (<http://sgn.cornell.edu/>; <http://www.tigr.org/tdb/lgi>), Van der Hoeven et al. (2002) estimated that the tomato transcriptome consists of approximately 35,000 genes. *N. tabacum* is an amphidiploid species derived from a cross of progenitor species *N. sylvestris* and an introgressed hybrid of *N. tomentosiformis* and *N. otophora* (Kenton et al. 1993, Reichers and Timko 1999), with the genome of *N. tabacum* consisting of duplicated genes contributed by each parent. If the size of the amphidiploid *N. tabacum* transcriptome is double the estimated size of the tomato transcriptome, the gene content of *N. tabacum* would be approximately 70,000 duplicated genes. Alternatively, the size of the tobacco transcriptome may be predicted based on the percentage of the tobacco genome that is thought to be transcribed. The tobacco genome is estimated to consist of 4.5 billion base pairs (Opperman et al. 2003). If 2.0% of the tobacco genome is assumed to be transcribed, with an average gene size of 1300 bp (Ferl and Paul 2000), then the tobacco transcriptome is estimated to consist of approximately 70,000 genes, which is consistent with the figure derived by analysis of the tomato EST database. The expression of 15% of all genes at a particular time in a eukaryotic cell (Liang and Pardee 1992) would generate 10,500 duplicated genes. Under the conditions of FDD analysis in this study, as many as 12,000 to 18,000 FDD amplified fragments were detected, which exceeds the number of anticipated expressed genes. The discrepancy between the number of FDD fragments and the expected number of expressed genes is due in part to sampling the same transcript more than once or sampling the same transcript with different arbitrary primers. Repeated sampling of the same transcript was observed on FDD gel images as multiple different-sized FDD bands (amplified with the same primer combination), showing the same pattern of differential expression. In the present study,

only 6 out of 14 fragments identified by FDD were found to represent unique sequences. Kuno et al. (2000) investigated irradiated *Arabidopsis* seedlings and found that 20 of 24 differentially expressed fragments isolated by FDD represented distinct mRNA species; the remaining 4 FDD fragments corresponded to mRNA species that were amplified more than once with different primers or with the same primers at multiple sites. The sampled mRNA population in this study was limited to transcript species that corresponded to the anchored-C primer, so that only a subset of the mRNA population that is inducible by conditions inducing alkaloid biosynthesis was sampled.

#### V.1.1 Effectiveness of FDD analysis was limited by experimental conditions

Nine of 14 cloned FDD bands that were identified as representing differentially expressed genes under conditions inducing alkaloid biosynthesis were subsequently determined to represent genes for rRNA or a ribosomal protein. Only one of the 14 clones was confirmed by Northern blot analysis to contain an FDD fragment corresponding to a gene that was inducible by conditions inducing alkaloid biosynthesis. As explained below, most of the differentially expressed FDD bands were therefore artifacts, likely due to experimental conditions for growth and induction of root cultures as well as lack of sufficient RNA lots for reproduction of FDD screening.

##### V.1.1.1 Gene inducibility may have been affected by induction period and time of root growth

Experimental conditions used to generate total RNA for FDD analysis were based on a previous study (Hibi et al. 1994) that showed inducibility of *PMT* after 1 hour of alkaloid induction of root cultures grown for 14 days. However, QRT-PCR analysis performed a year after the FDD screen indicated that nicotine biosynthetic genes (*PMT3*, *QPRT*, *ADC1*, and *ODC3*) were not induced with a 1 hour induction treatment, but rather were induced after 8 hours induction. Furthermore, a follow up study showed that root tissue was not reliably inducible at 14 days of growth, but rather was inducible at 10 to 12 days of growth (data not shown). In a study of the time course of nicotine production in tobacco callus in auxin-free media by Takahashi and Yamada (1972), the stationary phase of callus growth occurred 15 days after inoculation, with nicotine synthesis beginning at the end of the logarithmic growth phase. The inducibility of root tissue culture in auxin-free media may similarly depend on the stage of growth, and nicotine biosynthetic genes may already be highly induced at 14 days, when root growth was approaching stationary phase.

If alkaloid biosynthesis was initiated in the "non-induced" root culture approaching stationary phase, treatment of root tissue with alkaloid-inducing conditions may not have resulted in detectable nicotine biosynthetic gene induction, thus minimizing differences between non-induced and induced treatments. Therefore, the effectiveness of FDD as a screening tool may have been limited by both insufficient time of induction treatment and overgrowth of root culture that reduced the apparent differential expression of genes in samples used for FDD analysis.

#### V.1.1.2 Reproducibility of FDD analysis may have been limited by insufficient lots of RNA

The use of anchored oligo(dT) primers to generate cDNA for FDD analysis was expected to specifically amplify polyadenylated mRNA. However, non-specific PCR amplification occurred when oligo(dT) primers bound to A-rich regions of 25S rRNA and were subsequently detected during FDD due to the abundance of rRNA template material. In order to reduce the number of false positives that arise from reverse transcription and PCR artifacts and from variation within populations, the parallel analysis of several independent lots of total RNA are recommended for FDD screening (Stein and Liang 2002). For the present study, only two independent lots of RNA were available for FDD analysis, and differential expression of many FDD fragments used for cloning was not reproducible in FDD screens of both lots of RNA. The use of only two independent lots of RNA may therefore have been insufficient for this study, since most positive FDD bands were subsequently determined to correspond to either genes for rRNA or ribosomal protein or non-differentially expressed genes.

#### FDD clones organized according to expression pattern

Pattern 1 of differential expression (from Results section: Figure 1), predicted for genes induced by conditions inducing alkaloid synthesis and regulated by the *A* and/or *B* loci, was used as a target pattern to screen FDD bands. Differential expression of endogenous genes represented by cloned FDD fragments was confirmed by Northern blot analysis, and FDD clones are classified according to their validated expression pattern as follows. Northern blot analysis showed differential expression similar to pattern 1 for the gene represented by FDD clone Y18a-9, and for genes represented by FDD clones JGJ331, JGJ332, and JGJ334 (isolated in a previous study by Dr. John Jelesko). However, the gene represented by clone A11-7 appeared to show an anomalous differential expression pattern and the gene represented by clone Y2-6 did not show

differential expression. Genes represented by A11-7 and Y2-6 therefore do not appear to be regulated by the *A* and/or *B* loci or by conditions inducing alkaloid synthesis. As with the rRNA clones, A11-7 and Y2-6 were likely artifacts of FDD, because differential expression of these fragments was not confirmed in a second lot of RNA during initial FDD analysis.

### V.1.3 Characterization of differentially expressed genes represented by FDD clones

FDD clones Y18a-9, JGJ331, JGJ332, and JGJ334 each showed homology to genes associated with stress and/or wounding response.

#### V.1.3.1 FDD clone Y18a-9 (anionic peroxidase-like protein)

Clone Y18a-9 showed strong homology to an anionic peroxidase of potato (Roberts et al. 1988), tomato TAP1 and TAP2 (Roberts and Kolattukudy 1989), and petunia P17 (Tournaire et al. 1996), with less significant homology to previously cloned tobacco leaf anionic peroxidases (Hiraga et al. 1999), indicating that clone Y18a-9 may represent a novel anionic peroxidase in tobacco. Anionic peroxidases of potato and tomato are induced by suberization-associated conditions, including pathogen infection, elicitor and ABA treatment, or wounding (Roberts et al. 1988, Roberts and Kolattukudy 1989). In petunia, P17 is induced by a low cytokinin level, which is associated with the onset of senescence (Tournaire et al. 1996). Wang et al. (2000) used a subtractive hybridization procedure to isolate differentially expressed cDNAs in *N. tabacum* B21 plants induced for alkaloid synthesis by topping, and found several cell wall-related proteins, including a lignin-forming anionic peroxidase, PR-45. Collinge and Boller (2001) used differential display (DD) to screen for potato genes induced by pathogen infection and wounding, and isolated a putative peroxidase, *Stprx2*. Anionic peroxidase is classified as a secretory plant peroxidase (class III plant peroxidase, EC 1.11.1.7) (Welinder 1992), which catalyzes an oxidoreduction reaction between hydrogen peroxide and a reductant. Peroxide-yielding reactions include oxidative bursts associated with the hypersensitive response (HR) plant defense against pathogens (Lamb and Dixon 1997). Anionic peroxidase may function in polymerization reactions leading to cell wall synthesis and repair, including lignification (Hammerschmidt and Kuc 1982), suberization (Espelie et al. 1986), and cross-linking of cell wall proteins (Bradley et al. 1992). Taken together, these results support a role for the anionic peroxidase represented by clone Y18a-9 in stress response. Nakamura and Matsuoka (1993)

suggest that a hydrophobic/acidic amino acid motif structure in the C-terminal propeptide of certain vacuolar proteins directs the protein to the vacuole. A conserved vacuolar targeting sequence was identified in the middle of the coding region of clone Y18a-9; however, this targeting sequence was not located in the C-terminal region of the anionic peroxidase, where sorting signals of vacuolar proteins, including barley coleoptile peroxidase (Kristensen et al. 1999), barley lectin (Bednarek and Raikhel 1992), and tobacco chitinase (Nakamura and Matsuoka 1993), are found.

#### V.1.3.2 FDD clone pJGJ331 (subtilisin protease-like protein)

Clone pJGJ331 showed homology to a gene in tomato for P69D subtilisin protease, a subfamily of the subtilase serine protease superfamily (EC 3.4.21.25). Tomato subtilases are thought to be involved in pathogen (Tornerio et al. 1996, 1997) and/or wound (Schaller and Ryan 1994) response. Animal subtilases, also referred to as proprotein convertases (PCs), function in post-translational processing of signal proteins, including hormones, growth factors and receptor proteins and also process viral and bacterial toxins (Seidah et al. 1994 and Nakayama 1997). Plant subtilases may function similarly, as evidenced by the discovery of a protein in tomato that crossreacts with antiserum against a *Drosophila* PC and interacts with systemin, a peptide wound signal (Schaller and Ryan 1994). A viral antifungal toxin overexpressed in tobacco plants is secreted in the correctly processed form, suggesting that a tobacco PC-like protease exists (Kinal et al. 1995). Although the function of plant subtilases is not well understood, a substrate of P69 subtilase has been identified in diseased tomato plants: a leucine-rich-repeat-containing tomato protein (LRP) thought to mediate signal transduction. LRP is upregulated in virus-infected tomato plants and processed proteolytically by the host-induced P69 subtilase during disease conditions (Tornerio et al. 1996). The P69 subtilisin protease-like gene represented by clone pJGJ331 may therefore function in signaling of conditions related to wounding or pathogenesis. Genes of the P69 subtilase subfamily are expressed in the roots, cotyledons, leaves and flowers of tomato plants (Meichtry et al. 1999). Tomato subtilase genes lack introns and contain long open reading frames coding for preprotein with an N-terminal signal peptide that targets the protein to the secretory system (Meichtry et al. 1999).

#### V.1.3.3 FDD clone pJGJ332 (purine permease-like protein)

The homology of clone pJGJ332 to an Arabidopsis purine transporter, *AtPUP1* (Gillissen et al. 2000), suggests that a similar purine transporter may exist in tobacco. Purines and purine derivatives are required for primary metabolic functions such as nucleic acid and phytohormone synthesis (Chen 1997) and cell energization, as well as for synthesis of secondary metabolites such as alkaloids (Leete 1967). Translocation of purine and pyrimidine nucleosides (Kamboj and Jackson 1984, Kombrink and Beevers 1983, Lee and Moffat 1994) and purine derivatives, including cytokinins (Fusseder et al. 1989) and the alkaloids caffeine (Mazzafera and Gonçalves 1999) and nicotine (Dawson 1942) has been observed in plants, indicating that transport mechanisms exist; however, very few nucleobase transporter genes have been identified in eukaryotes. *AtPUP1* encodes an integral membrane protein that functions as a transporter for adenosine and cytosine and is inhibited by purine-related compounds, including cytokinins, caffeine, and, to a lesser extent, nicotine (Gillissen et al. 2000). *AtPUP1* belongs to a large *AtPUP* gene family consisting of at least 15 divergent members (Gillissen et al. 2000). Although *AtPUP*-related sequences have been identified in several plants, including tomato, clone pJGJ332 only shows significant homology to *AtPUP1* in Arabidopsis. A maize purine transporter, Leaf Permease 1 (LPE1), which is unrelated to *AtPUP* proteins, and which has ubiquitous homologs in prokaryotes and eukaryotes, has been functionally expressed in fungi (Argyou et al. 2001). In discussing the commonality of functions of LPE1 in prokaryotes and eukaryotes, Argyou et al. (2001) notes that the lack of *AtPUP*-related sequences in prokaryotic, fungal and animal genomes suggests that *AtPUP* proteins transport plant-specific compounds. Interestingly, *AtPUP1* is expressed in all tissues of Arabidopsis except roots, whereas the tobacco gene represented by clone pJGJ332 was isolated from RNA extracted from root tissue. Gillissen et al. (2000) speculate that the lack of expression of *AtPUP1* in roots indicates that this gene may encode a protein that takes up root-derived purine derivatives from xylem into shoots. Clone pJGJ332 may therefore contain a gene fragment that encodes a similar transport system for purine derivatives in root tissue, more specifically as mechanism for nicotine transport into xylem, since nicotine is known to be synthesized in roots and translocated through the xylem to shoots and leaves.

#### V.1.3.4 FDD clone pJGJ334 (lipoxygenase-like protein)

Clone pJGJ334 showed homology to lipoxygenases (LOX; EC 1.13.11.12) of potato (Royo et al. 1996), tomato (Heitz et al. 1997), and tobacco (Veronesi et al. 1995). LOXs catalyze the hydroperoxidation of fatty acids such as linolenic acid, which is metabolized to form MeJA. Accumulation of MeJA activates plant defense genes and LOXs are therefore predicted to function in plant wound signaling (Vick and Zimmerman 1983). Heitz et al. (1997) identified a tomato LOX (involved in MeJA synthesis) which is rapidly induced within 30 to 50 minutes of wounding or systemin or MeJA application. LOXs may also mediate the localized HR associated with pathogen infection by catalyzing lipid peroxidation in the plant cell membrane, causing plant cell death and thus limiting pathogen spread and further plant damage (Keppler and Novacky 1987). Durrant et al. (2000) identified a cDNA fragment representing a putative tobacco LOX that is inducible during a race-specific pathogen response and by plant wounding. Rancé et al. (1998) observed suppression of the HR following pathogen infection in transgenic tobacco expressing antisense LOX constructs. Several isoforms of lipoxygenases have been characterized in plants. Royo et al (1996) identified three classes of LOX isoforms in potato based on the similarity of their deduced amino acid sequences: *Lox1*, *Lox2*, and *Lox3*. *Lox1* is expressed in tubers and roots, *Lox2* is expressed in leaves, and *Lox3* is expressed in leaves and roots (Royo et al. 1996). Both *Lox2* and *Lox3* predicted proteins contain a chloroplast targeting signal sequence (Royo et al. 1996). Three tobacco LOX genes have been sequenced, *tpoxCI* and *tpoxNI* (Hiraga et al. 1999) and *LOX1* (Veronesi et al. 1995). The region of homology of FDD clone pJGJ334 to known plant LOXs was too small to permit identification of the specific class of LOX of the represented gene, and the predicted protein sequence of pJGJ334 shows the same homology to several plant LOXs, including tobacco LOX1.

#### V.1.4 Conclusions of FDD analysis

FDD screening was used to detect a single differentially expressed gene, represented by FDD clone Y18a-9, in roots of wild type Burley 21 and mutant LA21 tobacco grown under both alkaloid-inducing and non-inducing conditions for one hour. Differential expression indicating coordinate regulation of the gene represented by Y18a-9 by the *A* and/or *B* loci was subsequently confirmed by Northern blot analysis. The effectiveness and reproducibility of future FDD

analyses may be improved by modifying 1. duration of root culture growth and 2. duration of induction treatment to optimize inducibility of known alkaloid biosynthetic mRNAs and 3. by analyzing additional independent lots of RNA to reduce false positive FDD bands resulting from PCR artifacts.

#### V.1.4.1 *A/B* regulon may be larger than previously thought

The range of functions of genes represented by FDD clone Y18a-9 and by previously isolated FDD clones pJGJ331, pJGJ332, and pJGJ334 suggests that the *A/B* regulon is not limited to only alkaloid biosynthetic genes. The regulation by A and/or B of alkaloid biosynthetic genes is supported by previous studies showing that nicotine biosynthetic enzyme activities and alkaloid content are correlated to tobacco *A/B* genotype. Saunders and Bush (1979) showed that the *A/B* regulon included nicotine biosynthetic enzymes PMT, QPRT, and MPO, and induced enzyme activity is correlated to tobacco genotype according to the order B21 > HI21 > LI21 > LA21. Nicotine content is similarly correlated to tobacco genotype (Legg and Collins 1971), and no phenotype differences (i.e. plant height, leaves per plant or days to flower), other than alkaloid content and susceptibility to insect damage, are observed between wild type Burley 21 tobacco and single *A* or *B* mutants HI21 and LI21 or double *A* and *B* mutant LA21 (Legg et al. 1970). The conclusion of the present study, that A and/or B regulate additional genes not involved in nicotine biosynthesis, is supported by results of Hibi et al. (1994), who performed a subtractive hybridization screen of wild type B21 and low alkaloid (LA21) mutant and isolated both a known nicotine biosynthetic gene, *PMT*, and a gene for an isoflavone reductase-like protein, *A622*, that does not appear to be involved in alkaloid biosynthesis. FDD clones Y18a-9, pJGJ331, pJGJ332, and pJGJ334 appear to represent genes that are associated with plant stress or defense response but not required for alkaloid biosynthesis, and future FDD screens of RNA from tobacco genotypes differing at the *A/B* loci are therefore expected to reveal additional non-nicotine biosynthetic genes regulated by A and/or B, which will more completely define the *A/B* regulon.

## V.2 Northern blot analysis

### V.2.1 Characteristic pattern of differential expression pattern of analyzed genes was observed

Pattern 1 of differential expression used to screen FDD fragments (from Results section: Figure 1) was confirmed by Northern blot analysis for genes represented by FDD clones Y18a-9, pJGJ331, pJGJ332, and pJGJ334. A characteristic pattern of differential expression was observed during Northern blot analysis of nicotine biosynthetic genes *PMT3*, *QPRT*, *ODC3*, and *ADC1*, indicating that these genes were inducible in both B21 and LA21 genotypes by conditions inducing alkaloid synthesis. Northern blot analysis provides the novel result that *PMT3*, *QPRT*, *ODC3*, and *ADC1* were inducible in LA21, and that *QPRT*, *ODC3*, and *ADC1* were inducible by auxin removal from root culture media. Basal expression levels of *PMT3*, *QPRT*, *ODC3*, and *ADC1* were higher in B21 than in LA21, which suggests coordinate regulation of these genes by A and/or B. Likewise, genes represented by clones Y18a-9, pJGJ331 and pJGJ332 appeared to be coordinately regulated. The gene represented by clone pJGJ334 showed a pattern of differential expression similar to nicotine biosynthetic genes in B21, although no signal was detected in LA21 samples and inducibility of the gene represented by pJGJ334 in LA21 therefore could not be determined. The genes represented by clone A11-7 and Y2-6 did not appear to be regulated by A and/or B or by conditions inducing alkaloid synthesis.

### V.2.2 Inducibility of nicotine biosynthetic genes supports previous results

Northern blot analysis showed significant *PMT3* induction in B21 by removal of auxin from root growth media, which supports previous results showing differential expression of *PMT* in B21 and other tobacco cultivars by several conditions inducing alkaloid synthesis, including auxin removal, topping, MeJA treatment, and wounding. For example, *PMT* was shown to be inducible in B21 by auxin removal from root culture media for one hour (Hibi et al. 1994) and by topping (Reichers and Timko 1999). *PMT* induction by MeJA has been observed in tobacco cultivar cv. BY-2 (Imanishi et al. 1998a) and *N. sylvestris* (Shoji et al. 2000). *PMT* induction by wounding has been observed in tobacco cv. NC95, and in *N. sylvestris* and *N. glauca* (Sinclair et al. 2000). The present study also supports previous results showing induction of *PMT* enzyme activity by topping in B21 (Saunders and Bush 1979) and in cv. BY (Misuzaki et al. 1973). *PMT* inducibility in a variety of tobacco cultivars is therefore well established; however, Reichers and Timko (1999) did not observe induction of *PMT* by topping in the *A/B* double mutant, LA21.

Results of the present Northern blot analysis provide evidence that *PMT3* is inducible in LA21 as well as in B21, consistent with the finding by Saunders and Bush (1979) of PMT enzyme induction in LA21 by topping.

Northern blot analysis showing *QPRT* induction in B21 supports previous results showing differential expression of *QPRT* in tobacco cv. BY-2 by MeJA (Imanishi et al. 1998a) and in *N. sylvestris*, *N. glauca* and tobacco cv. NC95 by wounding (Sinclair et al. 2000). *QPRT* enzyme activity was also previously found to be inducible by topping in B21 (Saunders and Bush 1979) and in cv. Samsun (Wagner et al. 1986). Similar to *PMT3*, *QPRT* was inducible in LA21 as well as in B21, which contrasts to earlier evidence by Saunders and Bush (1979) showing that *QPRT* enzyme activity in LA21 was not inducible by topping.

*ODC3* was also shown by Northern blot analysis to be inducible in both B21 and LA21, supporting previous results showing induction of *ODC* in B21 by topping (Wang et al. 2000) and in cv. BY-2 by MeJA treatment (Imanishi et al. 1998a). Misuzaki et al. (1973) showed that *ODC* enzyme activity was inducible by topping in cv. BY.

Previous studies have shown that *ADC* is inducible in B21 by topping (Wang et al. 2000), but is not inducible in BY-2 by MeJA (Imanishi et al. 1998a). Tiburcio and Galston (1986) showed that *ADC* enzyme activity was correlated with nicotine content in tobacco calli. Consistent with results of both Wang et al. (2000) and Tiburcio and Galston (1986), Northern blot analysis results presented here showed very weak induction of *ADC1* in B21 and LA21. The weakness of the Northern blot signal of *ADC1* induction also suggests that although *ADC* was not reported to be inducible by MeJA (Imanishi et al. 1998a), induction may have occurred during that experiment that was below detectable levels.

### V.3 QRT-PCR analysis

#### V.3.1 Significance of correlation between gene expression levels and genotype

QRT-PCR analysis indicated that mRNA accumulation levels of *PMT3*, *QPRT*, *ODC3*, and *ADC1* after induction were correlated to tobacco genotype in the order B21 = HI21 > LI21 > LA21, which is generally consistent with previous results showing that PMT and *QPRT* enzyme

activities after induction are correlated to tobacco genotype in the order B21 > HI21 > LI21 > LA21 (Saunders and Bush 1979). Overall gene expression levels of *ODC3* and *ADC1* in tobacco genotypes B21, HI21, LI21, and LA21 have not been studied previously. Thus, the results of QRT-PCR analysis provide additional evidence for coordinate regulation of *PMT3* and *QPRT* by products of the *A* and/or *B* loci and novel evidence for similar coordinate regulation of *ODC3* and *ADC1*. Consistent with Northern blot analysis results and enzyme activity measurements of PMT after topping (Saunders and Bush 1979), QRT-PCR results indicated that *PMT3*, *QPRT*, *ODC3*, and *ADC1* were inducible in all genotypes tested. The inducibility of nicotine biosynthetic genes in single mutants HI21 and LI21 and double mutant LA21 supports the argument that *A* and *B* mutations affect overall mRNA accumulation levels rather than gene inducibility, per se.

Surprisingly, QRT-PCR results for the gene represented by Y18a-9 did not show the same pattern of overall gene expression in the tested genotypes that was observed during Northern blot analysis. QRT-PCR results were consistent with Northern blot analysis results in that induction of endogenous *Y18a-9* by alkaloid-inducing conditions was observed in all the tested genotypes. QRT-PCR results indicated, however, that endogenous *Y18a-9* was more strongly inducible in LA21 than in B21, and that induced endogenous *Y18a-9* levels were higher in LA21 than in B21 during alkaloid-inducing conditions. Thus, in contrast to Northern blot analysis results, which indicated that expression of the gene represented by Y18a-9 was coordinately regulated by *A* and/or *B*, QRT-PCR results did not show a genotype effect. Since Northern blot analysis was performed using a single lot of RNA, while QRT-PCR analysis results consisted of averaged results of 4 lots of RNA, further Northern blot analysis on additional independent RNA lots may be necessary to resolve the effect of genotype on *Y18a-9* gene expression. No genotype or induction effect on gene expression was observed during QRT-PCR analysis of genes represented by Y2-6 and A11-7, which was consistent with Northern blot analysis results.

### V.3.2 Significance of relative mRNA accumulation levels analyzed by QRT-PCR

Expression levels of nicotine biosynthetic genes and genes represented by FDD clones were determined by QRT-PCR analysis and relative mRNA accumulation levels of *β-ATPase*, *PMT3*, *QPRT*, *ODC3*, *ADC1*, and *Y18a-9*, *A11-7*, and *Y2-6* endogenous genes were compared. The

genes are presented in order of decreasing mRNA abundance following alkaloid induction as: *PMT3* > *β-ATPase* > *ODC3* > *QPRT* = *ADC1* = *Y18a-9* > *Y2-6* > *A11-7*, with mRNA levels of *PMT3* approximately 100 times that of *A11-7*. QRT-PCR primers for *QPRT*, *ADC1*, *Y18a-9*, *A11-7* and *Y2-6* were designed to be gene-specific, while primers for *PMT-3* and *ODC3* could potentially amplify additional *PMT* and *ODC* genes, and it is therefore not surprising that mRNA accumulation levels of *PMT3* and *ODC3* were considerably higher than the other genes. Relative mRNA levels must be considered in evaluating the significance of fold-increase of gene expression due to genotype effect or induction treatment. For example, the most significant increases in gene expression were observed with *PMT3*, which showed the highest relative mRNA accumulation of all the genes tested. Increased variance reduced the significance of differential expression of genes expressed at lower levels. Levels of mRNA accumulation may not reflect actual protein levels or protein activity, therefore a comparison of relative mRNA accumulation cannot provide an accurate measure of overall enzyme function.

#### V.4 Extent and inducibility of *A/B* regulon

The following statements regarding the extent and inducibility of the *A/B* regulon are presented for discussion:

1. The *A/B* regulon was not limited to alkaloid biosynthetic genes, but included multiple defense-related genes with roles in alkaloid synthesis, possible alkaloid transport, possible wound signaling, and defense response. The *A/B* regulon may also include genes coding for proteins with primary metabolic functions.
2. Some genes in the *A/B* regulon may be inducible by different conditions and signaling pathways, such as pathogenesis, wounding, MeJA, and/or auxin treatment.
3. Transcriptional regulation of the *A/B* regulon by overlapping signaling pathways is consistent with multiple stimuli response either at the level of cis-acting promoter elements or at the level of transcription factors.

#### V.4.1 The A/B regulon may include genes with a range of defense-related functions

Taken together, the results of FDD, Northern blot and QRT-PCR analysis indicated that the *A/B* regulon includes previously identified nicotine biosynthetic genes *PMT3*, *QPRT*, *ODC3*, and *ADC1*, as well as genes represented by FDD clones pJGJ331, pJGJ332, and pJGJ334. Northern blot analysis results indicated that the gene represented by FDD clone Y18a-9 was coordinately regulated by A and/or B, whereas QRT-PCR analysis indicated no genotype effect on *Y18a-9* gene expression. The *A/B* regulon therefore may potentially coordinate the expression of genes with a range of defense-related functions, including alkaloid synthesis, possible alkaloid transport (purine-permease-like protein), possible wound signaling (subtilisin protease-like protein), and defense response (anionic peroxidase-like protein, lipoxygenase-like protein).

Previous studies have not definitively established the roles of ODC and ADC in providing the primary source of putrescine in nicotine synthesis. Tiburcio and Galston (1986) concluded that ADC is the primary route in generating putrescine for nicotine synthesis, and that ODC functions primarily in polyamine synthesis and cell growth. Imanishi et al. (1998a), however, demonstrated that mRNA levels of *ODC* in tobacco cell suspension cultures are increased by MeJA treatment, while mRNA levels of *ADC* are unaffected. The present study showed that *ODC3* and *ADC1* were coordinately regulated by A and/or B and inducible by conditions inducing alkaloid synthesis, which supports a role for both *ODC3* and *ADC1* in alkaloid synthesis. The present study also supported previous results showing that a gene with a role in primary metabolism, *QPRT*, is a member of the *A/B* regulon (Saunders and Bush 1979). The coordination of primary and secondary metabolic pathways in plant has been previously reported. For example, tryptophan is a primary metabolite precursor in terpenoid indole alkaloid (TIA) synthesis, and the transcription factor ORCA3 activates genes leading to both tryptophan and TIA synthesis, in a stress response mediated by MeJA (van der Fits and Memelink 2000). Induction of tryptophan biosynthetic genes in *Arabidopsis* is also coordinately regulated with accumulation of the indolic phytoalexin, camalexin, in response to pathogen infection (Zhao and Last 1996).

#### V.4.2 Previous studies show that multiple genes are induced by different conditions leading to alkaloid biosynthesis

Experimental treatment conditions inducing alkaloid synthesis include MeJA treatment (Imanishi et al. 1998a), removal of auxin from root culture media (Takahashi and Yamada 1972), and mechanical or insect-associated plant wounding (Baldwin 1989, Baldwin et al. 1994a, Baldwin 1999, Baldwin and Prestin 1999). Previous studies have shown that multiple genes with a range of diverse functions are differentially expressed in response to conditions inducing alkaloid synthesis. For example, Hibi et al. (1994) identified genes for both PMT and A622, (a putative isoflavone reductase involved in biosynthesis of isoflavonoid phytoalexins that accumulate at sites of pathogen infection) in a subtractive hybridization screen of *N. tabacum* cv. B21 and LA21 induced for alkaloid synthesis by auxin removal. Imanishi et al. (1998a, 1998b) used 2-D electrophoresis to screen translation products inducible by MeJA in cultured *N. tabacum* cells, and found cDNAs with homology to a putative glycosyltransferase, which is believed to be an early stress response gene, and to nicotine biosynthetic genes *ODC*, *SAMS*, and *QPRT*. Wang et al. (2000) performed a subtractive hybridization screen of *N. tabacum* cv. B21 root tissue induced by topping, and isolated 60 cDNAs with homology to diverse genes, including nicotine biosynthetic genes *ODC*, *SAMS*, *ADC*, and cell wall synthetic and signal transduction genes. A study by Hermsmeier et al. (2001) examined transcriptional changes in *N. attenuata* following insect attack, using differential display (DD) to isolate 27 differentially expressed cDNA fragments. Putative functions assigned to 15 of the 27 transcripts included primary metabolic functions, i.e. photosynthesis, electron transport, cytoskeleton, carbon and nitrogen metabolism and signaling, as well as secondary metabolic functions associated with wounding and pathogen response. Although most cDNAs representing genes with primary metabolic functions were down-regulated in response to insect attack, a putative Fd-GOGAT gene, coding for an enzyme that catalyzes the assimilation of nitrogen into glutamic acid, was up-regulated. Up-regulation of Fd-GOGAT may therefore facilitate the allocation of nitrogen resources to defense-related metabolites, consistent with previous studies showing that labeled nitrate is rapidly assimilated for nicotine synthesis following MeJA treatment and herbivory (Baldwin et al. 1994b and Baldwin 1998). The studies by Wang et al. (2000) and Hermsmeier et al. (2001) suggest that the topping- and/or wound-inducible transcriptome of tobacco is extensive. Based on the percentage

of the *N. attenuata* transcriptome that was analyzed by DD, Hermsmeier et al. (2001) predicted that the insect-responsive transcriptome of *N. attenuata* contains more than 500 different genes.

#### V.4.3 Different signaling pathways regulate common plant defense genes

Several signaling molecules are associated with wound response, including MeJA, auxin, salicylic acid (SA), and ethylene. The signaling pathways that regulate pathogen and wound response in plants have been reported to overlap, since pathogen infection is often associated with wounding or insect-caused plant damage (Reymond and Farmer 1998). Several defense related genes have been shown to be induced by more than one signaling pathway or induction stimuli. For example, Wang et al. (2001) identified topping-inducible tobacco cDNAs with homology to a putative ethylene responsive element binding (EREB) protein and to an auxin-regulated gene, and Hermsmeier et al. (2001) found that tobacco genes that were up- or down-regulated in response to insect attack were similarly induced or repressed by MeJA treatment. Mazeyrat et al. (1998) identified a sunflower gene, HaAC1, showing homology to auxin-inducible genes, that is inducible by pathogen infection. Sitbon and Perrot-Rechenmann (1997) identified several auxin-inducible genes in plants that were also induced by SA application or by wounding. Consistent with these studies, the present study identified three FDD clones by differential expression in response to removal of auxin from root culture, that putatively coded for subtilisin protease, anionic peroxidase and lipoxygenase, thought to function in pathogen response.

#### V.4.4 Promoter elements permit induction of defense-related genes by different stimuli

In an effort to understand how common plant defense responses may be inducible by different conditions, Rushton et al. (2002) showed that a range of cis-acting synthetic promoter sequences were responsive to both pathogens and to wounding. Several cis-acting elements, i.e. GCC boxes (Ohme-Tagaki et al. 2000), found in defense genes, jasmonate and elicitor response elements (JERE) (Menke et al. 1999), which bind ORCA transcription factors, and W boxes (Rushton et al. 1996 and Eulgem et al. 2000), which bind WRKY transcription factors, were able to mediate gene transcription in response to both pathogens and wounding. Inducibility of these elements by multiple stimuli supports convergence of pathogen and wound response at the level of promoter elements. Cis-acting elements have been located in alkaloid biosynthetic genes, although not in

nicotine biosynthetic genes. The promoter of the strictosidine synthase gene (*Str*), leading to TIA synthesis, has been found to contain two jasmonate and elicitor responsive sequences: the BA region and the jasmonate- and elicitor-responsive element (JERE) (Menke et al. 1999; van der Fits et al. 2000). Shoji et al. (2000) found that approximately 0.25 kb of the conserved 5'-flanking region of three *PMT* genes in *N. sylvestris* was sufficient to mediate MeJA induction of a reporter gene, although no JERE boxes or known cis-acting elements have been identified in *PMT*. This result leads to speculation that inducibility of defense-related genes putatively regulated by A and/or B may be due to an unknown promoter element(s) that is inducible by several induction factors, such as MeJA, auxin removal, pathogen infection and wounding.

#### V.4.5 MAP kinase cascades mediate transduction of multiple signaling pathways

Mitogen-activated protein kinases (MAPKs) or proteins that interact with MAPKs may be a factor in the convergence of plant defense responses to pathogen infection and wounding (Bent 2001). MAP kinase cascades consist of MAP kinase kinase kinase (MAPKKK) proteins, which phosphorylate MAP kinase kinase (MAPKK) proteins, which phosphorylate MAPKs.

Phosphorylated MAPKs are then transported to the nucleus, in order to phosphorylate specific transcription factors. Different signaling pathways may activate a MAPK that in turn activates a specific transcription factor, thus inducing expression of a common gene(s) in response to different stimuli. For example, two MAPKs, which are induced by pathogen infection in tobacco, are also induced by wounding and SA: wound-induced protein kinase (WIPK) and SA-induced protein kinase (SIPK), respectively (Romeis et al. 1999). Work by Kotvun et al. (2000) suggests that three closely related MAPKKKs in *Arabidopsis* both mediate the activation of WIPK and SIPK and negatively regulate auxin-induced gene expression. Although the identity and function of the proteins coded by the *A* and *B* loci is unknown, the results of the present study showing that the *A/B* regulon consists of genes inducible by multiple signaling pathways is consistent with speculation that regulation by A and/or B may involve a MAP kinase cascade.

#### V.4.6 Future investigation of A/B regulon: characterization and transcriptional regulation

Future experimentation to determine the role of different environmental stimuli and signaling pathways in transcriptional regulation and to identify genes regulated by A and/or B and will be necessary to characterize the *A/B* regulon. As a first step, identification of full-length tobacco

cDNAs corresponding to the differentially expressed genes represented by FDD clones Y18a-9, pJGJ331, pJGJ332, and pJGJ334, will facilitate analysis of gene flanking sequences to identify regions that confer gene inducibility. To investigate any involvement of kinase and MeJA signaling cascades in transcription of the *A/B* regulon, the identification of tobacco homologs of signaling pathway mutants identified in other plants may be useful. For example, an *mpk4* mutant has been identified in Arabidopsis that is activated for SA responses but blocked for MeJA responses, suggesting both a positive and negative role for MAPK cascades in defense response (Petersen et al. 2000). The octadecanoid pathway tomato mutant, JL5, which is unable to accumulate MeJA in response to wounding and elicitor induction, shows increased susceptibility to insect attack (Howe et al. 1996). The identification of homologous mutations in tobacco might promote study of signal transduction and transcriptional response of the *A/B* regulon, and ultimately, facilitate the functional characterization of A and/or B.

#### V.5 Conclusions of HPLC analysis

HPLC analysis of nicotine content in root tissue of B21, HI21, LI21, and LA21 supported previous results showing that nicotine content is correlated to genotype in the order B21 > HI21 > LI21 > LA21. Root nicotine levels of each genotype relative to B21 were: B21 = 100, HI21 = 88.5, LI21 = 68.5, and LA21 = 37.7. Saunders and Bush (1979) measured relative nicotine levels as: B21 = 100, HI21 = 71, LI21 = 46, LA21 = 26. Although Legg and Collins (1971) found significantly lower relative nicotine levels in LA21, similar relative nicotine levels were reported for HI21 and LI21: B21 = 100, HI21 = 91.7, LI = 55.5, and LA21 = 7.1. Differences in relative nicotine levels may be due in part to different experimental conditions used in the previous studies: nicotine was analyzed in different tissues (roots versus leaves), under different sampling conditions, and using different quantification methods. This correlation between nicotine content and genotype is consistent with the results of QRT-PCR analysis which indicated a similar correlation between levels of nicotine biosynthetic gene mRNA and genotype. In this study, intercellular nicotine levels did not increase following alkaloid induction. The lack of nicotine synthesis following auxin removal from culture media indicated that the conditions of alkaloid induction, specifically the 8 hour induction period, did not result in a detectable difference in nicotine accumulation within root tissue. Previous studies have shown that leaf nicotine content increases within 24 hours of topping (Saunders and Bush 1979) and that nicotine content of

tobacco cv. BY cell culture increases approximately 12 hours after MeJA treatment Imanishi et al 1998a). Additional HPLC analyses of root tissue exposed to longer induction treatment periods may therefore be necessary in order to measure increased nicotine synthesis resulting from induction of nicotine biosynthetic genes. Since nicotine is transported out of the root cells, additional studies measuring the nicotine content of the root culture media are also necessary to determine overall nicotine accumulation in each genotype.

#### V.6 Summary

FDD was used to screen total RNA isolated from B21 and LA21 tobacco root cultures that were induced for alkaloid synthesis. Four of thirteen cloned FDD fragments showed sequence homology to genes with defense-related functions but no known role in alkaloid biosynthesis: anionic peroxidase, subtilisin protease, purine permease, and lipoxygenase. The effectiveness of the FDD procedure in detecting differentially expressed gene fragments was limited by experimental conditions, which may be improved by modifying the duration of root growth and induction treatment, and by analyzing multiple independent lots of total RNA. Future FDD analyses incorporating these modifications is expected to be a valuable technique for identifying additional genes coordinately regulated by A and/or B.

Northern blots of transcripts of defense-related genes identified by FDD and known alkaloid biosynthetic genes, *PMT3*, *ODC3*, *ADC1*, and *QPRT* showed a similar pattern of differential expression. The coordinate regulation by A and B of genes with defense related functions but no known role in alkaloid biosynthesis suggests that the *A/B* regulon is not limited to alkaloid biosynthetic genes, but includes multiple genes with defense-related functions. QRT-PCR analysis of nicotine biosynthetic genes and genes represented by confirmed differentially expressed FDD clones showed increased mRNA accumulation in response to alkaloid induction in WT and *A/B* single and double mutant genotypes, which suggests that the *A* and *B* mutations affect overall mRNA accumulation levels, rather than gene inducibility, per se. QRT-PCR analysis also showed that mRNA accumulation levels of *PMT3* were highest relative to the other tested genes and that mRNA accumulation levels of the endogenous genes represented by tested FDD clones were relatively low, although mRNA levels are not necessarily correlated with protein activity and a comparison of relative mRNA levels cannot provide an accurate measure

of overall enzyme function. The identification of relatively low abundance gene fragments by FDD demonstrates the sensitivity of FDD as a method for gene discovery.

HPLC analysis of nicotine accumulation in root tissue of all tested genotypes supported previous studies showing that nicotine accumulation is correlated to genotype, but an 8 hour alkaloid induction period did not result in detectable increases of intercellular nicotine. Additional HPLC analyses of root tissue exposed to longer induction treatment periods and analysis of the nicotine content of the root culture media may provide a better assessment of increased nicotine synthesis resulting from induction of nicotine biosynthetic genes.

## V.7 Bibliography

- Argyrou, E., Sophianopoulou, V., Schultes, N., Diallinas, G. 2001. Functional characterization of a maize purine transporter by expression in *Aspergillus nidulans*. *Plant Cell* 13: 953-964.
- Baldwin, I.T. 1989. Mechanism of damage-induced alkaloid production in wild tobacco. *J. Chem. Ecol.* 15(5): 1661-1680.
- Baldwin, I.T., Schmelz, E.A., and Ohnmeiss, T.E. 1994a. Wound-induced changes in root and shoot jasmonic acid pools correlate with induced nicotine synthesis in *Nicotiana sylvestris* Spegazzini and Comes. *J. Chem. Ecol.* 20: 2139-2157.
- Baldwin, I.T., Karb, M.J., Ohnmeiss, T.E. 1994b. Allocation of <sup>15</sup>N from nitrate to nicotine: production and turnover of a damage-induced mobile defense. *Ecology* 75: 1703-1713.
- Baldwin, I.T. 1998. Jasmonate-induced responses are costly but benefit plants under attack in native populations. *Proc. Natl. Acad. Sci. USA* 95: 8113-8118.
- Baldwin, I.T., 1999. Inducible nicotine production in native *Nicotiana* as an example of adaptive phenotypic plasticity. *J. Chem. Ecol.* 25: 3-30.
- Baldwin, I.T., Prestin, C.A. 1999. The eco-physiological complexity of plant responses to insect herbivores. *Planta* 208: 137-145.
- Bent, A.F. 2001. Plant mitogen-activated protein kinase cascades: negative regulatory roles turn out positive. *Proc. Natl. Acad. Sci. USA* 98: 784-786.
- Bradley, D.J., Kjellborn, P., Lamb, C.J. 1992. Elicitor- and wound-induced oxidative cross-linking of a proline-rich plant cell wall protein: a novel, rapid defense response. *Cell* 70: 21-30.
- Chaplin, J.F. and Weeks, W.W. 1976. Association between percent total alkaloids and other traits in the flue-cured tobacco. *Crop Sci.* 16(3): 416-418.
- Chen, C.M. 1997. Cytokinin biosynthesis and interconversion. *Physiol. Plant.* 101: 665-673.
- Collinge, M. and Boller, T. 2001. Differential induction of two potato genes, *Stprx2* and *StNAC*, in response to infection by *Phytophthora infestans* and to wounding. *Plant Mol. Biol.* 46: 521-529.
- Creelman, R.A., Tierney, M.L., and Mullet, J.E. 1992. Jasmonic acid/methyl jasmonate accumulation in wounded soybean hypocotyls and modulate wound gene expression. *Proc. Natl. Acad. Sci. USA* 89: 4938-4941.
- Dawson, R.F. 1942. Accumulation of nicotine in reciprocal grafts of tomato and tobacco. *Am. J. Bot.* 29: 66-71.

- Doares, S.H., Syrovets, T., Weiler, E.W., Ryan, C.A. 1995 Oligogalactouronides and chitosan activate plant defensive genes through the octadecanoid pathway. *Proc. Natl. Acad. Sci. USA* 92: 4095-4098.
- Durrant, W.E., Rowland, O., Piedras, P., Hammond-Kosack, K.E., Jones, J.D.G. 2000. cDNA-AFLP reveals a striking overlap in race-specific resistance and wound response gene expression profiles. *Plant Cell* 12: 963-977.
- Espelie, K.E., Fransechi, V.R., Kolattukudy, P.E. 1986. Immunocytochemical localization and time course of appearance of an anionic peroxidase associated with suberization in wound-healing potato tuber tissue. *Plant Physiol.* 81: 487-492.
- Eulgem, T., Rushton, P.J., Robatzek, S., Somssich, I.E. 2000. The WRKY superfamily of plant transcription factors. *Trends Plant Sci.* 5: 199-206.
- Ferl, R. and Paul, A-L. 2000. Genome organization and expression. In: *Biochemistry and Molecular Biology of Plants*. Buchanan, B., Gruissem, W., Jones, R. eds. American Society of Plant Physiologists, Rockville, MD. p. 324.
- Fusseder, A., Siegler, P., Peters, W., Beck, E. 1989. Turnover of O-glucosides of dihydrozeatin and dihydrozeatin-9-riboside during the cell growth cycle of photoautotrophic cell suspension cultures of *Chenopodium rubrum*. *Bot. Acta* 102: 335-340.
- Geerts, A., Feltkamp, D., Rosahl, S. 1994. Expression of lipoxygenase in wounded tubers of *Solanum tuberosum* L. *Plant Physiol.* 105: 269-277.
- Hammerschmidt, R. and Kuc, J. 1982. Lignification as a mechanism for induced systemic resistance in cucumber. *Physiol. Plant Pathol.* 20: 61-71.
- Heitz, T., Bergey, D.R., Ryan, C.A. 1997. A gene encoding a chloroplast-targeted lipoxygenase in tomato leaves is transiently induced by wounding, systemin and methyl jasmonate. *Plant Physiol.* 114: 1085-1093.
- Hermesmeier, D., Schittko, U., Baldwin, I.T. 2001. Molecular interactions between the specialist herbivore *Manduca sexta* (Lepidoptera, Sphingidae) and its natural host *Nicotiana attenuata*. I. Large-scale changes in the accumulation of growth- and defense-related plant mRNAs. *Plant Physiol.* 125: 683-700.
- Hiraga, S., Ito, H., Matsui, H., Honma, M., Ohashi, Y. 1999. cDNA sequences for two novel tobacco peroxidase isoenzymes (Accession Nos. AB027752 and AB027753). (PGR99-109) *Plant Physiol.* 120: 1205.
- Howe, G.A, Lightner, J., Browse, J., Ryan, C.A. 1996. An octadecanoid mutant (JL5) of tomato is compromised in signaling for defense against insect attack. *Plant Cell* 8: 2067-2077.

- Imanishi, S., Hashizumi, K., Nakakita, M., Kojima, H., Matsubayashi, Y., Hashimoto, T., Sakagami, Y., Nakamura, K. 1998a. Differential induction by methyl jasmonate of genes encoding ornithine decarboxylase and other enzymes involved in nicotine biosynthesis in tobacco cell cultures. *Plant Mol. Biol.* 38: 1101-1111.
- Imanishi, S., Hashizumi, K., Kojima, H., Ichihara, A., Nakamura, K. 1998b. An mRNA of tobacco cell that is rapidly inducible by methyl jasmonate in the presence of cycloheximide codes for a putative glycosyltransferase. *Plant Cell Physiol.* 39: 202-211.
- Kamboj, R.K. and Jackson, J.F. 1987. Purine nucleoside transport in *Petunia* pollen is an active, carrier-mediated system not sensitive to nitrobenzylthioinosine and not renewed during pollen tube growth. *Plant Physiol.* 84: 688-691.
- Kenton, A., Parokony, A.S., Gleba, Y.Y., Bennett, M.D. 1993. Characterization of the *Nicotiana tabacum* L. genome by molecular cytogenetics. *Mol. Gen. Genet.* 240: 159-169.
- Keppler, L.D. and Novacky, A. 1987. The initiation of lipid peroxidation during bacteria-induced hypersensitive reaction. *Physiol. Mol. Plant Pathol.* 30: 233-245.
- Kinal, H., Park, C-M., Berry, J.O., Koltin, Y., Bruenn, J.A. 1995. Processing and secretion of a virally encoded antifungal toxin in transgenic tobacco plants: evidence for a *kex2p* pathway in plants. *Plant Cell* 7: 677-688.
- Kombrink, E. and Beevers, H. 1983. Transport of purine and pyrimidine bases and nucleosides from endosperm to cotyledons in germinating castor bean seedlings. *Plant Physiol.* 73: 370-376.
- Kovtun, Y., Chiu, W.L., Zeng, W., Sheen, J. 1998. Suppression of auxin signal transduction by a MAPK cascade in higher plants. *Nature* 395(6703): 716-720.
- Kovtun Y, Chiu WL, Tena G, Sheen J. 2000. Functional analysis of oxidative stress-activated mitogen-activated protein kinase cascade in plants. *Proc. Natl. Acad. Sci. USA.* 97(6): 2940-2945.
- Kuno, N., Muramatsu, T., Hamazato, F., Furuya, M. 2000. Identification by large-scale screening of phytochrome-regulated genes in etiolated seedlings of *Arabidopsis* using a fluorescent differential display technique. *Plant Physiol.* 122: 15-24.
- Lamb, C. and Dixon, R.A. 1997. The oxidative burst in plant disease resistance. *Annu. Rev. Plant Physiol. Plant Mol. Biol.* 48: 251-275.
- Lee, D. and Moffat, B.A. 1994. Adenine salvage activity during callus induction and plant growth. *Physiol. Plant.* 90: 739-747.
- Leete, E. 1967. Biosynthesis of the *Nicotiana* alkaloids XI. Investigation of tautomerism in N-methyl-D-pyrrolinium chloride and its incorporation into nicotine. *J. Am. Chem. Soc.* 89: 7081.

- Legg, P.D., Collins, G.B., Litton, C.C. 1970. Registration of LA Burley 21 tobacco germplasm. *Crop Sci.* 10:212.
- Legg, P.D. and Collins, G.B. 1971. Inheritance of percent total alkaloids in *Nicotiana tabacum* L. II. Genetic effects of two loci in Burley 21 X LA Burley 21 populations. *Can. J. Cytol.* 13: 287-291.
- Liang, P., Pardee, A.B. 1992. Differential display of eukaryotic messenger RNA by means of the polymerase chain reaction. *Science* 257: 967-971.
- Mazeyrat, F., Mouzeyar, S., Nicholas, P., Tourvielle de Labrouhe, D., Ledoigt, G. 1998. Cloning, sequence and characterization of a sunflower (*Helianthus annuus* L.) pathogen-induced gene showing sequence homology with auxin-induced genes from plants. *Plant Mol. Biol.* 38: 899-903.
- Mazzafera, P. and Gonçalves, K.V. 1999. Nitrogen compounds in the xylem sap of coffee. *Phytochemistry* 50: 383-386.
- Menke, F.L.H., Champion, A., Kijne, J.W., Memelink, J. 1999. A novel jasmonate- and elicitor-responsive element in the periwinkle secondary metabolite biosynthetic gene *Str* interacts with a jasmonate- and elicitor-inducible AP2-domain transcription factor, ORCA2. *EMBO J.* 18: 4455-4463.
- Misuzaki, S., Tanabe, Y., Noguchi, M., Tamaki, E. 1973. Changes in the activities of ornithine decarboxylase, putrescine N-methyltransferase and N-methylputrescine oxidase in tobacco roots in relation to nicotine biosynthesis. *Plant Cell Physiol.* 14: 103-110.
- Nakayama, K. 1997. Furin: a mammalian subtilisin/kex2p-like endoprotease involved in processing of a wide variety of precursor proteins. *Biochem J.* 327: 625-635.
- Ohme-Tagaki, M., Suzuki, K., Shinshi, H. 2000. Regulation of ethylene-induced transcription of defense genes. *Plant Cell Physiol.* 41: 1187-1192.
- Opperman, C.H., Lommel, S.A., Sosinski, B., Burke, M., Lakey, N., He, L., Brierly, R., Salstead, A., Gadani, F., Hayes, A. 2003. Poster P32: Genome sequencing and EST's. The tobacco genome initiative. Plant & Animal Genomes XI Conference. San Diego, CA. [http://www.intl-page.org/11/abstracts/P01\\_P32\\_XI.html](http://www.intl-page.org/11/abstracts/P01_P32_XI.html).
- Petersen, M., Brodersen, P., Naestaed, H., Andreasson, E., Lindhart, U., Johansen, B., Nielsen, H.B., Lacy, M., Austin, M.J., Parker, J.E., Sharma, S.B., Klessig, D.F., Martienssen, R., Mattsson, O., Jensen, A.B., Mundy, J. 2000. Arabidopsis map kinase 4 negatively regulates systemic acquired resistance. *Cell* 103: 1111-1120.
- Rancé, I., Fournier, J., Esquerré-Tugayé, M-T. 1998. The incompatible interaction between *Phytophthora parasitica* var. *nicotianae* race 0 and tobacco is suppressed in transgenic plants expressing antisense lipoxygenase sequences. *Proc. Natl. Acad. Sci. USA* 95: 6554-6559.

- Reichers, D.E. and Timko, M.P. 1999 Structure and expression of the gene family encoding putrescine N-methyltransferase in *Nicotiana tabacum*: new clues to the evolutionary origin of cultivated tobacco. *Plant Mol. Biol.* 41: 387-401.
- Reymond, P. and Farmer, E.E. 1998. Jasmonate and salicylate as global signals for defense gene expression. *Curr. Opin. Plant Biol.* 1: 404-411.
- Romeis, T., Piedras, P., Zhang, S., Klessig, D.F., Hirt, H. Jones, J.D.G. 1999. Rapid Avr9- and Cf-9-dependent activation of MAP kinases in tobacco cell cultures and leaves: convergence of resistance gene, elicitor, wound, and salicylate responses. *Plant Cell* 11: 273-287.
- Royo, J., Vancanneyt, G., Perez, A.G., Sanz, C., Stormann, K., Rosahl, S., Sanchez-Serrano, J.J. 1996. Characterization of three potato lipoxygenases with distinct enzyme activities and different organ-specific and wound-regulated expression patterns. *J. Biol. Chem.* 274: 36446-36455.
- Rushton, P.J., Torres, J.T., Parniske, M., Wernert, P., Hahlbrock, K., Somssich, I.E. 1996. Interaction of elicitor-induced DNA binding proteins with elicitor response elements in the promoters of parsley PR1 genes. *EMBO J.* 15: 5690-5700.
- Rushton, P.J., Reinstadler, A., Lipka, V., Lippok, B., Somssich, I.E. 2002. Synthetic plant promoters containing defined regulatory elements provide novel insights into pathogen- and wound-induced signaling. *Plant Cell* 14: 749-762.
- Saunders, J.W. and Bush, L.P. 1979. Nicotine biosynthetic enzyme activities in *Nicotiana tabacum* L. genotypes with different alkaloid levels. *Plant Physiol.* 64: 236-240.
- Schaller, A. and Ryan, C.A. 1994. Identification of a 50-kDa systemin-binding protein in tomato plasma membranes having Kex2p-like properties. *Proc. Natl. Acad. Sci. USA* 91: 11802-11806.
- Seidah, N.G., Chrétien, M., Day, R. 1994. The family of subtilisin/kexin likepro-protein and pro-hormone convertases: Divergent or shared functions. *Biochimie* 76: 197-209.
- Sembdner, G. and Parthier, B. 1993. The biochemistry and the physiological and molecular actions of jasmonates. *Annu. Rev. Plant Physiol Plant Mol. Biol.* 44: 569-589.
- Shoji, T., Yamada, Y., Hashimoto, T. 2000. Jasmonate induction of putrescine N-methyltransferase genes in the root of *Nicotiana glauca*. *Plant Cell Physiol.* 41(7): 831-839.
- Sinclair, S.J. Murphy, K.J. Birch, C.D., Hamill, J.D. 2000. Molecular characterization of quinolinate phosphoribosyltransferase (*QPRTase*) in *Nicotiana*. *Plant Mol. Biol.* 44: 603-617.
- Sitbon, F. and Perrot-Rechenmann, C. 1997. Expression of auxin-regulated genes. *Physiol. Plant.* 100: 443-455.
- Stein, J. and Liang, P. 2002. Differential display technique: a general guide. *CMLS* 59: 1235-1240

- Takahashi, M. and Yamada, Y. 1972. Regulation of nicotine production by auxins in tobacco cultured cells in vitro. *Agr. Biol. Chem.* 37(7): 1755-1757.
- Tiburcio, A.F., and Galston, A.W. 1986. Arginine decarboxylase as the source of putrescine for tobacco alkaloids. *Phytochemistry* 25: 107-110.
- Tornero, P., Mayda, E., Gomez, M.D., Canas, L., Conejero, V., Vera, P. 1996. Characterization of LRP, a leucine-rich-repeat (LRR) protein from tomato plants that is processed during pathogenesis. *Plant J.* 10: 315-330.
- Tornero, P., Conejero, V., Vera, P. 1996. Primary structure and expression of a pathogen-induced protease (PR-P69) in tomato plants: similarity of functional domains to subtilisin-like endoproteases. *Proc. Natl. Acad. Sci. USA* 93: 6332-6337.
- Tornero, P., Conejero, V., Vera, P. 1997. Identification of a new pathogen-induced member of the subtilisin-like protease family from plants. *J. Biol. Chem.* 272: 14412-14419.
- Tournaire, C., Kushnir, S., Bauw, G., Inze, D., Teysseidier de la Serve, B., and Renaudin, J-P. 1996. A thiol protease and an anionic peroxidase are induced by lowering cytokinins during callus growth in *Petunia*. *Plant Physiol.* 11: 159-168.
- van der Fits, L. and Memelink, J. 2000. ORCA3, a jasmonate-responsive transcriptional regulator of plant primary and secondary metabolism. *Science* 289: 295-297.
- Van der Hoeven, R., Ronning, C., Giovannoni, J., Martin, G., Tanksley, S. 2002. Deductions about the number, organization, and evolution of genes in the tomato genome based on analysis of a large expressed sequence tag collection and selective genomic sequencing. *Plant Cell* 14: 1441-1456.
- Véronési, C., Fournier, J., Rickauer, M., Marolda, M., Esqerré-Tugayé, M-T. 1995. Nucleotide sequence of an elicitor-induced tobacco lipoxygenase cDNA (GenBank X84040). *Plant Physiol.* 108: 1342.
- Vick, B.A and Zimmerman, D.C. 1983. The biosynthesis of jasmonic acid: a physiological role for plant lipoxygenase. *Biochem. Biophys. Res. Commun.* 111: 470-477.
- Wagner, R. Feth, F., Wagner, K.G. 1986. The regulation of enzyme activities of the nicotine pathway in tobacco. *Physiol. Plant.* 68: 667-672.
- Wang, J., Sheehan, M., Brookman, H., Timko, M. 2000. Characterization of cDNAs differentially expressed in roots of tobacco (*Nicotiana tabacum* cv Burley 21) during the early stages of alkaloid biosynthesis. *Plant Sci.* 158: 19-32.
- Welinder, K.G. 1992. Superfamily of plant, fungal and bacterial peroxidases. *Curr. Opin. Struct. Biol.* 2: 388-393.

Zhao, J. and Last, R.L. 1996. Coordinate regulation of the tryptophan biosynthetic pathway and indolic phytoalexin accumulation in *Arabidopsis*. *Plant Cell* 8: 2235-2244.

## APPENDIX A. Nucleotide sequences of cloned FDD fragments

Arbitrary 10mer primers and anchored-C oligo(dT) primer sites are underlined and stop codons are indicated by \*. Translation frame for BLASTX protein homology is indicated.

### HIGH-PRIORITY REED FDD CLONES

#### 1. A11-7 (glucosyltransferase/cellulose synthase-like protein) frame + 2

```
S I A V R A H L C G W K F I Y V D D V R
2  tcaatcgccgtcagagcacacttgtgtggctggaaatctatggtgatgacgtaagg 61

A L C E L P E S Y E A Y K K Q Q H R W H
62  gcgctttgtgagttgccagaatcatatgaagcttacaaaaagcagcagcaccggttgcat 121

S G P M Q L F R L C L P S I L K S K I S
122 tctggtccaatgcagctcttttagactatgtctcccttcaatcttgaagtccaagatctct 181

V W K K A N L I F L F F L L R K L I L P
182 gtctggaagaaggccaacctgatattcctattctttcttctaaggaagctgatattacct 241

F Y S F T L F C I I L P L T M F I P E A
242 ttttactcattcacactgttctgtattatacttccactaacaatgttcataccggaagcc 301

E L P P W V I C Y I P I V M S I L N I L
302 gagttaccccccttgggtgatctgttatatccctatagtcatgtccattttgaacatcctt 361

P S P K S F P F L M P Y L L F E N T M S
362 ccatcgccaaagtctttccctttcctgatgccataccttctattcgagaacacaatgtcc 421

V T K F N A M V S G L F Q L G S A Y E W
422 gtgacaaaattcaatgccatggtgtcgggactatctcagtttaggcagcgcctacgaatgg 481

V V T K K T G R A S E S D L V A L A E R
482 gtagtcaccaagaaaacaggtagagcatctgagtcggacttagtagcacttgctgagagg 541

E S K N M N E E K I S R R L S E S G L E
542 gaatcgaagaatatgaacgaagagaaaatctcaagaaggttgtctgaatctggtctagaa 601

L F E K K K K
602 ctattcgaaaaaaaaaaaaaac 623
```

#### 2. Y18a-9 (anionic peroxidase-like protein) frame + 2

```
V E S A A S I L T L N N N N A E Q N S D
2  gtggagtcagcagccagcattttaaccctaaataataataatgctgagcaaaattcagac 61

S K L T Q P L S P S A C I F S A V R R V
62  agcaagttaactcaaccattatctccatcggcacatcttctctgctggttcgacgagtt 121

V N R A I D R E R R M G A S L I R L H F
```

122 gttaacagagccattgatagagaaagacgcatgggagcttctctcattcgtctccatttc 181  
 H D C F V D G R D G G V L L D D I P G S  
 182 catgactgctttgttgatggtcgcatggaggagttcttctagacgatattcccggatca 241  
 F Q G E K T S P P N N N S A R G F E V I  
 242 ttccaaggggaaaaaacctcgccaccaacaactcagccagaggttttgaagtcata 301  
 E Q A K Q R V K D T C P N T P V S C A D  
 302 gaacaagctaaacaaagagtaaaagatacttgtcccaacacgcctgtatcttgcgagac 361  
 I L A I A A R D S V V K L G G Q G Y N V  
 362 atcttagctattgctgctcgtgattctgttggttaaactaggaggacaaggctataacggt 421  
 A L G R R D A R A A N F T G A L T Q L P  
 422 gcacttgggagaagagatgcaagagcggccaacttcactgggtgctttaactcagcttcca 481  
 A P F D N L T V Q I R K K K K N  
 482 gctccggttcgacaatctaaccgtccaataagaaaaaaaaaaaaaaaaaac 529

### 3. D15-12 (disease resistance-like protein) frame +1

S S V L E E L Q I L X C T E L M E I P D  
 1 tcatccgtgcttgaggaattacaataactagrctgtactgagcttatggagatcccggac 60  
 S F G D I F S L K Y I S L L G S G Q L E  
 61 agttttggcgatattttttcattaaagtatatctcactggtgggcagcgggtcaacttgaa 120  
 V S A T R I K E Y V A D M T G E D K L E  
 121 gtttcagccacaaggattaaggaatatggttcagatatgacgggagaagacaagcttgag 180  
 V K C N W \* V H A R D G S \* \* V R N Y L  
 181 gtaaagtgcaactggtgagtgcatgctcgagatggatcatagtaggtccgtaattatctt 240  
 D K S L \* L G H T N L L T S F L H \* F P  
 241 gacaaatctctgtgactaggtcatacgaatttattaacttcattcctacattaatttcct 300  
 F I L F F P I V V \* Y S N D Y Q V L L K  
 301 tttatattattttttcccattgtggtttaatacagtaatgattatcaagtattactgaaa 360  
 K K K N  
 361 aaaaaaaaaaaaaac 372

### 4. Y2-6 ( tumor-related protein) frame +3

I A A S W K L Y K N G V G C G A C Y Q V  
 3 atcgccgcatcctggaaactctataagaatggagttggttggtgcatgttatcaggtg 62  
 R C K D K A L C S D V G V K V K V T D S  
 63 aggtgcaaggacaaggcactatgcagtgacgtgggagtttaaggtgaaggtgacagacagt 122  
 G E G P G T D F I L S S D A F A K M A K  
 123 ggagaagggccaggaactgacttcattctaagctcagatgctttcgccaaaatggctaaa 182

H P K L A H M L F P K G V V D V D Y K R  
 183 catcctaagtttagctcacatggttcccaaagggcgtggctgatgtcgattacaaaaga 242  
 V S C K Y G N L I I K V N E H S N Y N G  
 243 gtttcttgcaaatatggcaatctcattatcaaggtcaatgaacatagcaactataatggc 302  
 Y L A I L L L N N G G Y A D I L A V E I  
 303 taccttgccatacttctattgaacaacggtggttacgctgatatacctagccgtagagata 362  
 Y E E K S H K W I A M R R L Y G A V F D  
 363 tacgaggaaaaaagccacaaatggatagcaatgaggaggttatatggagcagtattcgac 422  
 L S N P P K G N L K L K I Q I K E D G K  
 423 ttgtccaaccaccaaagggaaatctgaagctgaagatccaaataaaagaagatggaaaa 482  
 T K W V Q S D K T V I P D H W K A G S A  
 483 accaaatgggtgcagtctgacaagactggtatccctgatcactggaaggctggatctgcc 542  
 Y E T D I Q I P \* T S I Y N S L V C N F  
 543 tatgaaactgacattcagattccttgaacaagtatatataattcgctagtttgtaatttc 602  
 S V M V W S Q M K F V \* V I S H C G L T  
 603 tctgttatggtttggagtc aaatgaagtttgtgtaggtcatcagccattgtggtttaacc 662  
 K C L F V N N K A E I R V L L \* R E Y E  
 663 aaatggttggttgtaataataaggctgaaattcgtgtattggttgaagagaatataaa 722  
 I K H C R I L C \* K K K K K  
 723 ataaaaacattgccgtatcttgtgtagaaaaa aaaaaaaac 765

## HIGH-PRIORITY JELESKO FDD CLONES

### 1. JGJ331 (serine protease-like protein) frame +3

N V G E A K S S Y R V E I V S P R S X S  
 3 aacgtcggggaggcaaaatcatcttatcgcgtagagatagtttcaccacgaagtstytcc 62  
 V V V K P S T L K F T K L N Q K L T Y R  
 63 gtggttgtaagccttcaactctaaagtttacgaagttgaatcagaagttgacataccga 122  
 V T F S A T T N I T N M E V V H G Y L K  
 123 gtgaccttttctgcaacaacaacatcacaacatggaagttggtcatggatacttgaaa 182  
 W S S N R H F V R S P I A V I L Q E S E  
 183 tggagtagtaataggcattttgtaagaagtc caattgctgttattctacaagagtctgaa 242  
 T P E D \* C L S F L I I C S I I I S L Y  
 243 acaccagaagattagtgcttttctttttaataatttgttcaattataataagcctgtat 302  
 \* W L V S K M \* N E C K I Y S C F I L K  
 303 taatggcttgatccaaaatgtagaatgagtgcaaaatttactcatgttttattctaaaa 362  
 K K K N  
 363 aaaaaaaaaaac 374

## 2. JGJ332 (purine permease-like protein) frame + 3

N V G E A R Y Y T V I V C T A A I W Q X  
3 aacgtcgggagaagctagatattatacagttatagatgcaactgccgctatttggcagts 62

F F V G I I G V I Y R S S S L M S G V M  
63 ttcttcgtgggtattattggagttatctaccgctcttcttctttgatgtctggggttatg 122

I A V L L P V T E V L A V I F F K E N F  
123 attgcagtttttgctccccgttactgaggtattagctgtaattttctttaaggaaaat 182

S G E K G L A L F L S L W G F V S Y F Y  
183 tcaggtgaaaagggtcttgctcttttctttctttggggtttcgtctcatacttctat 242

G E F R Q T K K Q K N T S P E A E M T I  
243 ggagagttcagacaaacaagaagcagaagaatacaagtccagaagctgagatgacaatt 302

T T H T E S V \* F T I H G Y K D N \* F L  
303 acgacacatactgaatctgtttgatttactattcatggttataaggataactagttt 362

F F V Q N N V R R F P F I A T F I M F V  
363 ttttttgtacaaaataatgtacgtcgttttctttcattgctactttcattatgttt 422

K R V S L F E I S D V A L K S V I Q H L  
423 aaaagggtctctctctttgaaatttctgatggtgctcttaaatccgtaatacaacact 482

K Y L Q F K K K K T  
483 aaatatttgcagtttaaaaaaaaaaaaaac 511

## 3. JGJ334 (lipoxygenase-like protein) frame +2

G G L T A K G I P N S V S I \* T L L L R  
2 gggggactcacagccaaaggaattcctaacagtgatctatataaaccttattattaaga 61

N E P C E Q V W K W R M K K A G V S I N  
62 aatgagccatgtgaacaagtctggaaatggagaatgaagaaagctgggtgtttcaataaat 121

L V M K F H Y F K F I C L I S I C L I P  
122 cttgtaatgaagtttcattactttaagtttattttgccttattttctatatgtttgataccc 181

L S S F I S L L A Q L V I W F Q F V G R  
182 ttaagttcctttattttcccttttagcacaacttgtcatttgggtccagtttgttgggaga 241

I M Q I T N P I Y S A T C N Y S E Y \* S  
242 ataatgcagataacaaatcccatatattctgcaactgtaattattctgagtattaatca 301

Y I H L R I M Y \* K K K K  
302 tatatacatctcagaatcatgtattaaaaaaaaaaaaaac 341

## LOW-PRIORITY FDD CLONES

### 1. D15-11 (no significant BLASTN or BLASTX homology)

1 catccgtgctgtcaattaacatgtctggatccttgatccctgactgattacgagtagcg 60  
61 tgtattttaagtctatgcaactaagtaatttctttgctttaccttaccccaagacgcctc 120  
121 ccttgcatggctctgatattgctcctatttgcctttcaattgatgtaagaattcgtaa 180  
181 acttacattggatctctttccagatgatggattagataaaactccaagacgatttagaaat 240  
241 tttcgtctgttgggagttcatctagctcgagtgattgtcttaagttatatggtagatgg 300  
301 tgtccttgaacattgtgcctgtcttcaaagtaattacaaaatggtggatttctcatttga 360  
361 aaaaaaaaaaaaaac 375

### 2. D15-9 (100% nucleotide identity from position 16 to 378 of *N. tabacum* (TSC40-4) 60S ribosomal protein L34 mRNA)

1 catccgtgctcagcgccgcccgtgaaaaatgggtccaacgattaacttaccgtaaacggcac 60  
61 agctatgccaccaaatacctaaccaacataggggtgtcaaaaccccagggtggaaagctgatt 120  
121 taccagagtaccaagaagaggggctagtggacctaagtgcctgttactggaaaaagaatt 180  
181 caagggattcctcacttgaggcctactgaatacaagaggtcaagattgtcgagaaacagg 240  
241 aggactgtgaaccgtgcttatgggtgggtgtgttgtcaggcagtgctgtacgtgaaaggatc 300  
301 ataagagcctttttgggtggaagaacaaaagattgtgaagaaggttttgaagatccagaaa 360  
361 aaaaaaaaaaaaaac 373

## FDD clones with homology to *Nicotiana tabacum* 26S rRNA (GBPLN: 19919613) **A19-11, Y19a-3, Y19-9**

### 1. A19-11 (99% nucleotide identity to 2256-2671 region of *N. tabacum* 26S rRNA)

1 caaacgtcggtgccctcgtcatctaattagtgacgcgcatgaatggattaacgagattccc 60  
61 actgtccctgtctactatccagcgaaaccacagccaaggggaacgggcttggcagaatcag 120  
121 cggggtaagaagaccctgttggagcttgactctagctccgactttgtgaaatgacttgaga 180  
181 ggtgtagtataagtgggagccgaaaggcgaaagtgaaataccactacttttaacgattatt 240

241 ttacttattccgtgaatcggaagcggggcactgccctctttttggacccaaggcttgctt 300  
301 gcaggccgatccgggcggaagacattgtcaggtggggagtttggctggggcggcacatct 360  
361 gttaaaagataacgcaggtgtgcctaagatgagctcaacgagaaacagaaatctcgtgtgg 420  
421 aaaaaaaaaaaaaac 436

## 2. Y19a-3 (99% nucleotide identity to 2142-2653 region of *N. tabacum* 26S rRNA)

1 ttgaggggtccctgcggtatgtttacgcaatgtgatttctgccagtgctctgaatgtcaaa 60  
61 gtgaagaaattcaaccaagcgcgggtaaacggcgaggtaactatgactctcttaaggta 120  
121 gccaaatgcctcgtcatctaattagtgacgcgcatgaatggattaacgagattcccactg 180  
181 tccctgtctactatccagcgaaaaccacagccaagggaaacgggcttggcagaatcagcggg 240  
241 gaaagaagaccctggttgagcttgactctagtcggactttgtgaaatgacttgagaggtgt 300  
301 agtataagtgggagccgaaaggcgaaagtgaaataccactacttttaacgttattttact 360  
361 tattccgtgaatcggaagcggggcactgccctctttttggacccaaggcttgcttgag 420  
421 gccgatccgggcggaagacattgtcaggtggggagtttggctggggcggcacatctgtta 480  
481 aaagataacgcagtgctcctaagatgagctcaacgagaaaaaaaaaaaaaac 532

## 3. Y19-9 (99% nucleotide identity to 2142-2269 region of *N. tabacum* 26S rRNA)

1 ttgaggggtccctgcggtatgtttacgcaatgtgatttctgccagtgctctgaatgtcaaa 60  
61 gtgaagaaattcaaccaagcgcgggtaaacggcgaggtaactatgactctcttaaggta 120  
121 gccaaatgcctcgtcatctaattagtgacgcgcatgaatggattaacgagattcccactg 180  
181 tccctgtctactatccagcgaaaaccacagccaagggaaacgggcttggcagaatcagcggg 240  
241 gaaagaagaccctggttgagcttgactctagtcggactttgtgaaatgacttgagaggtgt 300  
301 agtataagtgggagccgaaaggcgaaagtgaaataccactacttttaacgttattttact 360  
361 tattccgtgaatcggaagcggggcactgccctctttttggacccaaggcttgcttgag 420  
421 gccgatccgggcggaagacattgtcaggtggggagtttggctggggcggcacatctgtta 480  
481 aaagataacgcaggtgtcctaagatgagctcaacgagaaacagaaatctcgtgtgaaaaaa 540  
541 aaaaaaaaaac 551

FDD clones with homology to *Oenothera berteriana* mitochondrial 26S rRNA (GBPLN: 13185)  
**D2-10, X4-3, X7-10, Y18-1, Y2a-6**

1. D2-10 (98% nucleotide identity to 1159-1710 region of *O. berteriana* mitochondrial 26S rRNA)

1 ggacccaacccacgtatgtggcaaaatacggggatgacttgtggctaggggtgaaaggcc 60  
61 aaccaagatcggatatagctagttttccgcgaaatctatttcagtagagcgtatgatgtc 120  
121 gatggccccgaggtagagcactcaatgggctaggggtggcctcatttcgccttaccaacccc 180  
181 agggaaactccgaatacaggcctagatcgtttgtacagacagactttttgggtgctaaga 240  
241 tccaaagtcgagaggggaaacagcccagatcgtagcctaaggccctaagcaatcacttag 300  
301 tggaaaaggaagtgatcgagcgtatgacaaccaggaggtgggcttgggaagcagccatcctt 360  
361 tgaagaaagcgtaatactcactgggtctagctccatggcaccgaaaatgtatcagggctc 420  
421 aagtgattcaccgaagcgcagacaccttgaaagctgctttttcaagtgtcagtagcggaa 480  
481 cgttctgtcaatcggggaaggtttttgggtgacaagacctggagatatcagaagtgagaat 540  
541 gctgacatgagtaacgaaaaaaaaaaaaaaaaaac 572

2. X4-3 (97% nucleotide identity to 1119-1712 region of *O. berteriana* mitochondrial 26S rRNA)

1 ccgctaccgaagggttgaagagagctctaacaggccttggaggaccgaaccacgtatgtg 60  
61 gcaaaatacggggatgacttgtggctaggggtgaaaggccaaccaagatcggatatagct 120  
121 ggtttttccgcgaaatctatttcagtagagcgtatgatgtcgtatggccccgaggtagagcac 180  
181 tcaatgggctaggggtggcctcatttcgccttaccaaccccagggaaactcccgaatacag 240  
241 gcctagatcgtttgtacagacaagactttttgggtgctaagatccaaagtcgagagggaa 300  
301 acagcccagatcgtagcctaaggccctaagcaatcacttagtggaaggaagtgatcg 360  
361 agcgtatgacaaccaggaggtgggcttgggaagcagccatcctctgaagaaagcgtaatagc 420  
421 tcaactgggtctagctccatggcaccgaaaatgtatcagggctcaagtgattcaccgaagc 480  
481 gacagagaccttgaaagctgctttttcaagtgtcagtagcggaaacgcttctgtcaatcggg 540  
541 gaaggtttttgggtgacaagacctggagatatcagaagtgagaatgctgacatgagtaacg 600

601 agaaaaaaaaaaaaaaaaaac 618

### 3. X7-10 (97% nucleotide identity to 950-1712 region of *O. berteriana* mitochondrial 26S rRNA)

1 gagcgaggctttttgattctattagtaaagcgactcactctaacggcgctaccttttgca 60  
61 tgatgggtcagcgaggaaatgggaacagcggcttaagccattaggtgtaggcgctttcca 120  
121 gaggtggaatcttctagttcttcctatTTTgacccgaaaccgatcgatctagccatgagca 180  
181 ggttgaagagagctctaacaggccttggaggaccgaaccacgtatgtggcaaaatacgg 240  
241 ggatgacttgtggctaggggtgaaaggccaaccaagatcggatatagctggTTTTccgcg 300  
301 aaatctatTTTcagtagagcgtatgatgtcgatggcccagggtagagcactcaatgggcta 360  
361 gggTggcctcatttcgccttaccacccccagggaaactcccgaatacaggcctagatcgt 420  
421 ttgtacagacaagactTTTTgggtgctaagatccaaagtcgagaggggaaacagcccagat 480  
481 cgtacgctaaggTccctaagcaatcacttagtggaaggaagtgatcgagcgatgacaa 540  
541 ccaggaggtgggcttggaaagcagccatcctctgaagaaagcgtaatagctcactggTcta 600  
601 gctccatggcaccgaaaatgtatcacgggctcaagtgattcaccgaagcgacagagacct 660  
661 tgaaagctgctTTTTcaagtgtcagtagcggaaacgTtctgtcaatcggggaaggTTTTg 720  
721 gtgacaagacctggagatatcagaagtgagaatgctgacatgagtaacgagaaaaaaaaa 780  
781 aaaaaac 787

### 4. Y18-1 (98% nucleotide identity to 1011-1712 region of *O. berteriana* mitochondrial 26S rRNA)

1 gtggagtcagcgaggaaatgggaacagcggcttaagccattaggtgtaggcgctttccag 60  
61 aggtggaatcttctagttcttcctatTTTgacccgaaaccgatcgatctagccatgagcag 120  
121 gttgaagagagctctaacaggccttggaggaccgaaccacgtatgtggcaaaatacggg 180  
181 gatgacttgtggctaggggtgaaaggccaaccaagatcggatatagctggTTTTccgca 240  
241 aatctatTTTcagtagagcgtatgatgtcgatggcccagggtagagcactcaatgggctag 300  
301 ggtggcctcatttcgccttaccacccccagggaaactcccgaatacaggcctagatcgtt 360  
361 tgtacagacaagactTTTTgggtgctaagatccaaagtcgagaggggaaacagcccagatc 420  
421 gtacgctaaggTccctaagcaatcacttagtggaaggaagtgatcgagcgatgacaac 480

481 caggaggtgggcttgggaagcagccatcctctgaagaaagcgtaatagctcactgggtctag 540  
541 ctccatggcaccgaaaatgtatcacgggctcaagtgattcaccgaagcgacagagacctt 600  
601 gaaagctgctttttcaagtgtcagtagcgcaacggttctgtcaatcggggaagggtttttgg 660  
661 tgacaagacctggagatatcagaagtgagaatgctgacatgagtaacgagaaaaaaaaaa 720  
721 aaaaac 726

5. Y2a-6 (98% nucleotide identity to 2786-3449 region of *O. berteriana* mitochondrial 26S rRNA)

1 catcgccgcaccgatcattcggggggaggcgggacactgcgatgcgaggtgggtagttta 60  
61 tctggggcggatgcctcctaaagagtaacggaggtgtgcaaggtaggctcaagctaaga 120  
121 ttctgctcgtgagcgtaatgggtataagcctgcctgactgtgagaccgactggtcgaacag 180  
181 agacgaaagtcggccatagtgatccgggagtcctggtggaagggctctcgctcaacgga 240  
241 tcaaaggtacgcccgggataacaggtgatgactccaagagctcttatcgacggagtcg 300  
301 tttggcacctcgatgtcgactcatcacatcctgggggtgaagaaggtcccaaggggttcgg 360  
361 ttgttcgccgattcaagtggtagctgagttgggtttagaacgctcgtgagacagttcggtt 420  
421 cctatctaccgttgggtgttaaagggagaactgcgaggagccaaccctagtagagaggac 480  
481 tgggttgggctaacctatgggtgtaccggttgggtatgccaatagcagcgccgggcagctaa 540  
541 gttggtatggaagaactgctgcccggggaaatccttctctatacaagttctcggacga 600  
601 ggtttttgaacagaacttcgataggcgagaggtgtaagcaccggggtgtgaagcgatc 660  
661 tcgtactaaacaaaaaaaaaaaaaaaaaac 688

## CURRICULUM VITAE

Deborah G. Reed (formerly Deborah G. Goldman) was born in Bloomington, Indiana on January 18<sup>th</sup>, 1966. She grew up in Pennsylvania, Virginia, and Maryland, and graduated from Rockville High School, in Rockville, Maryland, in 1983. She received a B.S. in Biochemistry with a minor in Chemistry from Virginia Tech in 1987. Deborah completed her Master of Science degree in Plant Pathology, Physiology and Weed Science with a major emphasis in Plant Physiology in June 2003, under the direction of Dr. John J. Jelesko.